Physics – Uspekhi **38** (1) 39 – 86 (1995)

PACS numbers: 76.30.Pk; 72.15.Gd; 71.25.Hc

Magnetic breakdown with spin flip

Yu N Proshin, N Kh Useinov

Contents

Abstract. A review is given of the theory of magnetic breakdown with consistent account for the spin degrees of freedom of conduction electrons. An analysis is made of the spectrum of conduction electrons in regions with anomalous approach of the orbits belonging to the different bands. The principal dynamic characteristic of magnetic breakdown in the form of a fourth-rank s matrix is derived. It is shown that the spin – orbit coupling leads to a probability of spin-flip magnetic breakdown. The main assumptions of the theory of coherent magnetic breakdown are summarised and analysed in the case of simple examples. The spectrum of conduction electrons under magnetic breakdown conditions is discussed. Applications of the theory to the galvanomagnetic effects, to the de Haas – van Alphen effect, and to the conduction-electron spin resonance are considered.

Yu N Proshin Physics Faculty, Kazan State University, ul. Lenina 18, Kazan, 420008. Tel. (8-432) 31 81 92; Fax (8-432) 38 09 94.
E-mail: proshin@phys.ksu.ras.ru
N Kh Useinov Physicotechnical Faculty, Branch of the Moscow State University, ul. L'va Tolstogo 42, Ul'yanovsk, 42700. Tel. (8-422) 32 15 98; Fax (8-422) 31 86 51. E-mail: nhu@dl.univ.simbirsk.su

Received 4 August 1994; in revised form 31 October 1994
Uspekhi Fizicheskikh Nauk **165** (1) 41 – 87 (1995)
Translated by A Tybulewicz

1. Introduction

Cohen and Falicov [1] put forward the following hypothesis: in a sufficiently strong magnetic field, conduction electrons may tunnel between orbits passing along different parts of the Fermi surface if these orbits are separated by a small energy gap. This hypothesis has been

confirmed strikingly in a period of over thirty years of progress in metal physics. This hypothesis and the term 'magnetic breakdown' (MB)† were proposed by Cohen and Falicov [1] in 1961 to explain an unexpected result reported by Priestley [2]. Priestley carried out experiments on the de Haas–van Alphen (dHvA) effect in magnesium and discovered a 'giant' orbit of area exceeding the cross section of the hexagonal Brillouin zone.

The history of MB actually begins with the work of Dhillon and Shoenberg in 1955 [3], who studied the dHvA effect in zinc. However, not until 1964 did Pippard [4] show that the mysterious fall of the amplitude of the oscillations associated with 'needles' with increase in a magnetic field, discovered by Dhillon and Shoenberg [3], is a consequence of MB.

Numberous experimental and theoretical investigations which followed the paper of Cohen and Falicov [1] not only have confirmed the correctness of the initial hypothesis, but have also revealed a number of interesting phenomena associated with MB. The majority of these results have been reviewed in detail by Stark and Falicov [5] and by Kaganov and Slutskin [6]. A thorough review of the experimental methods and the results of investiga-tions of MB can be found in the paper of Alekseevskii, Nizhankovskii [7], and in Shoenberg's monograph [8].

We are therefore dealing with a thoroughly investigated effect. Nevertheless, it has been found that a consistent account for the spin–orbit coupling (SOC) in the theory of MB demands a review of some of the ideas relating to this breakdown. It has usually been assumed [1–8] that under MB conditions there are two possible types of behaviour of conduction electrons reaching regions of anomalous orbit approach: electrons can remain in their own band or can jump to an adjacent band. It has been assumed that the conduction electron spin is conserved. It has been found, however, that [9] in the case of metals (or other systems containing conduction electrons) for which the role of the SOC is important in the formation of the band spectrum, conduction electrons may tunnel to an adjacent band with spin flip under MB conditions. We shall show that the appearance of this additional tunnelling channel complicates greatly the pattern of motion of conduction electrons under MB conditions and in some cases may alter significantly the macroscopic properties of a system.

In the semiclassical approximation, when the spin degrees of freedom in a static magnetic field are taken into account at absolute zero, the electron orbits are formed by a section of the Fermi surface cut by a plane perpendicular to the magnetic field $\boldsymbol{H}(0, 0, H)$:

$$\varepsilon_{m\sigma}(\boldsymbol{p}) = \varepsilon_{\mathrm{F}} = \mathrm{const}, \quad p_z = p_{z0} = \mathrm{const}, \tag{1}$$

where ε_{F} is the Fermi energy: $\varepsilon = \varepsilon_{m\sigma}(\boldsymbol{p})$ is an arbitrary dispersion law of conduction electrons in the absence of a magnetic field but subject to the SOC [10]; $\boldsymbol{p}$ is the quasimomentum; $\boldsymbol{p}_z$ is the projection of the quasimomentum along the direction of the magnetic field $\boldsymbol{H}$; m is the band number; $\sigma = \uparrow\downarrow$ is the spin index. In the absence of an MB and for sufficiently pure metals at low temperatures the quantities m, p_z, and σ are 'good' quantum numbers.

† Sometimes also called 'magnetic breakthrough', especially in the older literature. *Translator's note*.

The electron orbit topology determines many properties of metals in a magnetic field (both transport and thermodynamic properties; see, for example, Refs [11–13]. Magnetic breakdown changes drastically the topology of conduction electron orbits described by expression (1) and the nature of their motion. This is related to the possibility of conduction electron tunnelling from band to band, as the orbits described by expressions (1) approach one another. Blount [14] demonstrated the probability of such tunnelling is

$$w = \exp\left(-\frac{H_0}{H}\right), \tag{2}$$

i.e. the probability is governed by the ratio of the magnetic field to $H_0 = H_0(\varepsilon_{\mathrm{F}}, p_z)$, which is known as the MB field. Each orbit is characterised by its own breakdown field. The order of magnitude of this field is $H_0 \approx \Delta^2/\varepsilon_{\mathrm{F}}$, where the interband energy gap is $\Delta \approx v_M\,\delta p$ (v_M is the velocity of conduction electrons near the maximum approach of the orbits and δp is the minimum separation between the orbits in the $\boldsymbol{p}$ space).

In addition to these changes in the nature of motion of conduction electrons, the macroscopic properties of a system are influenced also by quantum interference of conduction electrons participating in MB in sufficiently pure metals. All the phenomena due to interband quantum transitions of conduction electrons between the orbits in different bands in the magnetic field and their interference are known as 'coherent magnetic breakdown' [6]. MB alters the response of a metal to external agencies (electric and magnetic fields, sound) and this is manifested in almost all the electronic properties when the applied magnetic field is sufficiently strong.

MB has been observed in over twenty metals, intermetallic compounds, and some alloys [15]. The evidence for MB is based on the dHvA and Shubnikov–de Haas effects, the Hall and other galvanomagnetic effects, conduction-electron spin resonance [16, 17], and some other phenomena and properties of metals [5–8]. For example, MB leads to giant oscillations of the magnetoresistance and to unusual oscillations of the magnetic susceptibility and the acoustic absorption coefficient of metals. Characteristic nonlinear effects in the attenuation of waves [18], in the static conductivity [19–21], and in the propagation of sounds [22] are also due to MB.

The number of chemical compounds exhibiting MB is increasing continuously. In the years since the last review, it has been found that in addition to normal metals (such as Mg, Al, Zn, etc.) [23], MB has been observed in ferromagnets [24–26], in two-dimensional heterostructures [27–29], and in rare-earth hexaborides [30]. When $NbSe_3$ is subjected to strong magnetic fields (up to 520 kG), MB manifests itself by giant oscillations of the resistance in the ultraquantum limit [31].

Intensive studies of the Fermi surface of organic conductors, representing a new class of superconductors with fairly high superconducting transition temperature (of the order of 10 K) [32], have provided a stimulus for a large number of reports of observations of MB in these conductors [33–43]. Practical applications of MB are also being proposed: beryllium has been used in measuring a magnetic field and its gradients [44]. The widespread occurrence of MB and the variety of the associated effects have stimulated further theoretical and experimental investigations of the topic.

The smallness of the regions of the anomalous approach of two bands (MB regions) makes it possible to consider them as characteristic points of quantum scattering of conduction electrons that move along semiclassical orbits in a magnetic field. Frequently these small regions are called MB nodes: they link the semiclassical parts of the orbits described by expressions (1) associated with different bands into a single planar network. Such a planar system of orbits in $\boldsymbol{p}$ space is called an MB configuration [6, 45] and the corresponding system of orbits in the real $\boldsymbol{r}$ space is called an MB network [5, 46]. It should be pointed out that there is no special MB region in the $\boldsymbol{r}$ space.

The main dynamic characteristic of MB is a unitary MB scattering matrix or s matrix [6, 9, 45]. This matrix relates semiclassical wave functions of conduction electrons of parts of orbits which merge at an MB node and are associated with two bands. Knowledge of the s-matrix elements makes it possible to derive readily the probability of MB and of a jump in the wave-function phase as a result of this breakdown. For example, the sum of the squares of the moduli of the off-diagonal (in respect of the band number) s-matrix elements determines the total probability, given by formula (2), of the transition of a conduction electron to another band [9].

A mathematical formalism based on the s matrix and fit for the task in question has made it possible to develop a consistent MB theory and to describe a number of effects. Among the most interesting are giant quantum oscillations due to coherent MB [6, 18] and small-orbit interference transparency [6]. The possibility of quantum localisation of conduction electrons under MB conditions has been predicted [47] (see also Ref. [48], where the effect is considered from a different standpoint).

However, in all these theoretical investigations of various aspects of MB the spin degrees of freedom of conduction electrons have been effectively ignored. MB theories developed on the basis of the s-matrix formalism by Slutskin [6, 49] and the concept of coupled-orbit networks, proposed by Pippard [4, 46, 50] and developed later by Chambers [51–53], and by Falicov and Stark [5, 48, 54–58], postulate that conduction electrons with opposite spins move completley independently. MB scattering has been regarded as a two-channel process and it has been suggested that there are two independent patterns of the motion of conduction electrons: spin up and spin down.

On the other hand, it is known (see, for example, Refs [10, 59]) that the SOC makes a considerable contribution to the band spectrum specifically in those parts of the quasimomentum space where the energy gap between the various bands is small. Consequently, the SOC should play a significant role in a quantum analysis of the motion of conduction electrons in the small regions responsible for MB.

A simple model of a metal with its Fermi surface intersecting the Brillouin zone only in one direction has been used [60] to show that the SOC does indeed lead to a nonzero probability of conduction-electron spin flip under MB conditions.

Somewhat later, a complete s matrix including the SOC has been developed for a metal with an arbitrary dispersion law [9]. It has been found not only that the spin doubles the rank of the s matrix, but the matrix has nonzero off-diagonal (in terms of the spin index and band number) elements. This leads to a new (third!) MB tunnelling channel with conduction-electron spin flip.

The SOC does not alter formula (2). However, w is now the total probability of conduction electron tunnelling to an adjacent band, equal to the sum of the probabilities of magnetic breakdown with (w^s) and without (w^0) spin flip:

$$w^s = \frac{\alpha^2 w}{1+\alpha^2}, \quad w^0 = \frac{w}{1+\alpha^2}. \tag{3}$$

The SOC parameter $\alpha = \alpha(\varepsilon_F, p_z)$ is determined by the ratio of the off-diagonal (in respect of the spin index and band number) matrix elements of the conduction-electron velocity operator near the closest approach of the orbits [9]. In the absence of the SOC there is no conduction electron spin flip: $\alpha \equiv 0$. Inclusion of the SOC also leads to renormalisation of the characteristic breakdown field H_0.

It follows that a consistent MB theory should take into account the spin degrees of freedom of conduction electrons. The orbits of conduction electrons with opposite spins merge because of the SOC under MB conditions.

However, if the theory of MB with spin flip is considered formally, it is found that it differs in the following ways from the 'zero-spin' case [6]: the s matrix is converted from 2×2 to 4×4 and the number of sections in the MB configuration doubles. That is all! However, this is sufficient to complicate greatly the description of the effect.

Fortunately, the MB theory developed by Slutskin [18–20, 45, 47, 49] and discussed in Kaganov and Slutskin's review [6] *places no restrictions on the rank and form of the s matrix*. This enabled Slutskin and his colleagues to use the s-matrix approach to describe a completely different effect, which is multichannel specular reflection of conduction electrons from surfaces and the phenomena associated with this effect [61–63].

In our case this property of the MB theory makes it possible to generalise its fundamental concepts given in Kaganov and Slutskin's review [6]. This review deals with coherent MB and is full of new concepts and complex formulas. It is therefore difficult to digest it at first reading, particularly in the case of people not specialising in this branch of physics. We would therefore like to, first, demonstrate the consequences of taking into account the spin degrees of freedom of conduction electrons under MB conditions and, second, to use the theory of spin-flip MB to illustrate the ideas underlying Slutskin's approach but at a more accessible level. The need for this is particularly great because it has been found that the SOC affects all the properties of MB systems [9, 17, 60, 64–71]. For example, there is a major change in the energy spectrum of conduction electrons participating in breakdown and this alters greatly the classification of the conduction-electron states. Under MB conditions the small-orbit interference transparency effectively disappears and there are changes in the galvanomagnetic properties and in the dHvA effect. The reliability of theoretical calculations, which are continued until numerical results have been obtained, is supported by experimental data.

We shall consider in greater detail these and some other topics in the theory of MB with a possible spin flip of conduction electrons.

2. Fundamentals of magnetic breakdown theory including the spin degrees of freedom

2.1 Motion of conduction electrons with an arbitrary dispersion law along semiclassical orbits in a magnetic field

The treatment of conduction electrons as weakly interacting quasiparticles [72] with an arbitrary dispersion law [11]

$$\varepsilon = \varepsilon_{m\sigma}(\boldsymbol{p})\,. \tag{4}$$

has played a special role in the physics of metals. The energy of quasiparticles varies periodically with $\boldsymbol{p}$ and the period is the same as that of the reciprocal lattice. Many conclusions can be drawn without specifying the actual dependence of energy on quasimomentum.

Moreover, we must stress another important circumstance which facilitates greatly the solution of many problems. Conduction electrons are ultimately quantum objects. The band nature of the energy spectrum and the concepts of the 'spin', 'quasiparticle', 'quasimomentum', 'degeneracy', 'Fermi surface', etc. are the results of application of the laws of quantum mechanics to conduction electrons. However, the motion of a quasiparticle with a quasimomentum $\boldsymbol{p}$, a spin state σ, a band number m, and an energy given by the dispersion law (4) in external fields is in most cases semiclassical [11]. This is due to the fact that external fields are relatively weak compared with the internal atomic fields and they vary significantly over distances which are large compared with the atomic spacings.

In other words, typical dimensions of electron orbits are large compared with the de Broglie wavelength $\hbar/p_0$, where p_0 is the characteristic Fermi momentum. In the case of conduction electrons moving in a magnetic field this condition is equivalent to the inequality

$$\kappa = \frac{\hbar\omega_c}{\varepsilon_0} \ll 1\,, \tag{5}$$

where ω_c is the characteristic cyclotron frequency of conduction electrons in a magnetic field and ε_0 is the characteristic energy of these electrons, which is of the order of the Fermi energy ε_F.

Inequality (5) is satisfied by fields $H \ll 10^8 - 10^9$ G, which makes it possible to express the one-electron Hamiltonian $\hat{H}$ in a magnetic field in terms of the dispersion law of conduction electrons, in accordance with the familiar correspon-dence principle [11]

$$\varepsilon_{m\sigma}(\boldsymbol{p}) \to \hat{H}_{m\sigma} = \varepsilon_{m\sigma}(\hat{\boldsymbol{p}})\,, \quad \hat{\boldsymbol{P}} = \hat{\boldsymbol{p}} + \frac{e}{c}\hat{\boldsymbol{A}}\,. \tag{6}$$

Here $\hat{\boldsymbol{P}}$ is the generalised momentum operator; $\hat{\boldsymbol{A}} = \boldsymbol{A}(\hat{\boldsymbol{r}})$ is the vector potential of the magnetic field; $\hat{\boldsymbol{p}}$ is the kinematic momentum operator.

In the zeroth-order approximation (with respect to κ), conduction electrons can be regarded as classical particles whose motion obeys the equations

$$\frac{\mathrm{d}\boldsymbol{p}}{\mathrm{d}t} = \frac{e}{c}[\boldsymbol{v}_{m\sigma} \times \boldsymbol{H}], \quad \frac{\mathrm{d}\boldsymbol{r}}{\mathrm{d}t} = \boldsymbol{v}_{m\sigma} = \frac{\partial\varepsilon_{m\sigma}}{\partial\boldsymbol{p}}. \tag{7}$$

The spin index σ is retained in these equations only for completeness, because in the adopted approximation the system of equations (7) describes the motion of a zero-spin particle. If the first of these equations is multiplied scalarly once by $\boldsymbol{v}_{m\sigma}$ and then by $\boldsymbol{H}$, it is found that in a static homogeneous magnetic field $\boldsymbol{H} = \boldsymbol{H}(0, 0, H)$ the motion of conduction electrons in the $\boldsymbol{p}$ space follows orbits which are on a constant-energy surface, by analogy with expressions (1):

$$\varepsilon_{m\sigma}(\boldsymbol{p}) = E = \text{const}\,, \quad p_z = p_{z0} = \text{const}\,, \tag{8}$$

where the energy E and the projection of the quasimomentum p_{z0} along the magnetic field are conserved.

There is a close relationship between the orbits in the quasimomentum and ordinary ($\boldsymbol{r}$) spaces. It follows from the system of equations (7) that the xy projection of an orbit in the $\boldsymbol{r}$ space essentially repeats the $\boldsymbol{p}$ orbit and differs from the latter only by its orientation and scale: the former is obtained from the latter by the substitution

$$p_x = -\frac{e}{c}Hy\,, \quad p_y = \frac{e}{c}Hx\,. \tag{9}$$

The orbit described by expressions (8) represents geometrically the contour of a section of a constant-energy surface $E = \text{const}$ cut by a plane perpendicular to the magnetic field. The orbit of expression (8) is usually complex because of the periodicity and anisotropy of the dispersion law (4). If the Fermi surface is closed, then all its sections are closed contours (see Fig. 1a given later). The sections of an open Fermi surface may be closed or open, i.e. they may extend over the whole of the reciprocal lattice. (The influence of the Fermi surface topology on the macroscopic properties of metals in magnetic fields is discussed in the very detailed review of Kaganov and Lifshitz [12].)

We shall now consider the next approximation in terms of κ and $\hbar$ and include the spin degrees of freedom of conduction electrons. If the vector potential of a homogeneous magnetic field, directed along the z axis, is selected in the form $\boldsymbol{A} = \boldsymbol{A}(Hy, 0, 0)$, then in that region of the $\boldsymbol{p}$ space where the semiclassical approximation is valid, the motion of conduction electrons is described by the Hamiltonian [73]

$$\hat{H}_{m\sigma}(\hat{\boldsymbol{p}}) = \varepsilon_{m\sigma}(\hat{\boldsymbol{p}}) + g_m(\boldsymbol{p})\,\mu_B H\hat{\sigma}_z\,, \tag{10}$$

where $\hat{\boldsymbol{p}}$ is given by expression (6):

$$(\hat{p}_x, \hat{p}_y, \hat{p}_z) \to \left(\hat{P}_x + \frac{e}{c}H\hat{y}, \hat{P}_y, \hat{P}_z\right), \tag{11}$$

$g_m(\boldsymbol{p})$ is the $\boldsymbol{p}$-dependent scalar g factor of conduction electrons [10]; $\hat{\sigma}_z$ is the Pauli spin matrix; μ_B is the Bohr magneton.

The second term in the Hamiltonian (10) represents only the interaction of the magnetic moment of conduction electrons with the field if the SOC is ignored. A complete picture is obtained by noting that, in general, this interaction can be written in the tensor form [10, 59, 74], which naturally leads to the appearance of the g tensor†. The Hamiltonian (10) does in fact introduce the scalar g factor (or effective spin) of conduction electrons.

The linearity of the approximation in terms of $\hbar$ makes it possible to adopt the following sequence of operations [73]: an orbit is quantised first ignoring the spin and then the spin splitting is superimposed. It therefore follows from

† With the exception of several papers in which the phenomenological g tensor is introduced for the purpose of theoretical interpretation of the experimental data on conduction-electron spin resonance in Ag, Cu [75, 76], and Al [77], in most of the theoretical analyses of the g factor of metals it is regarded as a scalar quantity.

the Hamiltonian (10) that the Zeeman splitting of the 'spin' levels appears in $H \neq 0$ (Fig. 1b):

$$\varepsilon_{m\uparrow}(p_z) - \varepsilon_{m\downarrow}(p_z) = g_m(p_z)\,\mu_B H \ll \varepsilon_0\,. \tag{12}$$

The inclusion of the SOC makes the g factor of conduction electrons different from the value $g_0 = 2.0023$ for free electrons. For clarity, we can assume that conduction electrons belonging to one band (i.e., with the same number m but with different spin indices σ) generally move along slightly different orbits described by expression (8) (Fig. 1c).

Inclusion of the spin of conduction electrons gives rise, in a magnetic field, to a Fermi surface of conduction electrons with the spins parallel and antiparallel to the field. Such splitting of the Fermi surface is particularly important in the case of ferromagnetic metals [8, 24]. The splitting is small for normal metals.

In this approximation the quasiclassical wave function of conduction electrons has the following form in the p representation [9, 73, 78]:

$$\Psi_{m\sigma}(P_y) = \frac{c_{m\sigma}}{|v^x_{m\sigma}|^{1/2}} \exp\left[\varphi_{m\sigma}(E, p_z)\right] \chi_\sigma\, \delta_{P_{x0}P_x}\, \delta_{P_zP_{z0}}\, \delta_{\sigma_{z0}\sigma_z}\,, \tag{13}$$

where the Kronecker deltas indicate that P_x, $P_z = p_z$, and σ_z are conserved. It should also be pointed out that the selected gauge leads to $P_y = p_y$. The following notation is used in formula (13): $c_{m\sigma}$ is an arbitrary constant factor; $v^x_{m\sigma} = \partial\varepsilon_{m\sigma}/\partial P_x$ is the x component of the velocity along an orbit described by expression (8); χ_σ is the 'spin' function of the type $\chi_\sigma = \lambda\chi^0_\uparrow + \mu\chi^0_\downarrow$, where

$$\chi^0_\uparrow = \begin{pmatrix}1\\0\end{pmatrix}, \quad \chi^0_\downarrow = \begin{pmatrix}0\\1\end{pmatrix}. \tag{14}$$

If the spin degrees of freedom are taken into account, the phase $\varphi_{m\sigma}(E, p_z)$ of the wave function (13) is [9, 73]:

$$\varphi_{m\sigma}(E, p_z) = \frac{1}{\hbar}\, S_m(E, p_z) \pm \frac{1}{2\hbar}\, g_m\, \mu_B H t_m\,. \tag{15}$$

The first term in formula (15) is the zero-spin contribution to the phase, where

$$S_m(E, p_z) = \frac{c}{eH} \int^{p_y} p_x^{(m)}(p'_y)\, \mathrm{d}p'_y \tag{16}$$

is the increment in the transverse effect in the absence of the spin splitting; $p_x^{(m)}(p_y, E, p_z)$ is the solution of Eqn (8). The second term in formula (15) is the spin contribution to the phase; $t_m = t_m(E, p_z)$ is the zero-spin duration of motion of a conduction electron along an orbit in the mth band; $g_m = g_m(E, p_z)$ is the g factor of conduction electrons averaged over the orbit described by expression (8) [9, 73, 79–82]. The plus and minus signs in expression (15) correspond to $\sigma = \uparrow, \downarrow$. In the derivation of expression (15) use is made of the quasiclassical equations of motion (7).

Along a closed orbit of expression (8) the motion of a conduction electron is naturally periodic and its revolution (cyclotron) frequency is

$$\omega_m = \frac{eH}{cm_m(E, p_z)} = \frac{2\pi}{T_m(E, p_z)}. \tag{17}$$

Here, $T_m(E, p_z)$ is the period and

$$m_m = \frac{1}{2\pi}\, \frac{\partial S_m(E, p_z)}{\partial E} \tag{18}$$

is the effective cyclotron mass of a conduction electron in the mth band, which depends on E and p_z. Here, $S_m(E, p_z)$ is the zero-spin area under the curve. Formulas (17) and (18) are written down ignoring the spin index σ, which is important only in the case of ferromagnetic metals [24].

The finite motion of conduction electrons leads to the appearance of discrete energy levels corresponding to each fixed value of the longitudinal quasimomentum p_z. These levels are governed by the general semiclassical Lifshitz–Onsager quantisation rules [11]. The quantisation condition for this case is obtained from the requirement that the phase, described by expression (15), of the wave function (13) changes by $2\pi n$ in the case of a passage along any closed orbit given by expression (8). If the spin of conduction electrons and the SOC are taken into account, this condition can be written in the following form [11, 73] on the basis of formulas (17) and (18):

$$S_m(E, p_z) \pm \pi g_m m_m\, \mu_B H = \frac{2\pi e\hbar H}{c}\,(n + \gamma)\,, \tag{19}$$

where n is an integer ($n \gg 1$), and γ is a correction (of the order of unity) to the number n which is introduced in order to refine semiclassical quantisation conditions. This correction can be determined by considering the motion of conduction electrons near the 'stopping points' [11, 83, 84].

It therefore follows that semiclassical quantisation in the case of closed orbits leads to the appearance of discrete energy levels $E_{m\sigma}(n, p_z)$. An energy band, for example the mth band, splits into a number of Landau subbands and each of these represents a band of energy levels which differ in respect of the values of the continuous variable p_z. Inclusion of the spin of conduction electrons splits each of these levels into two. If in a plane perpendicular to the field the motion of a conduction electron is infinite, the spectrum changes and it consists then of continuous finite-width bands [11, 83].

The description of motion of conduction electrons along orbits described by expression (8), which includes the spin splitting of expression (12), can be provided conveniently if conduction electrons are represented by semiclassical wave packets. Such a representation is particularly useful in studies of transport phenomena [11, 13]. The quantum uncertainty of a wave packet in respect of its quasimomentum Δp is small compared with the characteristic momentum p_0 (it is of the order of p_F or of the order of the reciprocal lattice constant b) and the corresponding uncertainty of the coordinate $\hbar\Delta p$ is much greater than its de Broglie wavelength, but much less than the characteristic electron orbit radius cp_0/eH.

It follows from the above that the state of a conduction electron (packet) can be described by two vectors: $\boldsymbol{P}$ and $\boldsymbol{R}$, which are the centres of its localisation in the p and r spaces, as well as by the band number m and the spin index σ. Then the motion of a quasiparticle along an orbit, described by expression (8) and governed by the system of equations (7), results in an acquisition of a semiclassical phase of expression (15).

2.2 Condition for the appearance of magnetic breakdown

In some cases it is not possible to use a semiclassical description of the motion of conduction electrons in the $\boldsymbol{p}$ space given by the system of equations (7). The description loses its meaning near the points of approach of the orbits,

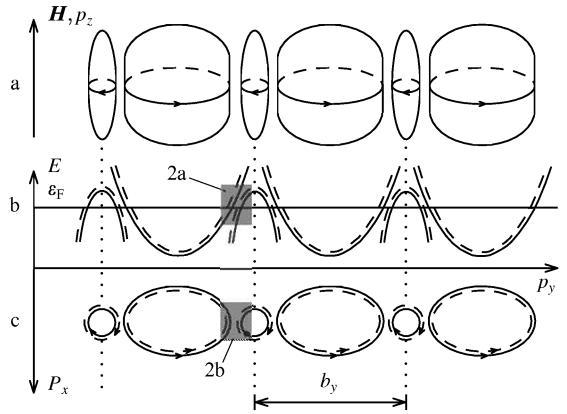

Figure 1. Schematic representation of the band pattern resulting in MB: (a) Fermi surface consisting of two sheets [the arrows give the direction of motion of conduction electrons along orbits described by expression (8) in a magnetic field; the spin splitting is not shown]; (b) nominal band spectrum in a magnetic field; (c) periodic system of semiclassical orbits, described by expression (8), in the $p_z = 0$ plane. The continuous curves in Figs 1b and 1c correspond to the states of conduction electrons with spin up and the dashed curves correspond to those with spin down. The regions of closest approach of the orbits belonging to different bands are shown (see Figs 2a and 2b).

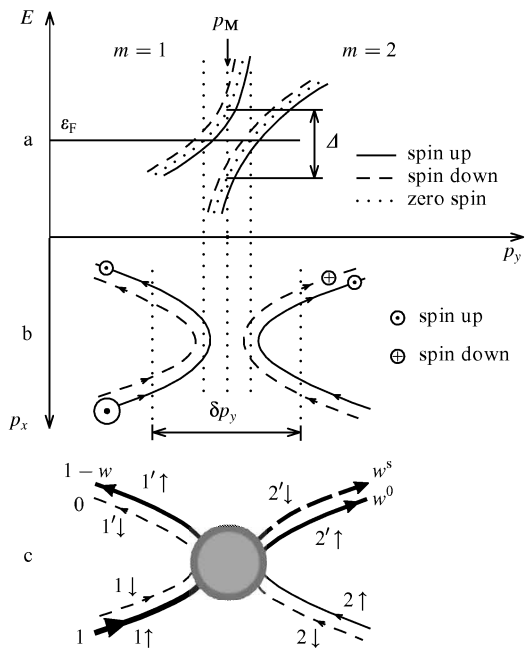

Figure 2. (a) Region of closest approach of the bands, identified in Fig. 1b ($\boldsymbol{p}_M$ is the point of maximum approach; the dashed curves give the zero-spin spectrum of conduction electrons). (b) Region of maximum approach of the orbits, identified in Fig. 1c (δp_y is the dimension of the MB region; the circles show schematically the process of MB scattering of conduction electrons). (c) Schematic representation of an MB node (demonstrating the scattering of a wave packet which enters an MB node in the first Brillouin zone with spin up). The amplitudes of the packet are represented nominally by the thickness of the lines (c) and by the dimensions of the circles (b). The arrows identify the direction of motion of conduction electrons and the orientation of their spin.

described by expression (8) with different numbers m i.e. where the following inequality is obeyed:

$$\Delta(\boldsymbol{p}) = \Delta_{mm'}(\boldsymbol{p}) = |\varepsilon_{m\sigma}(\boldsymbol{p}) - \varepsilon_{m'\sigma}(\boldsymbol{p})| \ll \varepsilon_0\,, \qquad (20)$$

where $\Delta_{mm'}(\boldsymbol{p})$ is the width of the interband gap. In the case of some values of m and m' the gap $\Delta(\boldsymbol{p})$ may vanish along certain lines of points of degeneracy in the $\boldsymbol{p}$ space. As pointed out in Ref. [11], such degeneracy lines should be exhibited by approximately half of all the metals.

For the majority of polyvalent metals the smallness of the pseudopotential means that the anomalous band approach occurs near the Bragg reflection faces [50]. In these planes the band gap $\Delta(\boldsymbol{p})$ reaches its minimum, which is typically $(0.01-0.1)\varepsilon_F$. Such small values of $\Delta(\boldsymbol{p})$ have been deduced experimentally specifically from MB observations. Formation of small gaps is also possible because of the SOC, which lifts the degeneracy of the dispersion law (4) [10]. The existence of a small gap affects macroscopic properties if the gap is close to the Fermi surface. This is a fairly common occurrence and it has been observed, for example, for such metals as Mg, Zn, Cd, etc. In discussing the motion of conduction electrons in these parts of the $\boldsymbol{p}$ space it is necessary to adopt a quantum description, which is given in Sections 2.3–2.5.

To gain a better understanding let us turn to Fig. 1a where the extended zone scheme is used to show a model Fermi surface, consisting of a large electron 'packet' at the centre of the Brillouin zone and a hole 'cigar' at its boundary. Orbits with extremal areas ($p_z = 0$) are shown for both sheets and the arrows identify the direction of motion of a conduction electron in a magnetic field.

In the regions of anomalous approach of the orbits we can expect quantum interband transitions of conduction electrons, including those involving spin flip. For simplicity, the spin splitting is not shown in Fig. 1a. The Fermi surfaces corresponding to conduction electrons with different spins nest in one another and in this case the outer hole and electron sheets correspond to opposite spin orientations. This is illustrated clearly in Fig. 1b, which shows the band spectrum corresponding to a given Fermi surface. The dependence of the conduction-electron energy on the quasimomentum projection is given for different spin orientations (the continuous curves correspond to spin up and the dashed curves to spin down). In this case the spin splitting is greatly exaggerated for clarity. Fig. 1c shows the electron orbits obtained when the Fermi surface is cut by the $p_z = 0$ plane. In the absence of magnetic breakdown, these orbits are closed (as shown in Fig. 1c).

The regions of anomalous approach, identified in Figs 1b and 1c, are shown on an enlarged scale in Figs 2a and 2b: $\boldsymbol{p}_M$ is the point of maximum breakdown where $\Delta(\boldsymbol{p})$ has its minimum, and δp_y is the characteristic size of the MB region.

Fig. 2b demonstrates also the MB scattering process. The arrows identify the direction of motion of electron wave packets along the orbits. The sizes of the circles represent the relative amplitudes of the wave packets (conduction electrons). A spin-up packet (represented by the large circle) reaching an MB region splits into three smaller wave packets: two in the second band and one in the first. The spin degrees of freedom will be discussed in greater detail below in the derivation of the s matrix. In particular, it follows from the form of the s matrix that a conduction electron which remains in its *own* band after MB *cannot* experience a change in the *initial* spin orientation.

As pointed out in Section 1, the smallness of the MB region makes it possible to replace it with an MB node, which is shown schematically in Fig. 2c. MB scattering of a

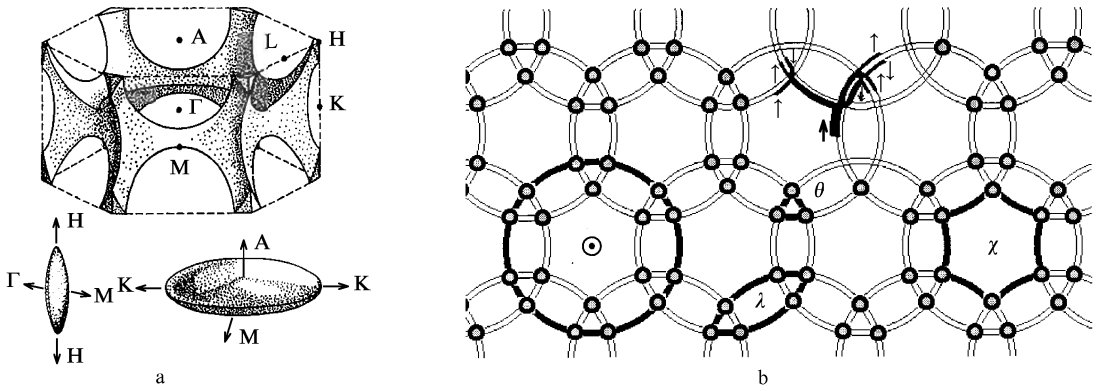

Figure 3. (a) The most important (in subsequent analysis) parts of the Fermi surface of a divalent metal with the hcp crystal structure (Be, Mg, Zn, Cd). The Brillouin zone and the hole monster lying in the second zone are at the top; below on the left is the electron cigar (Mg) or needle (Zn) in the third zone, centred on the edge of the Brillouin zone relative to the point K; below on the right is the electron lens centred relative to the point Γ. (b) Two-dimensional MB configuration, which appears in metals with the hcp crystal structure when $\boldsymbol{H}\|\boldsymbol{c}$ in the $p_z = 0$ plane. The MB nodes are identified by circles. Some orbits ($\odot$, λ, θ, χ) are discussed in Section 5. The centre of the figure shows schematically the evolution of a semiclassical packet which starts with a unit amplitude and spin up. After two successive MB scattering events it splits into seven packets. The arrows identify the final spin orientations. The thickness of the lines corresponds nominally to the packet amplitudes.

conduction electron in the first spin-up band is identified by lines whose thickness represents the relative amplitudes of the wave packets of the electrons. When the MB regions in Fig. 1c are replaced with the MB nodes in Fig. 2c, the result is an MB configuration which is open for $w = 1$ along the p_y axis. Other possible MB configurations are shown in Figs 3b and 4.

We shall now discuss qualitatively the magnetic field which can induce interband transitions of conduction electrons. Naturally, it should be possible to express the MB field H_0 in terms of the parameters of the band spectrum in the region of anomalous orbit approach (Fig. 2). The field H_0 should depend primarily on the interband gap Δ.

The condition for the appearance of MB was first formulated by Cohen and Falicov [1]. According to this condition, in order to observe MB the measure $\hbar\omega_c$ of the quantisation of the motion of electron wave packets in a magnetic field should be greater than or approximately equal to the interband gap Δ. Cohen and Falicov estimated that fields of at least 10^3 kG would be needed to observe MB for the smallest known interband gap $\Delta \approx 10^{-2}\varepsilon_F$. However, in many cases it is possible to observe MB in much weaker fields, which raises doubts about the Cohen–Falicov criterion.

Blount [14] considered the behaviour of electrons in the limits of strong and weak magnetic fields. He found that the probability of transitions depended exponentially on the ratio H_0/H and he obtained the correct expression (2) for the field H_0. Harrison [85] demonstrated that this expression is valid also in moderate fields. A different approach to MB was used by Pippard [46]. He drew attention to the fact that after partial reflection of an electron from an MB node, the subsequent reflections may result in interference of the reflected and transmitted waves.

Pippard was thus the first to consider the coherent effects associated with MB. He investigated the structure of the energy levels that appear as a result of such processes in the case of some MB networks: he discussed a one-dimensional network of the kind shown in Fig. 4d (in

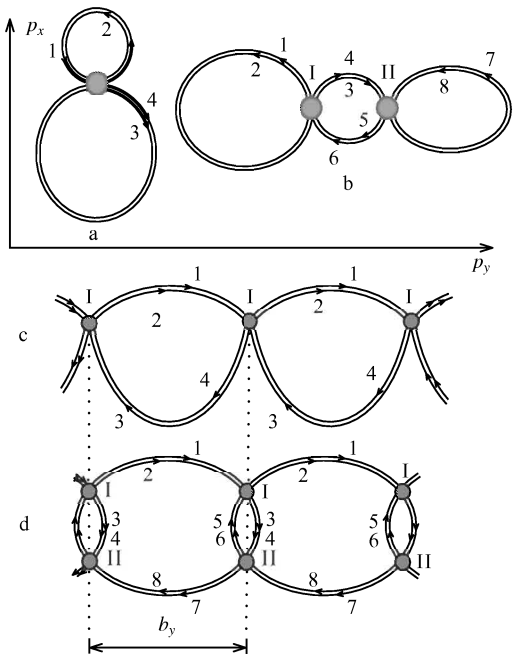

Figure 4. Simple MB configurations taking account of the spin splitting: (a) double figure-of-eight, showing nominally the MB scattering of conduction electrons in Section 1 (spin up); (b) closed MB configuration with inequivalent sites I and II; (c) and (d) open MB configurations with the period b_y. The inequivalent sections have Arabic numbers: the odd numbers correspond to the motion of spin up conduction electrons and the even numbers to spin down electrons. Inequivalent MB nodes are identified by Roman numerals. The arrows identify the direction of motion of conduction electrons.

Pippard's case it consisted of regular circles) and a two-dimensional network (Fig. 3b) [4]. The quantum-mechanical problem of finding the MB probability in the specific case of almost-free electrons was solved by Reitz [86]. Inclusion of the SOC in the Reitz model gives rise to the probability of conduction-electron spin flip under MB conditions [60].

A consistent solution of the Schrodinger equation was first obtained, ignoring the SOC, by Slutskin [45] who considered MB as a transition of conduction electrons between closely spaced energy terms under the influence of an adiabatic perturbation.† Slutskin used only the smallness of the semiclassical parameter κ and the smallness of the ratio $\Delta(\boldsymbol{p})/\varepsilon_0$. This procedure involved finding the dispersion law for an MB region and the coefficients in the expansion of the Bloch factors in terms of wave eigenfunctions. Matching of the solutions obtained to the semiclassical wave functions (13) yields the principal characteristic of MB, which is the unitary second-rank s matrix describing two-channel scattering of conduction electrons on MB nodes. It relates the coefficients of the wave functions of conduction electrons from expression (13) on different sides of MB regions. The complete s matrix, which takes account of the SOC, is calculated in Ref. [9] (see below).

For simplicity, we shall consider qualitatively the situation when the spin degrees of freedom are ignored. The MB field of formula (2) can be estimated by making use of a readily understood interpretation of MB given in Ref. [87]. MB represents quantum tunnelling of conduction electrons accompanied by a change in a discrete quantum number, which is the number m of the energy band. The dispersion law $\varepsilon_{m\sigma}(\boldsymbol{p})$ represents essentially the discrete levels of terms of the quantum system that are continuous functions of the vector parameter $\boldsymbol{p}$ (Figs 1b and 2a). The magnetic field creates a transient perturbation, inducing a time dependence of the parameter $\boldsymbol{p}$ and a consequent variation of the separation between the terms $\Delta_{mm'}(\boldsymbol{p})$. This leads to transitions of electrons from one level to another (interband transitions). A characteristic magnitude of this perturbation δE is equal to the change in the interband gap in a time $\Delta t \sim \hbar\Delta_{mm'}$. If $\delta E \ll \Delta_{mm'}$, the probability of a transition between the bands m and m' is negligible. However, if $\delta E \sim \Delta_{mm'}$, the transitions become possible: MB takes place.

We shall now estimate the perturbation δE. By definition, it can be described by

$$\delta E \approx \Delta t \frac{\mathrm{d}(\delta E)}{\mathrm{d}t} = \frac{\hbar}{\Delta_{mm'}} \left| \frac{\partial \Delta_{mm'}}{\partial \boldsymbol{p}} \cdot \frac{\mathrm{d}\boldsymbol{p}}{\mathrm{d}t} \right|, \tag{21}$$

where the derivatives obey the classical equations of motion (7). Since far from the points of closest approach of the bands the quantity $|\partial\Delta_{mm'}/\partial\boldsymbol{p}|$ is of the order of the characteristic electron velocity v_0, it follows that for $\Delta(\boldsymbol{p}) \sim \varepsilon_0 \approx mv_0^2/2$ and from the semiclassical condition (5) that

$$\delta E \sim \hbar\omega_c < |\Delta_{mm'}|.$$

Therefore, the smallness of the parameter κ makes it possible to ignore interband transitions in those parts of the $\boldsymbol{p}$ space where the band gap is not small. At the closest approach of the bands, when $\Delta_{mm'} = \Delta(\boldsymbol{p}_M) \ll \varepsilon_0$, the estimate $|\partial\Delta_{mm'}/\partial\boldsymbol{p}| \sim v_0$ is not affected, since the Fermi surface has an anomalous curvature. Then the perturbation is $\delta E \sim \hbar\omega_c\varepsilon_0/\Delta_{mm'} \gg \hbar\omega_c$, and the criterion $\delta E \geqslant \Delta_{mm'}$ becomes

$$\hbar\omega_c \geqslant \frac{\Delta^2}{\varepsilon_0}. \tag{22}$$

† This is an analogue of predissociation of molecules [84].

Since the ratio Δ/ε_0 can frequently be less than 0.01, the criterion (22) imposes much less stringent constraints on the magnetic field and ensures that the breakdown field

$$H_0 \approx \frac{c\Delta^2}{e\hbar v_0^2} \tag{23}$$

can readily be achieved in experiments. For example, $\Delta \approx 10^{-2}$ eV corresponds to $H_0 \approx 10-100$ kG. A rigorous analysis (without allowance for the SOC) gives [5, 14, 45]

$$H_0 = \frac{\pi}{4} \frac{c\Delta^2}{e\hbar v^x v^y_{1,2}}, \tag{24}$$

where $v^y_{1,2}$ is the interband matrix element of the operator representing a component of the conduction-electron velocity perpendicular to the field $\boldsymbol{H}$ (the subscripts 1 and 2 are the numbers of the bands which are coupled by MB). All the quantities in formula (24) are determined at the MB point.

It follows that expression (23) gives the correct order of magnitude of H_0. It also makes it possible to find the width δp of the MB region in the $\boldsymbol{p}$ space where interband transitions take place (Fig. 2b) and which is very small (of the order of Δ/v_0). The time needed for an electron to cross this region $\delta t \approx \hbar/\Delta = (\kappa)^{-1/2}\omega_c^{-1}$ is also small. Hence, we can regard the MB region in the $p_z = \text{const}$ plane as a zero-dimensional point (Fig. 2c). An electron following a semiclassical path described by expression (8) associated with a given band has a nonzero probability (2) of transition to a semiclassical orbit in another band. The probability that a conduction electron remains in its own band is equal to $1 - w$. We shall show later that taking the SOC into account adds one more MB channel: it represents an interband transition of a conduction electron to an adjacent band, accompanied by spin flip; its probability is w^s, given by expression (3).

2.3 Effects of the spin degrees of freedom of conduction electrons in magnetic breakdown regions

A consistent inclusion of the spin degrees of freedom of conduction electrons in the band theory of metals is usually carried out in two stages. The energy spectrum and the wave functions of conduction electrons are found in the absence of a magnetic field, but taking the SOC into account; next, when these functions are known, the spin splitting of the levels induced by a magnetic field is calculated.

We shall not consider the relevant fairly complex theory (for details, the reader is directed to Jafet's review [10] and to the books of Bir and Pikus [59] and of Gantmakher and Levinson [88], where the literature of the topic is given). We shall provide here only a relatively simple treatment which helps to understand the importance of inclusion of the SOC in studies of the properties of metals under the MB conditions and we shall estimate the characteristic energy of the interaction in the MB regions.

We shall consider a conduction electron in $\boldsymbol{H} = 0$ in the presence of the SOC. The one-particle Schrodinger equation can be written as follows [11, 59]:

$$\begin{aligned} &\hat{H}(\boldsymbol{p})\, u_{mp\sigma}(\boldsymbol{r}) = \varepsilon_{m\sigma}(\boldsymbol{p})\, u_{mp\sigma}(\boldsymbol{r}), \\ &\hat{H}(\boldsymbol{p}) = \exp\left(-\frac{\mathrm{i}\boldsymbol{p}\cdot\boldsymbol{r}}{\hbar}\right)\hat{H}\exp\frac{\mathrm{i}\boldsymbol{p}\cdot\boldsymbol{r}}{\hbar}. \end{aligned} \tag{25}$$

Here, $\hat{H} = \hat{H}_0 + \hat{H}_{s\text{-}o}$ is the complete Hamiltonian of a conduction electron, where

$$\hat{H}_0 = \frac{\hat{p}^2}{2m} + V(\boldsymbol{r}), \tag{26a}$$

whereas

$$\hat{H}_{s\text{-}o} = \frac{\hbar}{(2mc)^2}[\hat{\sigma} \times \nabla V(\boldsymbol{r})]\cdot\hat{\boldsymbol{p}} \tag{26b}$$

is the Hamiltonian of the spin–orbit interaction which has the same translation properties as the periodic field of a crystal $V(\boldsymbol{r})$.

The quasimomentum $\boldsymbol{p}$ occurs in the system (25) as a parameter. In the presence of the SOC the Bloch factor $u_{mp\sigma}(\boldsymbol{r})$ of the stationary wave function

$$\Psi_{mp\sigma}(\boldsymbol{r}) = \exp\frac{i\boldsymbol{p}\cdot\boldsymbol{r}}{\hbar}\, u_{mp\sigma}(\boldsymbol{r}) \tag{27}$$

becomes a spinor [10, 88]:

$$u_{mp\sigma}(\boldsymbol{r}) = \begin{pmatrix} \lambda_{mp\sigma}(\boldsymbol{r}) \\ \mu_{mp\sigma}(\boldsymbol{r}) \end{pmatrix}. \tag{28}$$

We shall assume that $|\lambda_{mp\sigma}(\boldsymbol{r})| > |\mu_{mp\sigma}(\boldsymbol{r})|$ [10]. Then, the eigenvalue of the Pauli matrix $\langle\sigma_z\rangle_{\uparrow,\uparrow}$ is finite:

$$\langle\Psi_{mp\uparrow}|\hat{\sigma}_z|\Psi_{mp\uparrow}\rangle > 0.$$

In the case of normal metals in the absence of a magnetic field and when the SOC is ignored, each energy level found from the Schrodinger equation is doubly spin-degenerate. In the presence of the SOC, this degeneracy is retained for centrosymmetric metals:

$$\varepsilon_{m\uparrow}(\boldsymbol{p}) = \varepsilon_{m\downarrow}(\boldsymbol{p}) = \varepsilon_m(\boldsymbol{p}). \tag{29}$$

The symmetry of the Schrodinger equation under time reversal and space inversion means that the wave functions of conduction electrons $\Psi_{mp\uparrow}(\boldsymbol{r})$ and $\Psi_{mp\downarrow}(\boldsymbol{r})$ are coupled by the conjugation operation $\hat{C}$:

$$\Psi_{mp\downarrow} = \pm\hat{C}\Psi_{mp\uparrow}, \quad \Psi_{mp\uparrow} = \mp\hat{C}\Psi_{mp\downarrow}, \quad \hat{C} = i\hat{\sigma}_y\hat{T}\hat{K}. \tag{30}$$

Here, $\hat{T}$ and $\hat{K}$ are, respectively, the space inversion and complex conjugation operators. A unit cell is selected in such a way that the centre of inversion of a centrosymmetric metal coincides with the point $\boldsymbol{r} = 0$. The plus and minus signs depend on the parity of the wave function of a conduction electron at the centre of the mth band [10]: the upper (plus) sign corresponds to an even function and the lower (minus) sign to an odd function. It should be pointed out that physically significant results should be independent of the selection of the signs in the definitions given by expression (30).

In accordance with the terminology of Ref. [10], a conduction electron state described by formula (29) is called 'nondegenerate', because random degeneracy or crossing of the energy levels is still possible at some point of the $\boldsymbol{p}$ space. This degeneracy or crossing of levels is associated with the crystal symmetry and the situation is then called 'degenerate'.

In this case the SOC can lift the degeneracy and alter drastically the electron energy spectrum. In general, the degree of influence of the SOC on the band spectrum and on the wave functions of conduction electrons depends on the ratio of the characteristic interaction energy $\varepsilon_{s\text{-}o}$ to the width of the forbidden band in the absence of a magnetic field

$$\Delta^0_{mm'}(\boldsymbol{p}) = |\varepsilon^0_{m\sigma}(\boldsymbol{p}) - \varepsilon^0_{m'\sigma}(\boldsymbol{p})|, \tag{31}$$

where $\varepsilon^0_{m\sigma}(\boldsymbol{p})$ is the eigenenergy of the Hamiltonian (26a). For example, if $\varepsilon_{s\text{-}o} \ll \Delta^0_{mm'} \sim \varepsilon_0$, the SOC has little influence on the spectrum in this part of the $\boldsymbol{p}$ space and we can assume that the width of the interband gap (20) is of the order of the width of the forbidden band: $\Delta_{mm'}(\boldsymbol{p}) \sim \Delta^0_{mm'}(\boldsymbol{p})$. Therefore, in calculations of the energy band structure subject to the SOC it is usual to employ perturbation theory (see, for example, Refs [59, 81, 89–91]). This applies also to MB metals (Zn, Mg, Be, Al, etc.) when the characteristic SOC energy $\varepsilon_{s\text{-}o}$ is usually much less than the Fermi energy ε_F.

In the first order of perturbation theory in $\hat{H}_{s\text{-}o}$ the wave function $\Psi_{mp\sigma}$ is given by

$$\Psi_{mp\sigma} = \Psi^0_{mp\sigma} + \sum_{m'\neq m,\,\sigma} \frac{\langle m\sigma|\hat{H}_{s\text{-}o}|m'\sigma'\rangle}{\varepsilon^0_{m\sigma}(\boldsymbol{p}) - \varepsilon^0_{m'\sigma'}(\boldsymbol{p})}\, \Psi^0_{m'p\sigma'}. \tag{32}$$

Here, $\Psi^0_{mp\sigma} = \Psi^0_{mp}\,\chi^0_\sigma$ is the eigenfunction of the ground-state Hamiltonian. Since in the case of real metals the SOC is determined by the processes which occur inside the ions [50, 90], in estimates we can replace a matrix element of $\hat{H}_{s\text{-}o}$ based on the Bloch functions with the matrix element of the atomic Hamiltonian of the SOC based on atomic wave functions. In other words, the Bloch functions can be represented in the form of orthogonalised plane waves or augmented plane waves [81, 90, 92]. Then the energy $\varepsilon_{s\text{-}o}$ is replaced with the SOC energy for the relevant level in an atom of a metal in the relevant crystal.

Therefore, if $\varepsilon_{s\text{-}o} \ll \Delta(\boldsymbol{p})$, it follows from formula (32) that in this approximation

$$\left|\frac{\mu_{p\uparrow}}{\lambda_{p\uparrow}}\right| \approx \frac{\varepsilon_{s\text{-}o}}{\Delta(\boldsymbol{p})}. \tag{33}$$

The relative value of the SOC correction to the energy of the ground-state Hamiltonian is of the order of $(v_0/c)\,f(Z)$, where $f(Z)$ is a rising function of the atomic number Z. Since the velocity is $v_0 \sim 10^6$ m s^{-1}, it follows that this energy is usually of the order of 10^{-2}–10^{-3} eV [10, 13]. This is obviously a small effect, but it may be significant if we are dealing with the SOC lifting of the level degeneracy in a given part of the $\boldsymbol{p}$ space.

If $\varepsilon_{s\text{-}o} \approx \Delta(\boldsymbol{p})$, we can find $\lambda_{p\uparrow}$ and $\mu_{p\uparrow}$ provided we solve the appropriate secular equation, the form of which depends on the band structure of the metal [59, 81, 90, 91]. Then $\mu_{p\uparrow}$ can become of the order of $\lambda_{p\uparrow}$ and for $\Delta^0(\boldsymbol{p}) = 0$ the SOC may lift degeneracy, i.e. we may find that $\Delta(\boldsymbol{p}) \neq 0$.

It follows from these estimates that in the parts of the $\boldsymbol{p}$ space where inequality (20) is obeyed and $\varepsilon_{s\text{-}o} \approx \Delta(\boldsymbol{p})$, the SOC influences significantly the wave functions and the structure of the conduction-electron band spectrum. Turning back to the MB problem, we can say that a region of the $\boldsymbol{p}$ space, 'susceptible' to MB, is also 'susceptible' to the influence of the SOC. The degree of influence of the SOC on the spectrum of conduction electrons can be judged indirectly on the basis of the g factor of these electrons. An estimate $\Delta g(\boldsymbol{p})/g_0 = (g(\boldsymbol{p}) - g_0)/g_0$ gives the same result as that obtained from expression (33) [10, 81, 89].

2.4 Spectrum of conduction electrons for $\boldsymbol{H} = \boldsymbol{0}$ in magnetic breakdown regions

We shall now consider in greater detail the conduction electron spectrum subject to the SOC when $\boldsymbol{H} = \boldsymbol{0}$ inside a region is 'susceptible' to MB [9]. This is essential to the

derivation of the effective Hamiltonian which describes interband transitions in a magnetic field. It is also necessary to find the regions of the $\boldsymbol{p}$ space where the interband gap is minimal.

Let us assume that two bands approach each other closely in the vicinity of some point $\boldsymbol{p}'$ when $\boldsymbol{H}=\boldsymbol{0}$ and that $\Delta(\boldsymbol{p}') \ll \varepsilon_0$. Since for a given $\boldsymbol{p}'$ we find that $u_{mp'\sigma}(\boldsymbol{r})$ gives rise to a complete set of orthonormalised functions, we can expand $u_{mp\sigma}(\boldsymbol{r})$ in terms of these functions at any other point $\boldsymbol{p}$:

$$u_{mp\sigma}(\boldsymbol{r}) = \sum_{m',\sigma'} R_{m\sigma,m'\sigma'}(\boldsymbol{p}|\boldsymbol{p}')\, u_{m'p'\sigma'}(\boldsymbol{r}),$$
$$R_{m\sigma,m'\sigma'}(\boldsymbol{p}|\boldsymbol{p}') = \langle u_{m'p'\sigma'}|u_{mp\sigma}\rangle\,. \tag{34}$$

In a small region near the point $\boldsymbol{p}'$ ($|\delta\boldsymbol{p}| \ll p_0$, $\delta\boldsymbol{p} = \boldsymbol{p} - \boldsymbol{p}'$) we can ignore the influence of the other bands:

$$R_{m\sigma,m'\sigma'}(\boldsymbol{p}|\boldsymbol{p}') \sim \begin{cases} 1, & m,\, m' = 1,\, 2, \\ O\left(\dfrac{|\delta\boldsymbol{p}|}{p_0}\right), & m,\, m' \neq 1,\, 2. \end{cases} \tag{35}$$

We are assuming here specifically that two anomalously approaching bands have the numbers $m = 1,\ 2$.

The smallness of $\delta\boldsymbol{p}$ together with Eqns (25) and (26) can be used to write down the following expansion for $\hat{H}(\boldsymbol{p})$:

$$\hat{H}(\boldsymbol{p}) = \hat{H}(\boldsymbol{p}') + \hat{\boldsymbol{v}}(\boldsymbol{p}')\,\delta\boldsymbol{p} + O\left(\frac{|\delta\boldsymbol{p}|^2}{p_0^2}\right), \tag{36}$$

where

$$\hat{\boldsymbol{v}}(\boldsymbol{p}) = \exp\left(-\frac{\mathrm{i}\boldsymbol{p}\cdot\boldsymbol{r}}{\hbar}\right)\hat{\boldsymbol{v}}\exp\frac{\mathrm{i}\boldsymbol{p}\cdot\boldsymbol{r}}{\hbar},$$
$$\hat{\boldsymbol{v}} = \frac{\mathrm{i}}{\hbar}\,[\hat{H}\times\hat{\boldsymbol{r}}] = \frac{\hat{\boldsymbol{p}}}{m} + \frac{\mathrm{i}}{\hbar}\,[\hat{H}_{\mathrm{s\text{-}o}}\times\hat{\boldsymbol{r}}] \tag{37}$$

is the operator representing the velocity of conduction electrons when $H = 0$. Substitution of expressions (34) and (37) into the Schrodinger equation (25) and application of the conditions (35) leads to the following system of four equations for $R_{m\sigma,m'\sigma'}(\boldsymbol{p}|\boldsymbol{p}')$:

$$\sum_{m',\sigma'}\left\{\left[\varepsilon_{m',\sigma'}(\boldsymbol{p}') - E\right]\delta_{m',m''}\delta_{\sigma',\sigma''} + \boldsymbol{v}_{m''\sigma'',m'\sigma'}(\boldsymbol{p}')\,\delta\boldsymbol{p}\right\} \times R_{m\sigma,m'\sigma'}(\boldsymbol{p}|\boldsymbol{p}') = 0\,. \tag{38}$$

Here, ($m,\ m',\ m'' = 1,\ 2$)

$$E = \varepsilon_{m\sigma}(\boldsymbol{p}), \quad \boldsymbol{v}_{m\sigma,m'\sigma'}(\boldsymbol{p}) = \langle u_{mp\sigma}\,|\hat{\boldsymbol{v}}(\boldsymbol{p})|\,u_{m'p\sigma'}\rangle.$$

Symmetry in respect of the wave-function conjugation $\hat{C}$ described by expression (30) imposes the following restrictions on the matrix elements $\hat{\boldsymbol{v}}(\boldsymbol{p})$:

$$\boldsymbol{v}_{m\uparrow,m\uparrow} = \boldsymbol{v}_{m\downarrow,m\downarrow}, \quad \boldsymbol{v}_{m\uparrow,m\downarrow} = \boldsymbol{v}_{m\downarrow,m\uparrow} = 0\,.$$

The matrix $\hat{\boldsymbol{v}}(\boldsymbol{p})$ now becomes

$$\hat{\boldsymbol{v}} = \begin{bmatrix} \boldsymbol{v}_{1,1}(\boldsymbol{p}) & 0 & \boldsymbol{c}(\boldsymbol{p}) & \boldsymbol{d}(\boldsymbol{p}) \\ 0 & \boldsymbol{v}_{1,1}(\boldsymbol{p}) & \mp\boldsymbol{d}(\boldsymbol{p}) & \pm\boldsymbol{c}(\boldsymbol{p}) \\ \boldsymbol{c}(\boldsymbol{p}) & \mp\boldsymbol{d}(\boldsymbol{p}) & \boldsymbol{v}_{2,2}(\boldsymbol{p}) & 0 \\ \boldsymbol{d}(\boldsymbol{p}) & \pm\boldsymbol{c}(\boldsymbol{p}) & 0 & \boldsymbol{v}_{2,2}(\boldsymbol{p}) \end{bmatrix} \tag{39}$$

where the matrix elements are described by ($m = 1,\ 2$)

$$\boldsymbol{v}_{m,m}(\boldsymbol{p}) = \boldsymbol{v}_{m\sigma,m\sigma}(\boldsymbol{p}),\ \boldsymbol{c}(\boldsymbol{p}) = \boldsymbol{v}_{1\uparrow,2\uparrow}(\boldsymbol{p}),\ \boldsymbol{d}(\boldsymbol{p}) = \boldsymbol{v}_{1\uparrow,2\downarrow}(\boldsymbol{p}). \tag{40}$$

The upper signs in the matrix (39) correspond to the same parity of the conduction-electron wave functions and the lower ones correspond to different parities.

In accordance with the comments made immediately after expression (29), the results obtained below are independent of the selection of the signs in the matrix (39). Therefore, we shall omit the lower signs. Invariance of $\hat{H}$ under the space inversion operation $\hat{T}$ makes it possible to select the phase factors of the wave functions so that $\mathrm{Im}\,\boldsymbol{c}(\boldsymbol{p}) = \mathrm{Im}\,\boldsymbol{d}(\boldsymbol{p}) = \boldsymbol{0}$ at all points of the $\boldsymbol{p}$ space [45, 68].

It follows that inclusion of the SOC gives rise, in the matrix (39), to elements of the conduction-electron velocity operator which are off-diagonal in respect of the spin and band number. The existence of such matrix elements, i.e. elements characterised by $\boldsymbol{d}(\boldsymbol{p}) \neq \boldsymbol{0}$, leads in turn to the appearance of the probability of spin-flip MB. Therefore, it would be desirable to estimate the value of such a matrix element.

If $\varepsilon_{\mathrm{s\text{-}o}} \ll \Delta(\boldsymbol{p})$, we can use formulas (32) and (33) to obtain an estimate of $\boldsymbol{d}(\boldsymbol{p})$ from the main term of the velocity operator $\hat{\boldsymbol{p}}/m$ in expression (37):

$$|\boldsymbol{d}(\boldsymbol{p})| \approx \frac{\varepsilon_{\mathrm{s\text{-}o}} v_0}{\Delta(\boldsymbol{p})}, \tag{41}$$

where v_0 is the characteristic velocity of conduction electrons. If $\varepsilon_{\mathrm{s\text{-}o}} \geqslant \Delta^0_{mm'}(\boldsymbol{p})$, the estimate given by the above expression is naturally invalid and the modulus of the element $\boldsymbol{d}(\boldsymbol{p})$ can become of the order of v_0. In the absence of the SOC the matrix (39) splits into two independent matrices of second rank† and the system of equations (38) is transformed into two independent systems of two equations for each orientation of the spin of conduction electrons. In this limit, we obtain the results reported in Refs [6, 45].

If the determinant of the system of equations (38) is equated to zero, the result is the spectrum of conduction electrons near the point $\boldsymbol{p}'$ (we recall that $\boldsymbol{p} = \boldsymbol{p}' + \delta\boldsymbol{p}$):

$$\varepsilon_{1\uparrow,2\uparrow}(\boldsymbol{p}) = \varepsilon_{1\downarrow,2\downarrow}(\boldsymbol{p}) = \frac{1}{2}\sum_m \varepsilon_m(\boldsymbol{p}') + \frac{1}{2}\sum_m \boldsymbol{v}_{m,m}(\boldsymbol{p}')\cdot\delta\boldsymbol{p}$$
$$\pm\sqrt{\frac{1}{4}[\Delta(\boldsymbol{p}') + \boldsymbol{b}(\boldsymbol{p}')\cdot\delta\boldsymbol{p}]^2 + [\boldsymbol{c}(\boldsymbol{p}')\cdot\delta\boldsymbol{p}]^2 + [\boldsymbol{d}(\boldsymbol{p}')\cdot\delta\boldsymbol{p}]^2}, \tag{42}$$

where $\boldsymbol{b} = \boldsymbol{v}_{1,1} - \boldsymbol{v}_{2,2}$, $\Delta(\boldsymbol{p}') = \varepsilon_1(\boldsymbol{p}') - \varepsilon_2(\boldsymbol{p}')$. Obviously, for $\boldsymbol{H} = \boldsymbol{0}$ the spectrum remains doubly degenerate in spin.

The smallness of $\Delta(\boldsymbol{p}')$ in the spectrum (42) means that the dispersion law $\varepsilon_{m\sigma}(\boldsymbol{p})$ (and the corresponding Bloch factors) in the vicinity of $\boldsymbol{p}'$ are 'peaked' functions of the argument: a characteristic interval of their variation is less than $(\Delta/\varepsilon_0)p_0$ (for details see Refs [9, 45]). In an analysis of the behaviour of conduction electrons in MB regions when $H \neq 0$ we shall need functions which vary smoothly with at least one component of $\boldsymbol{p}$. In this case the effective Hamiltonian for an MB region can be found with the aid of modified Kohn– Luttinger functions [45]. Such functions are $\varepsilon_{m\sigma}(\boldsymbol{p})$ [and the corresponding factors are $u_{mp\sigma}(\boldsymbol{r})$], where $\boldsymbol{p}$ belongs to the part of the $\boldsymbol{p}$ space near $\boldsymbol{p}'$ where $\Delta(\boldsymbol{p}) = \varepsilon_{1\sigma}(\boldsymbol{p}) - \varepsilon_{2\sigma}(\boldsymbol{p})$ has its minimum.

† This becomes clear if, for $\boldsymbol{d}(\boldsymbol{p}) = \boldsymbol{0}$, we interchange the first and third rows, as well as the first and third columns, in the initial matrix. This gives rise to a block-diagonal matrix and each nonzero block then

It has been shown in Ref. [9] that the topology of the region of 'minimal Δ' depends strongly on the mutual orientation of the vectors $\boldsymbol{b}$, $\boldsymbol{c}$, and $\boldsymbol{d}$, which occur in the spectrum (42) and represent the matrix elements of the operator of the conduction electron velocity. The minimum of $\Delta(\boldsymbol{p})$ corresponds to the minimum of the radicand in the spectrum (42), which is governed by a system of linear algebraic equations

$$\boldsymbol{b}(\boldsymbol{p}')\cdot\delta\boldsymbol{p} + 4\boldsymbol{c}(\boldsymbol{p}')\cdot\delta\boldsymbol{p} + 4\boldsymbol{d}(\boldsymbol{p}')\cdot\delta\boldsymbol{p} = -\Delta(\boldsymbol{p}')\,\boldsymbol{b}(\boldsymbol{p}') \qquad (43)$$

with the unknowns δp_x, δp_y and δp_z.

Since the various projections of the matrix elements of the vector operator of the conduction electron velocity (39) can be calculated quite independently, it follows that generally there are no restrictions on the relative orientations of the vectors $\boldsymbol{b}$, $\boldsymbol{c}$, and $\boldsymbol{d}$, defined by expressions (40) and (42). In general, these vectors should be linearly independent. There is a unique solution of the system (43): it is a point of degeneracy in the $\boldsymbol{p}$ space (we shall call it $\boldsymbol{p}_{\mathrm{T}}$), defined by intersection of three planes:

$$\boldsymbol{b}(\boldsymbol{p}')\cdot\delta\boldsymbol{p} = -\Delta(\boldsymbol{p}'), \quad \boldsymbol{c}(\boldsymbol{p}')\cdot\delta\boldsymbol{p} = 0, \quad \boldsymbol{d}(\boldsymbol{p}')\cdot\delta\boldsymbol{p} = 0. \qquad (44)$$

At the point of degeneracy the value of $\Delta(\boldsymbol{p}_{\mathrm{T}})$ vanishes. This type of spectrum will be discussed later and at this stage we note that such a spectrum cannot appear in the absence of the SOC.

We shall consider in greater detail the cases when the determinant of the system (43) vanishes, i.e. when the vectors $\boldsymbol{b}$, $\boldsymbol{c}$, and $\boldsymbol{d}$ are linearly interdependent. The simplest and easiest to understand, from the point of view of physics, is the case when the vectors $\boldsymbol{b}$, $\boldsymbol{c}$, and $\boldsymbol{d}$ are collinear. It follows from the spectrum (42) that in this case we have $\varepsilon_0 \gg \Delta(\boldsymbol{p}) > 0$, everywhere near the point $\boldsymbol{p}'$ and the minimum of $\Delta(\boldsymbol{p})$ occurs in the plane of the closest approach of the bands [9], which we shall call the M plane [45]:

$$\boldsymbol{b}(\boldsymbol{p}')\cdot\delta\boldsymbol{p} = -\frac{\Delta(\boldsymbol{p}')\,|\boldsymbol{b}(\boldsymbol{p}')|^2}{|\boldsymbol{b}(\boldsymbol{p}')|^2 + 4|\boldsymbol{c}(\boldsymbol{p}')|^2 + 4|\boldsymbol{d}(\boldsymbol{p}')|^2}.$$

Since the pseudopotential of many metals is small, such a spectrum is frequently encountered. The M plane coincides with the boundary of the Brillouin zone [11, 50, 90, 92].

In Ref. [50] the smallness of the pseudopotential (but in this case compared with the SOC) is used as the argument for a strong influence of the SOC on the electron spectrum in the MB regions of Zn, Mg, and other hexagonal metals. The spectrum derived above can appear as a result of other mechanisms, such as doubling of one of the periods of the metal lattice as a result of a small displacement of its atoms [93].

Fig. 5a shows the approximate form of the constant-energy surface $\varepsilon_{m\sigma}(\boldsymbol{p}) = E$ near the M plane. In this region the dispersion law (42) is modified to

$$\varepsilon_{1\sigma,2\sigma}(\boldsymbol{p}) = \frac{1}{2}\sum_m \varepsilon_m(\boldsymbol{p}_{\mathrm{M}}) + \frac{1}{2}\sum_m v^n_{m,m}(\boldsymbol{p}_{\mathrm{M}})\delta p_n \pm \sqrt{\frac{1}{4}[\Delta(\boldsymbol{p}_{\mathrm{M}})]^2 + [c^n(\boldsymbol{p}_{\mathrm{M}})\delta p_n]^2(1+\alpha^2)}\,. \qquad (45)$$

Here, $\delta p_n = \boldsymbol{n}(\boldsymbol{p} - \boldsymbol{p}_{\mathrm{M}})$, $\alpha = |d^n(\boldsymbol{p}_{\mathrm{M}})/c^n(\boldsymbol{p}_{\mathrm{M}})|$, the point $\boldsymbol{p}_{\mathrm{M}}$ lies in the M plane, and $\boldsymbol{n}$ is a unit vector along the normal to the M plane, which makes an angle $\pi/2 - \theta$ with the magnetic field $\boldsymbol{H}$.

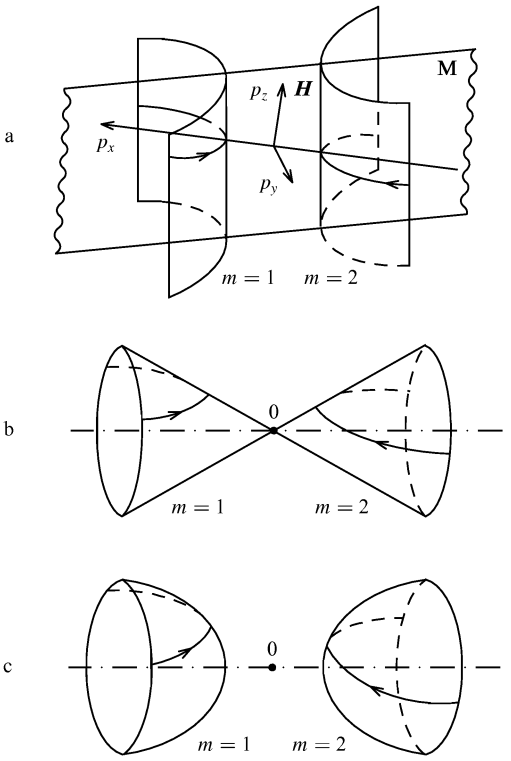

Figure 5. Schematic representation of the constant-energy surfaces in the region of anomalous approach of two bands: (a) spectrum of the M-plane type; the field H is inclined at an angle θ to the M plane; (b) spectrum of the p_0-line type, where the point 0 is the $p_0(E)$ point of degeneracy; (c) spectrum of the p_Δ-line type, where the point 0 is the $p_\Delta(E)$ point with the minimum interband gap. The arrows identify the directions of motion of conduction electrons along orbits described by expression (8). The spin splitting is not shown for the sake of clarity.

It should be noted that the functions $\varepsilon_{m\sigma}(\boldsymbol{p}_{\mathrm{M}})$ and $u_{m\boldsymbol{p}_{\mathrm{M}}\sigma}$ ($m = 1, 2$) now vary smoothly with $\boldsymbol{p}_{\mathrm{M}}$ and the interval of their variation in the M plane is of the order of p_0. Moreover, the smallest distance between the orbits $\varepsilon_{1\sigma}(\boldsymbol{p}) = E$, $p_z = p_{z0}$ and $\varepsilon_{2\sigma}(\boldsymbol{p}) = E$, $p_z = p_{z0}$ occurs at the point of their intersection with the M plane, where $\delta p(E, p_z) \sim \Delta/v_0$ is a smooth function of its arguments. We can see that the influence of the SOC reduces to the appearance of a renor-malisation factor $1 + \alpha^2$ in the radicand [compare formula (45) with the corresponding formula in Ref. [45]].

One more type of spectrum is predicted by the theory of MB [6, 45] in the case when the vectors $\boldsymbol{b}$, $\boldsymbol{c}$, and $\boldsymbol{d}$ are coplanar in such a way that $\boldsymbol{c} \parallel \boldsymbol{d}$, and $\boldsymbol{b}$ is not parallel to the other two. It readily follows from expressions (42) and (43) that in this case $\Delta(\boldsymbol{p})$ vanishes on the line of intersection of two planes:

$$\boldsymbol{b}(\boldsymbol{p}')\cdot\delta\boldsymbol{p} = -\Delta(\boldsymbol{p}'), \quad \boldsymbol{c}(\boldsymbol{p}')\cdot\delta\boldsymbol{p} = 0,$$

when this line passes near the point $\boldsymbol{p}'$.

If the constant-energy surface $\varepsilon_{m\sigma}(\boldsymbol{p}) = E$ is intersected by such an 'obligatory' degeneracy line [11] (called the $\boldsymbol{p}_0$ line in Ref. [45]), then parts of this line near the point of intersection form an elliptic cone (Fig. 5b). It should be noted that the inclusion of the SOC leads in this case to the appearance of the same renormalisation factor $1 + \alpha^2$ [see expression (45)] and does not lift the degeneracy. The sheets of the cone corresponding to different bands are separated

by a conical point $\boldsymbol{p}_0$ where $\varepsilon_1(\boldsymbol{p}_0) = \varepsilon_2(\boldsymbol{p}_0) = E$. This case is discussed in detail in Refs [6, 45, 68].

A qualitatively new type of spectrum appears if we assume that the vectors $\boldsymbol{b}$, $\boldsymbol{c}$, and $\boldsymbol{d}$ are in the same plane, but none of them are parallel. In this case it is important that $\boldsymbol{d}(\boldsymbol{p}) \neq \boldsymbol{0}$. We then have $\Delta(\boldsymbol{p}) \neq 0$ everywhere near the point $\boldsymbol{p}'$ and the minimum of $\Delta(\boldsymbol{p})$ occurs on the line of anomalous approach of the planes (which we can call the p_Δ line). If $\boldsymbol{b}$ is expressed in terms of $\boldsymbol{c}$ and $\boldsymbol{d}$, it is found that simple transformations of the system of equations (43) yield equations for two planes and the p_Δ line is the intersection of these planes. The first plane is described by the equation

$$\boldsymbol{c}\cdot\delta\boldsymbol{p} = -\frac{\Delta(\boldsymbol{p}')\,[\boldsymbol{c}\times\boldsymbol{d}]\,[\boldsymbol{b}\times\boldsymbol{d}]\,|[\boldsymbol{c}\times\boldsymbol{d}]|^2}{|[\boldsymbol{c}\times\boldsymbol{d}]\cdot[\boldsymbol{b}\times\boldsymbol{d}]|^2+|[\boldsymbol{c}\times\boldsymbol{d}]\cdot[\boldsymbol{b}\times\boldsymbol{c}]|^2+16|[\boldsymbol{c}\times\boldsymbol{d}]|^2},$$

where all the quantities are taken at the point $\boldsymbol{p}'$. The equation for the second plane differs from the above by the transposition $\boldsymbol{c} \leftrightarrow \boldsymbol{d}$ and by the opposite sign in front of the fraction.

The constant-energy surface near the p_Δ line is described by the equation for a two-sheet hyperboloid and the point itself with the minimum interband gap $p_\Delta = p_\Delta(E)$ is located between two sheets of this figure (Fig. 5c). A spectrum of this type can appear because of lifting of the degeneracy by the SOC along any line of symmetry.

We shall consider the spectrum (43) of the type encountered at the point $\boldsymbol{p}_\mathrm{T}$. The point $\boldsymbol{p}_\mathrm{T}$ lies on the constant-energy surface $\varepsilon_{m\sigma}(\boldsymbol{p}) = E$ only when the energy has the critical value $E = E_{\mathrm{cr}}$. In this case the point becomes conical and the spectrum is identical with that considered for the p_0 line. However, in general, the spectrum is of the 'neck-breaking' type [11, 12] and the situation depends strongly on the energy E (for conduction electrons participating in MB this energy is $E = \varepsilon_\mathrm{F}$). If the neck is broken, then for $E \neq E_{\mathrm{cr}}$ the spectrum near the point $\boldsymbol{p}_\mathrm{T}$ can be approximated by the equation for a two-sheet hyperboloid, but in contrast to the p_Δ line, a further increase in $|E - E_{\mathrm{cr}}|$ increases strongly the interband gap $\Delta(\boldsymbol{p}_\mathrm{T})$. If the neck 'thickens', the spectrum is described by the equation for a one-sheet hyperboloid which is contained entirely within a single Brillouin zone.

We have thus here the case of the electron topological Lifshitz transition [11, 12] with a conical point, which makes this case interesting for the study of the magnetic properties of conduction electrons as a function of the external pressure or of the alloy composition.† The influence of the conical point on MB under the conditions of the Lifshitz transition has been considered by Nedorezov [80]. In this review we shall assume that the energy E is fixed. In promising MB applications the spectrum of the $\boldsymbol{p}_\mathrm{T}$-point type, given by expression (43), reduces to a spectrum either of the p_0-line or the p_Δ-line type.

If we consider formally the semiclassical motion of conduction electrons in a magnetic field, we find that for all types of spectrum the orbits described by expression (8) with $\sigma = \mathrm{const}$ represent, in the regions of closest approach, different branches of the same hyperbola (Figs 5a–5c). In fact, the semiclassical equations (7) with the Hamiltonian (6) and wave functions (13) are inapplicable here. However, it has been shown [9, 45] that the smallness of the parameters κ and Δ/ε_0 makes it possible to generalise the correspondence principle (11) to the case of MB.

The most interesting, from the point of view of MB, and frequently encountered is the spectrum of the M-plane type. It readily follows from Fig. 5a that for this type of spectrum and a favourable direction of the magnetic field there is a fairly 'thick' layer of orbits along which conduction electrons can reach the MB region, since the minimum separation $\delta p \approx \Delta/v_0$ between the orbits associated with different bands depends very weakly on p_z. For all these conduction electrons the MB probability is significant. For example, magnesium is subjected to a magnetic field parallel to the hexagonal axis, the relative thickness of such a layer $\delta p_z^{\mathrm{MB}}/b_z$ can reach 0.14 [5] and this thickness is practically independent of the magnetic field.

In the case of the spectra corresponding to Figs 5b and 5c, the spacing $\delta p(E, p_z)$ increases rapidly as the plane $p_z = p_{z0}$ moves away from the symmetry axis. Consequently, the MB probability $w(p_z)$ decreases rapidly (in a given field). In other words, 'thin' MB layers are formed and their thickness depends on the magnetic field.

In exceptional cases even thin MB layers can give rise to giant oscillations of, for example, the static conductivity [6]. However, in general, the MB effects can be observed in practice if an MB layer is sufficiently thick (when the number of conduction electrons participating in MB is sufficiently large) or if MB layers are located near extremal sections of the Fermi surface. Therefore, we shall concentrate our attention on the spectrum of the M-plane type, especially as the structure of the s matrix is independent of the type of spectrum [9, 68].

The influence of the SOC on the spectrum of conduction electrons in a magnetic field ($\boldsymbol{H} \neq \boldsymbol{0}$) reduces qualitatively to the following. Far from the MB regions the semiclassical approximation works well and the spin degeneracy is lifted, as shown in Section 2.1. Pure spin states are then formed and their effective g factor is $g(\boldsymbol{p}) \approx g_0$ because in this case we have $\Delta(\boldsymbol{p}) \ll \varepsilon_0$. The spin degeneracy is also lifted in the MB region. If $\Delta(\boldsymbol{p}) \sim \varepsilon_{\mathrm{s-o}}$, mixed spin states belonging to different bands form in this small part of the $\boldsymbol{p}$ space. The semiclassical orbits of expression (8) with different spin directions and approaching closely one another are shown schematically in Fig. 2b.

2.5 The s matrix in the case of the spin–orbit coupling and an arbitrary dispersion law

When the spin degrees of freedom of conduction electrons are taken into account in a consistent manner in the theory of MB, it becomes necessary to calculate the principal dynamic characteristic of MB, which is the complete fourth-rank s matrix for an arbitrary dispersion law. Such a calculation is reported in Ref. [9] following generalisation of the rules for derivation of the effective Hamiltonian to the MB regions. We shall not go into details of calculation of the s matrix (details are given in Refs [9, 45, 94]), but instead we shall describe briefly how this matrix can be derived and we shall give the final expression in which the spin degrees of freedom are taken into account. All the expressions given below for the case when there is no SOC reduce to the familiar results presented in an earlier review [6].

The s matrix can be derived by finding, for $H \neq 0$, the effective Hamiltonian which determines the dynamics of conduction electrons in a nonsemiclassical region of charac-

†The position of the Fermi level can be altered by variation of these parameters.

teristic size $\delta p \ll p_0$ (Fig. 2b), where interband transitions of conduction electrons are important. Without loss of generality, we can avoid the change in the gauge of the vector potential in Section 2.1 by assuming that the M plane is intersected by the $p_z = p_z 0$ plane along the straight line $p_y = p_{My} = 0$ and the magnetic field $\boldsymbol{H}$ forms an angle θ with the M plane (Fig. 5a).

The s matrix can be written explicitly as a function of $\boldsymbol{H}$ and of the main parameters of the problem if the Schrodinger equation is investigated in a small region close to the point $p_{My} = 0$. After $p_y \leftrightarrow p_x$ redesignation of the axes, we can use here Fig. 2b. The appropriate Schrodinger equation for an MB region is obtained from the system of equations (38) if $\boldsymbol{p}$ is replaced with $\boldsymbol{P} - (e/c)\boldsymbol{A}$, $\boldsymbol{p}'$ with $\boldsymbol{p}_M$, the matrix elements $\boldsymbol{v}\delta\boldsymbol{p}$ with the matrix elements $v^y \delta p_y$ and $R_{m\sigma, m\sigma'}$ with $\beta_{m\sigma\sigma'}(\boldsymbol{P})$, where $\beta_{m\sigma}(\boldsymbol{P})$ are the coefficients in the expansion of a stationary wave function of conduction electrons in terms of the modified Kohn–Luttinger functions [95], in which the spin degrees of freedom are taken into account [9]:

$$\Psi^{KL}_{m\boldsymbol{P}\sigma} = u_{m; P_x + eHy/c,\, P_{My}, p_z; \sigma}(\boldsymbol{r}) \exp\left(\frac{i}{\hbar}\boldsymbol{P}\cdot\boldsymbol{r}\right).$$

Here the dependence on p_y occurs only in the exponential function and the dependence on P_x becomes smooth, since the P_x axis is parallel to the M plane.

The regions of validity of our quantum solutions and semiclassical functions (13) overlap. If we ignore a small quantum region, we obtain the s matrix relating the coefficients $c_{m\sigma}$ from the wave function (13) on opposite sides of an MB region. If the probability is $w \sim 1$, the size of the MB regions is of the order of $(\Delta/\varepsilon_0)p_0$, so that they can be replaced with MB nodes. A schematic representation of such an MB node is shown in Fig. 2c.

Each semiclassical section of an orbit (8) can be represented by a set $i_0\sigma$, where i_0 is the zero-spin number of that section [6], which depends on the band number m, and σ represents the orientation of the spin of conduction electrons in that section. In the presence of the SOC, the principal dynamic characteristic of MB (which is the s matrix) relates the amplitudes $c_{i_0\sigma}$ of eight semiclassical wave functions $\Psi_{i_0\sigma}$ at an MB node before and after the MB scattering [apart from the notation, these amplitudes are identical with those in the wave function (13)]:

$$c_{i_0\sigma} = \sum_{i_0'\sigma'} s_{i_0\sigma, i_0'\sigma'}\, c_{i_0'\sigma'}\,. \tag{46}$$

The primes denote the numbers of the semiclassical orbit sections which emerge from an MB node (Fig. 2c).

The matrix elements $s_{i_0\sigma, i_0'\sigma'}$ can be expressed in terms of the dispersion law [9] at the point of maximum breakdown $\boldsymbol{p}_M$ and can be written in the form

$$\hat{s} = \begin{bmatrix} \tau\exp(\mp i\Lambda) & 0 & \pm\rho/\beta & \pm\alpha\rho/\beta \\ 0 & \tau\exp(\mp i\Lambda) & \mp\alpha\rho/\beta & \pm\rho/\beta \\ \mp\rho/\beta & \pm\alpha\rho/\beta & \tau\exp(\pm i\Lambda) & 0 \\ \mp\alpha\rho/\beta & \mp\rho/\beta & 0 & \tau\exp(\pm i\Lambda) \end{bmatrix}, \tag{47}$$

where

$$\rho = \exp\left(-\frac{H_0}{2H}\right), \quad \rho^2 + \tau^2 = 1\,, \qquad \alpha = \left|\frac{d^y(\boldsymbol{p}_M)}{c^y(\boldsymbol{p}_M)}\right|, \quad \beta = (1+\alpha^2)^{1/2}. \tag{48}$$

The matrix elements of the velocity d^y and c^y, which are off-diagonal in respect of the band number, are defined by expression (40). It follows from formula (41) that if the influence of the SOC is strong, the parameter α in the second expression (48) is of the order of unity, but if the SOC is weak, then $0 \leqslant \alpha \ll 1$.

The phase shift Λ of the wave function (13) caused by MB is

$$\Lambda = \frac{\pi}{4} + \frac{H_0}{\pi H} + \arg\Gamma\left(\frac{H_0}{\pi H}\right) - \frac{H_0}{\pi H}\ln\frac{H_0}{\pi H}. \tag{49}$$

Here, $\Gamma(x)$ is the gamma function [96]. After breakdown, H_0 is renormalised by the SOC:

$$H_0 = \frac{\pi}{4}\,\frac{c\Delta^2}{e\hbar\beta\left|v^x v^n_{1,2}\cos\theta\right|} = \frac{H_0^0}{\beta}, \tag{50}$$

where the index n denotes the velocity component normal to the M plane and $H_0^0(p_z)$ is the characteristic breakdown field in the absence of the SOC ($\alpha = 0$, $\beta = 1$). This characteristic field depends smoothly on E and p_z, and also on θ, and it is practically identical with the field given by formula (24) if we bear in mind that $v^y = v^n \cos\theta$.

For the other types of the spectra corresponding to Fig. 5 there is no change in the structure of the s matrix. Only the expression for H_0 is different [6, 45, 68]. Belokolos [94] was the first to obtain the 4×4 s matrix: this was done by a group-theory approach to MB in a specific metal (thallium). However, the physical meaning of the matrix elements of the transitions is not stated in Ref. [94], although the general structure of the matrix derived there is identical with the structure of the matrix (47) which applies in the case of an arbitrary dispersion law [9].

The selection of the signs in the matrix (47) is determined by the sign of the difference

$$\varepsilon_{m\sigma}(\boldsymbol{p}_M) - \varepsilon_{m'\sigma}(\boldsymbol{p}_M), \quad m = m(i_0), \quad m' = m'(i_0')\,. \tag{51}$$

Here, m and m' are the serial numbers of the bands coupled by MB ($m \neq m'$). The upper signs in the matrix (47) correspond to the positive value of the difference in expression (51). It is evident from expression (47) that the probability of MB with spin flip of conduction electrons is

$$w^s = \left|s_{i_0\sigma, i_0'\sigma'}\right|^2 = \frac{\alpha^2}{1+\alpha^2}\,\exp\left(-\frac{H_0}{H}\right), \quad i_0 \neq i_0', \sigma \neq \sigma'\,. \tag{52}$$

The total probability of an interband transition [which should be compared with expressions (2) and (3)] is

$$w = w^0 + w^s = \rho^2 = 1 - \tau^2 = \exp\left(-\frac{H_0}{H}\right). \tag{53}$$

We must stress once again that this s matrix corresponds to *three-channel* scattering of conduction electrons. Spin flip of a conduction electron is forbidden if the electron remains in its own band. This follows from vanishing of the off-diagonal (in terms of the spin index) elements of the matrix (47) that belong to one band. It readily follows from the matrix (47) that in the absence of the SOC ($\alpha = 0$) the off-diagonal elements vanish. The s matrix then splits into two independent second-rank matrices for each orientation of the spin of conduction electrons [this can be demonstrated by a procedure described in a footnote following formula (3)]. Each such matrix is identical with the s matrix derived in Ref. [45].

3. Coherent magnetic breakdown

Mathematical formalism that takes account of the dual nature of the conduction electron dynamics, i.e. semiclassical motion along sections of an MB configuration and quantum scattering by MB nodes, is needed in the investigation of the properties of metals under MB conditions. It has been shown [6, 49] that the energy spectrum and macroscopic properties of a metal can be expressed in terms of semiclassical wave functions and s matrices. As pointed out earlier, the mathematical procedures used in the MB theory can be generalised quite simply, in the formal sense, to take account of the spin degrees of freedom and of the SOC. Therefore, a brief account of the formalism will be given here with stress on the features that arise from the inclusion of the SOC.

Interference processes are of decisive importance in the development of the mathematical formalism of the MB theory [18, 19]. Superposition of semiclassical wave functions (13) with different phases (15), the latter acquired by conduction electrons in different sections of an MB configuration, on multiple quantum scattering from MB nodes gives rise to an interference pattern which results in the appearance of a specific MB spectrum. When the influence of weakly inhomogeneous fields can be ignored, coherent effects appear and a steady MB spectrum is formed. This is known as the *coherent magnetic breakdown* [6].

A quantum interference pattern breaks down if an inhomogeneous perturbation is sufficiently strong to alter an increment of the action, described by expression (16), by an amount exceeding the Planck constant $\hbar$ in the time taken by an electron to travel along a section of an MB configuration. It follows that small-amplitude inhomogeneous fields influence very strongly the interference-type motion of a wave packet along an MB configuration but have practically no effect on the classical dynamics of conduction electrons in such a configuration [6, 57, 58].

The nature of motion of conduction electrons along an MB configuration depends strongly on the ratio of the characteristic times of the problems [6]:

$$\tau_{s.a} \gg \tau_p \gg T_c\,, \tag{54a}$$

$$\tau_p \gg \tau_{s.a} \gg T_c\,, \tag{54b}$$

$$\tau_p \gg T_c \gg \tau_{s.a}\,, \tag{54c}$$

$$T_c \gg \tau_p,\ \tau_{s.a}\,. \tag{54d}$$

Here, τ_p is the relaxation time of the momentum, governed by the electron – impurity scattering or by short-wavelength phonons [97]; $\tau_{s.a}$ is the small-angle scattering time;† $T_c = 2\pi/\omega_c$ is the characteristic time of motion of conduction electrons along a path in a magnetic field described by expression (17). In calculations that take account of the spin degrees of freedom we shall assume always that the spin relaxation time is much longer than any other characteristic time. This is true of pure metals at low temperatures [98, 99]. Therefore, spin flip of conduction electrons in the course of their motion along an MB configuration is solely due to MB scattering represented by the probability (52).

† The scattering of conduction electrons in weak inhomogeneous fields (due to dislocations, mosaic block boundaries, long-wavelength phonons, etc.), which is accompanied by small chnges in the quasimomentum $q_{s.a}$.

Coherent magnetic breakdown occurs when the inequalities (54a) and (54b) are satisfied. When the inequalities (54c) are obeyed, small-angle scattering destroys coherent interference when the electron dynamics becomes stochastic. The stochastisation field does not occur in the final expressions for the transport properties of a metal. All the phenomena which occur in this situation are called *stochastic magnetic breakdown.*

The inequalities in formula (54c) imply that one more inequality is also obeyed: $\tau^{tr}_{s.a} \sim \tau_{s.a}(p_0/q_{s.a})^2 \gg T_c$. This means that both the impurity and the small-angle scattering do not prevent conduction electrons from passing many times along a closed MB configuration until they are effectively scattered or from propagating for many periods along an open MB configuration.

When the inequality (54d) is satisfied, MB cannot be detected against the impurity scattering background resulting in interband transfer of conduction electrons.

3.1 Stationary wave function and motion of a wave packet along a magnetic breakdown configuration

The semiclassical theory of well-defined orbits on a Fermi surface, presented in Section 2.1, ceases to be valid under MB conditions. This theory can be used only in the limit of weak fields when MB does not appear. In the limit of very strong fields ($H \gg H_0$), when conduction electrons break through all the gaps, the influence of the SOC makes it necessary to take account of the probability of spin flip of conduction electrons, described by the matrix (47), in each such break-through (tunnelling) event. However, an intermediate situation, when features specific to both limiting cases are observed, is more typical. The semiclassical sections, described by expression (8), with oppositely oriented electron conduction spins, merge to form one MB configuration when $w^s \neq 0$ and the spin degrees of freedom are included. Each MB node now links eight semiclassical sections: four incoming and four outgoing (Fig. 2c).

The motion of conduction electrons along an MB configuration is described by the stationary wave function

$$\Psi = \sum_{i_0,\sigma}^{N_0} c_{i_0\sigma}\, \Psi_{i_0\sigma}(P_y)\, \delta_{p_{x0},p_x}\, \delta_{p_z,p_{z0}}\,, \tag{55}$$

which is a superposition of the wave functions $\Psi_{i_0\sigma}$ of separate sections, as described just before formula (46). The summation over i_0 in expression (55) is carried out up to N_0, which is the total number of inequivalent sections that occur in an MB configuration when the spin is ignored. Figs 1c, 3b, and 4 show schematically some MB configurations.

The requirement that the wave function (55) be unique imposes conditions on the amplitudes $c_{i_0\sigma}$. These amplitudes should satisfy the following system of linear equations:

$$c_{i_0\sigma} - \sum_{i'_0,\sigma'}^{N^0} V^{(0)}_{i_0\sigma,i'_0\sigma'} \exp\left(\mathrm{i}\gamma_{i'_0\sigma'}\right) c_{i'_0\sigma'} = 0\,. \tag{56}$$

Here $\hat{V}^{(0)}$ is a unitary matrix of rank $2N^0$ which has only three nonzero elements in each of the $i'_0\sigma'$ columns. These elements are in the rows $i_0\sigma$, whose numbers are identical with the numbers linked to $i'_0\sigma'$ by a shared node:

$$V^{(0)}_{i_0\sigma,i'_0\sigma'} = s^{(0)}_{i_0\sigma,i'_0\sigma'}\,, \tag{57}$$

where $\hat{s}^{(0)}$ is the matrix (47) in which it is assumed that all Λ vanish.

The system of equations (56) is derived by matching the functions (13) in such a way as to take account of the scattering channels [see formula (46)] and the phases acquired in a section $i_0\sigma$:

$$\gamma_{i_0\sigma}(E, P_z) = \varphi_{i_0\sigma}(E, P_z) + Rn_{i_0} + \frac{1}{2}(\Lambda_{\bar{i}_0} + \Lambda_{i_0}), \qquad (58)$$

where

$$\varphi_{i_0\sigma}(E, P_z) = \frac{1}{\hbar}\mathcal{S}_{i_0}(E, p_z) + \gamma^{s}_{i_0\sigma}(E, p_z) + \delta_{i_0} \qquad (59)$$

is the semiclassical phase of the wave function (13) acquired by a conduction electron in the section $i_0\sigma$ between two consecutive MB scattering events. The second term in expression (58) must be included in discussing open periodic MB configurations (with the period b_y; see Figs 1c, 4c, and 4d). It should be noted that $R = cb_yP_x/e\hbar H$; $n_{i_0} = 0$ if i_0 is an internal section and $n_{i_0} = \operatorname{sgn}(\partial P_y/\partial P_x)$ if a section intersects the boundaries of unit cells [6]. In the case of closed MB configurations (Figs 4a and 4b), we find that $n_{i_0} = 0$ in all cases. The phase shift Λ_{i_0} in expression (58) is defined by formula (49), where $\bar{i}_0$ is the number of a section entering an MB node from which a section i_0 emerges; $m(\bar{i}_0) = m(i_0)$.

It should be noted that in expression (59) the quantity $\mathcal{S}_{i_0}(E, p_z)$ is the increment in the transverse action of formula (16) and $\delta_{i_0} = \pm\pi/2$ is the sum of all the phase shifts that appear in the i_0th section crossing the classical turning points [45, 84]. The spin contribution $\gamma^{s}_{i_0\sigma}(E, p_z)$ to the phase (59) is

$$\gamma^{s}_{i_0\sigma}(E, p_z) = \pm\frac{1}{2\hbar}g_{i_0}\mu_B H T_{i_0}(E, p_z) = \pm\frac{\pi}{2}\frac{m_{i_0}}{m}g_{i_0} \qquad (60)$$

[see also expression (15)]. Here, $g_{i_0}(E, p_z)$ and $m_{i_0}(E, p_z)$ are, respectively, the g factor and the effective cyclotron mass of conduction electrons in the i_0th section; $T_{i_0}(E, p_z)$ is the time taken by a conduction electron to travel along the i_0th section. It should be stressed that these three quantities are independent of the spin index, i.e. they are 'zero-spin quantities'. It should be pointed out that $g^{s}_{i_0} = g_{i_0}m_{i_0}/2m$, sometimes called the spin splitting parameter [8, 11], is — like the SOC parameter α, defined in formula (48) — a parameter of the MB theory that takes account of the spin degrees of freedom.

A better understanding of the interference processes which appear in this situation can be obtained by relating the dual nature of the motion of conduction electrons to the evolution in time of a semiclassical wave packet moving along an MB configuration. A wave packet, localised in a section $i_0\sigma$ at a moment t, will be denoted by $|t; i_0\sigma\rangle$. This wave packet moves along the semiclassical section $i_0\sigma$ to the nearest MB node and it acquires the phase described by expression (59). When the wave packet crosses MB nodes, it splits into three:

$$|t; i_0\sigma\rangle = \sum_{i'_0\sigma'} s_{i_0\sigma, i'_0\sigma'}|t; i'_0\sigma'\rangle\,. \qquad (61)$$

We shall simplify the notation by replacing two $i_0\sigma$ indices with one symbol for a semiclassical section i in such a way that the odd numbers of the sections represent the spin-up states of conduction electrons and the even numbers represent the spin-down states, i.e. $\sigma = \uparrow$ and $\sigma = \downarrow$, respectively. The new section number i represents uniquely the number of the band in which the wave packet is located and the spin orientation: $m\sigma = m\sigma(i)$.

Inclusion of the spin degrees of freedom and the existence of the third scattering channel ($\alpha \neq 0$) double the number of semiclassical sections of the orbit [described by expression (8)] forming an MB configuration, compared with the number of such sections in the 'zero-spin' case [5–8]. The number of inequivalent sections is also doubled. We can use the results of Refs [6, 49] if we assign different numbers $(i, j, ...)$ from 1 to N to the inequivalent sections. In the case of a closed MB configuration, N represents the total number of sections. When the spin degrees of freedom are included, N is equal to four times the number of MB nodes, i.e. $N = 2N^0$, where N^0 is the number of MB-configuration sections in that version of the MB theory which ignores the SOC.

We thus find that each $|t; i\rangle$ packet, which appears after any MB scattering, evolves semiclassically until it is scattered by the next MB node, and so on. Such scattering occurs at the following moments:

$$t_{\boldsymbol{L}} = \sum_{i=1}^{N} l_i T_i \equiv \boldsymbol{L}\cdot\boldsymbol{T}\,, \qquad (62)$$

where T_i is the time of travel along a section i; l_i represents nonnegative integers, which are equal to the number of times that a conduction electron passes through a section i. The time $t_{\boldsymbol{L}}$ is measured from the moment of the first scattering event. The set N of quantities $\{A_i\}$ in expression (62), which represent quasiclassical sections of an MB configuration $(i = 1,, 2, ..., N)$, will be called the N vector and denoted by $\boldsymbol{A}$ [6]. Therefore, expression (62) is written in the form of a scalar product $\boldsymbol{L}\cdot\boldsymbol{T}$ of the vectors.

Multiple scattering of semiclassical packets multiplies their number, which rises exponentially with time (Fig. 3b). Each packet, which appears in some section (for example, a section i) can be assigned to a specific path, along which it travels in the time $\boldsymbol{L}\cdot\boldsymbol{T}$ between the sections i and j. This path can in general be closed or open and it is called the λ *path*. It corresponds to a packet of amplitude $a^{(\lambda)}_{i,j}(\boldsymbol{L})$, which contains a phase factor $\exp\{i\gamma^{(\lambda)}\}$ and the product of the elements of the s matrices of the MB nodes through which the λ path passes. The integers $l_1, l_2, ..., l_N$ indicate the number of times that each of the MB-configuration sections is included in the λ path, but some of these numbers may be zero.

The following feature of the MB theory plays a fundamental role: any pair of sections (i, j) and a time $\boldsymbol{L}\cdot\boldsymbol{T}$ can as a rule be matched to many λ paths differing in the sequence of passing along semiclassical sections. Packets corresponding to such λ paths differ only in respect of their amplitudes $a^{(\lambda)}_{i,j}(\boldsymbol{L})$ and, therefore, they interfere forming a packet with a combined amplitude

$$A_{i,j}(\boldsymbol{L}) = \sum_{\lambda} a^{(\lambda)}_{i,j}(\boldsymbol{L})\,. \qquad (63)$$

In quantum mechanics, expression (63) is a Feynman path integral, which is transformed into a sum over λ paths because of a characteristic combination, under the MB conditions, of semiclassical motion along sections and of smallness of the MB regions. In the semiclassical case ($w = 0$) there is only one λ path for each pair of sections (if they are linked by a classical path).

The combined amplitude of the interfering packets, given by expression (63), is the quantum amplitude of the probability of detection of conduction electrons in a section j at a moment $\boldsymbol{L}\cdot\boldsymbol{T}$ after the first scattering event in the first section i. A complete description of the dynamics of conduction electrons under the MB conditions requires the knowledge of the whole infinite series of amplitudes $A_{i,j}(\boldsymbol{L})$. These amplitudes can be calculated by combinatorial analysis [5]. In the simplest situations this presents no difficulties [8], but in the general case of an arbitrary MB configuration, such analysis proves very cumbersome. However, in practice the mathematical formalism of the MB theory makes it possible to avoid combinatorial analysis, since the amplitudes $A_{i,j}(\boldsymbol{L})$ satisfy recurrence relationships [18], which are derived in Ref. [18] ignoring the SOC and the conduction electron spin.

We shall illustrate the derivation of the recurrence relationships, which take account of the spin degrees of freedom of conduction electrons, by considering the simple example of a closed figure-of-eight MB configuration with one MB node and four inequivalent sections (Fig. 4a). In terms of the new notation we have $i = 1, 2$ for the motion of conduction electrons in the first band and $i = 3, 4$ for the second band.

In accordance with the structure of the s matrix (47), when a wave packet begins its motion in the section $i = 1$ and crosses an MB region, it splits into three packets: one in its own band with the initial spin orientation $(i' = 1)$ and two in the other band with opposite spin orientations $(i' = 3, 4)$. These packets in turn are scattered at times T_1, T_3, and $T_4 = T_3$, respectively. Next, the packet $|t; i\rangle$ is scattered again, creating each time three new states localised in the sections $i = 1-4$. It is clear that at moments $t_1 + \boldsymbol{L}\cdot\boldsymbol{T}$ the scattering is accompanied by interference between some packets which are encountered in a section j. Here, t_1 is the moment of the first splitting of the initial packet; $\boldsymbol{L} = \boldsymbol{L}(l_1, l_2, l_3, l_4)$. All the interfering packets have the same structure, but different amplitudes.

The combined amplitude (63) of all the packets which begin their motion in a section i and interfere at a moment $T_i + \boldsymbol{L}\cdot\boldsymbol{T}$ in a section j $(j = 1-4)$ satisfy the following relationships:

$$
\begin{aligned}
A_{i,1}(\boldsymbol{L}) &= \tau \exp(\mathrm{i}\gamma_1) A_{i,1}(\boldsymbol{L} - \boldsymbol{e}_1) \\
&\quad - \frac{\rho}{\beta} \exp(\mathrm{i}\gamma_3) A_{i,3}(\boldsymbol{L} - \boldsymbol{e}_3) + \frac{\alpha\rho}{\beta} \exp(\mathrm{i}\gamma_4) A_{i,4}(\boldsymbol{L} - \boldsymbol{e}_4), \\
A_{i,2}(\boldsymbol{L}) &= \tau \exp(\mathrm{i}\gamma_2) A_{i,2}(\boldsymbol{L} - \boldsymbol{e}_2) \\
&\quad - \frac{\rho}{\beta} \exp(\mathrm{i}\gamma_4) A_{i,4}(\boldsymbol{L} - \boldsymbol{e}_4) - \frac{\alpha\rho}{\beta} \exp(\mathrm{i}\gamma_3) A_{i,3}(\boldsymbol{L} - \boldsymbol{e}_3), \\
A_{i,3}(\boldsymbol{L}) &= \tau \exp(\mathrm{i}\gamma_3) A_{i,3}(\boldsymbol{L} - \boldsymbol{e}_3) \\
&\quad + \frac{\rho}{\beta} \exp(\mathrm{i}\gamma_1) A_{i,1}(\boldsymbol{L} - \boldsymbol{e}_1) + \frac{\alpha\rho}{\beta} \exp(\mathrm{i}\gamma_2) A_{i,2}(\boldsymbol{L} - \boldsymbol{e}_2), \\
A_{i,4}(\boldsymbol{L}) &= \tau \exp(\mathrm{i}\gamma_4) A_{i,4}(\boldsymbol{L} - \boldsymbol{e}_4) \\
&\quad + \frac{\rho}{\beta} \exp(\mathrm{i}\gamma_2) A_{i,2}(\boldsymbol{L} - \boldsymbol{e}_2) - \frac{\alpha\rho}{\beta} \exp(\mathrm{i}\gamma_1) A_{i,1}(\boldsymbol{L} - \boldsymbol{e}_1),
\end{aligned}
\tag{64}
$$

where $\boldsymbol{e}_j$ is the unit N vector with one nonzero component whose serial number is the same as the serial number of the section in which interference takes place, i.e. $\boldsymbol{e}_j = \{\delta_{1,j}, \delta_{2,j}, ..., \delta_{N,j}\}$.

Relationships (64) are obvious from the nature of the s matrix (47), from Fig. 4a, and from simple combinatorial considerations. Moreover, the following boundary conditions are assumed in the derivation of relationships (64):

$$
\begin{aligned}
&A_{i,j}(\boldsymbol{0}) = \delta_{i,j}, \\
&A_{i,j}(-1, l_2, l_3, l_4) = A_{i,j}(l_1, -1, l_3, l_4) \\
&\quad = A_{i,j}(l_1, l_2, -1, l_4) = A_{i,j}(l_1, l_2, l_3, -1) = 0,
\end{aligned}
\tag{65}
$$

where $\delta_{i,j}$ are the Kronecker deltas, each of which can be represented as a δ-like spike, which appears in a section $i = j$; $\boldsymbol{0} = \{0, 0, 0, 0\}$ is the null vector.

The boundary conditions (64) can be rewritten as an ordinary product of matrices:

$$
A_{i,j}(\boldsymbol{L}) = \sum_{k}^{N=4} A_{i,k}(\boldsymbol{L} - \boldsymbol{e}_k)\, V^{(0)}_{k,j} \exp(i\gamma_k), \tag{66}
$$

where on the left is the matrix of the amplitudes that interfere in a section j and on the right is the product of a matrix $A_{i,k}(\boldsymbol{L} - \boldsymbol{e}_k)$, interfering in a section k, and a dynamic matrix $V^{(0)}_{k,j'}$, which is defined by formula (57).

The above expressions (64)–(66) can be generalised directly to other types of MB configurations. In particular, the recurrence relationships (66) are valid in the case of all nonnegative values of $l_1, l_2, ..., l_N$ with the exception of $\boldsymbol{L} = \boldsymbol{0}$. Then $A_{i,k}(\boldsymbol{L})$ satisfies the boundary conditions

$$
A_{i,j}(\boldsymbol{0}) = \delta_{i,j}, \quad A_{i,j}[\boldsymbol{L} - (l_k + 1)\boldsymbol{e}_k] = 0, \tag{67}
$$

where k assumes values from 1 to N.

Introduction of a unitary matrix of rank N

$$
U_{k,j}(\boldsymbol{\gamma}) = V^{(0)}_{k,j} \exp(\mathrm{i}\gamma_k), \tag{68}
$$

expressed in terms of $\hat{V}^{(0)}$ and γ_k [see formulas (57) and (58)], yields the following form of relationship (66) valid for any MB configuration:

$$
A_{i,j}(\boldsymbol{L}) = \sum_{k}^{N} A_{i,k}(\boldsymbol{L} - \boldsymbol{e}_k)\, U_{k,j}, \tag{69}
$$

where for an arbitrary MB configuration the matrix $U_{k,j'}$ is constructed in such a way that there are only three nonzero elements in the jth column. These elements are on rows k, the serial numbers of which are identical with the serial numbers of the sections coupled to a section j by a shared MB node with a nonzero MB transition probability.

The system of recurrence relationships (69), together with the boundary conditions (67), can be represented in a compact form with the aid of the generating functions [6, 18]

$$
F_{i,j}(\boldsymbol{\gamma}) = {\sum_{\boldsymbol{L}}}' \bar{A}_{i,j}(\boldsymbol{L}) \exp(\mathrm{i}\boldsymbol{L}\cdot\boldsymbol{\gamma}), \tag{70}
$$

where the summation symbol is primed to indicate the absence of the term with $\boldsymbol{L} = \boldsymbol{0}$ and

$$
\bar{A}_{i,j}(\boldsymbol{L}) = \sum_{\lambda} \bar{a}^{(\lambda)}_{i,j}(\boldsymbol{L})
$$

is the smooth part of the combined amplitude (63). Here, $\bar{a}^{(\lambda)}_{i,j}$ is the product of the elements of the s matrix for the MB nodes traversed by the λ path, derived ignoring the

phases acquired in the sections and as a result of MB, because the phases occurring in $\boldsymbol{\gamma}$ are taken into account separately [see, for example, formula (70)].

The matrix described by formula (70) satisfies the following linear system of equations:

$$F_{i,j}(\boldsymbol{\gamma}) = \sum_{k}^{N} F_{i,k}(\boldsymbol{\gamma})\, V_{k,j}^{(0)} \exp(\mathrm{i}\gamma_k) + V_{i,j}^{(0)} \exp(\mathrm{i}\gamma_j)\,. \tag{71}$$

A similar system of equations is obtained for the above example of an MB configuration with one MB node (Fig. 4a) if the recurrence relationships (64) and (70) are substituted and the boundary conditions (65) are applied.

In view of the relationship between $\hat{U}$ and $\hat{V}$, the system of equations (71) can be written in the matrix form:

$$\hat{F}(\boldsymbol{\gamma}) = \hat{F}(\boldsymbol{\gamma})\,\hat{U}(\boldsymbol{\gamma}) + \hat{U}(\boldsymbol{\gamma})\,. \tag{72}$$

Therefore, we can find the amplitude $\bar{A}_{i,j}(\boldsymbol{L})$ by solving the system of N linear equations (71) and finding the relevant Fourier component of the resultant solution.

3.2 Dispersion equations and magnetic breakdown spectrum

It is pointed out in Section 2.1 that the energy levels of conduction electrons become quantised in a magnetic field and the quantisation rule is given by expression (19). It follows from this expression that the spacing between discrete energy levels $E_{m\sigma}(n, p_z)$ is $\Delta E_m = \hbar\omega_m(E, p_z)$ and that this spacing depends very weakly on the level number n. In the preceding section we have shown that under the MB conditions a simple periodic motion of the centre of a packet within one band is replaced by a complex pattern of quantum interference of an enormous number of packets. In this case the electron energy spectrum differs qualitatively from the semiclassical spectrum.

Pippard solved the difficult quantum-mechanical problem of the motion of conduction electrons under the MB conditions and derived the MB spectrum by introducing the concept of a *network of coupled orbits* in real space (see Refs [4, 46, 50]). This approach yields a fairly clear picture of the motion of conduction electrons, so that it is possible to utilise the probabilities of a jump of a conduction electron from one orbit to another and to consider a set of phases for the motion of conduction electrons along these orbits, deriving thus the dispersion equations the solution of which gives the MB energy spectrum.

The idea underlying this method is illustrated in sufficient detail in Shoenberg's book [8] on the basis of a simple model of a metal in which a network of coupled circular orbits is obtained along an $\boldsymbol{r}$-direction perpendicular to the direction of variation of the lattice potential. A similar network can be obtained from the MB configuration shown in Fig. 4d, if the relationship between the $\boldsymbol{p}$ and $\boldsymbol{r}$ paths given by expression (9) is utilised. One should mention also the work of Chambers [51–53], who analysed MB networks and found the MB spectrum by complex combinatorial procedures.

The mathematical procedures used in the preceding section make it possible to formalise and simplify the deriva-tion of the dispersion equations, at least in the case of simple one-dimensional periodic MB configurations [6, 49] or when the spin degrees of freedom are included [9]. This derivation reduces to the finding of the determinant of the system of equations (56) or of the matrix $\hat{E} - \hat{U}(\boldsymbol{\gamma})$, where $\hat{E}$ is a unit matrix. The matrix $\hat{E} - \hat{U}(\boldsymbol{\gamma})$ can also be derived from the matrix equation (72) and zeros of the determinant

$$\det|\hat{E} - \hat{U}(\boldsymbol{\gamma})| = 0 \tag{73}$$

yield the singularities of the generating function $F_{i,j}(\boldsymbol{\gamma})$.

It is clear from the general principles of quantum mechanics [84] that the roots of Eqn (73) give possible values of the energy of conduction electrons under the MB conditions, i.e. the MB spectrum, whereas the quantities $F_{i,j}(\boldsymbol{\gamma})$ represent a stationary quantum amplitude of a transition of a conduction electron from a section i to a section j. The unitary nature of the matrix $\hat{U}(\boldsymbol{\gamma})$ and the known properties of the determinants lead to

$$\det|\hat{E} - \hat{U}(\boldsymbol{\gamma})| = 2\exp\left\{\frac{\mathrm{i}}{2}\left[\sum_{i=1}^{N}\gamma_i + \chi_0\right]\right\} D(\boldsymbol{\gamma})\,, \tag{74}$$

where $\chi_0 = (\pi/2)[-1 + \mathrm{sgn}\,(\det|\hat{V}|)]$ and $D(\boldsymbol{\gamma})$ is a real function of the phases γ_i, which is periodic in the phases with the period 2π.

It follows from Eqn (74) that zeros of the spectral equation (73) are real and that $D(\{\gamma_i\})$ represents a finite trigonometric polynomial for N phases γ_i in which the coefficients depend only on the MB probabilities and on the SOC parameter, i.e. on ρ, τ, and α [see the matrix (47)]. It therefore follows that the MB spectrum can be deduced from the solution of the transcendantal equation

$$D(\{\gamma_i\}) = 0\,, \tag{75}$$

known as the dispersion equation.

The semiclassical nature of the motion between MB nodes implies the existence of large phases (59) of the wave functions of conduction electrons, which depend on the energy, on the projection of the momentum along the applied magnetic field, and on the field itself. The independence of the phases acquired in different sections i, and the incommensurability of these phases and their derivatives (in respect of their energy and momentum) has the effect that under the MB conditions the energy of conduction electrons becomes a quasirandom function of E and p_z [6]. If the spin is taken into account, these phases depend also on the value of the g factor of the conduction electrons in a section i, and, consequently, in general the g factor of conduction electrons representing the whole MB configuration can also become a quasirandom quantity.

We believe that it is *impossible* to separate (in general) the spin degrees of freedom from the 'orbital' degrees and, in our opinion, it is one of the most important results of the MB theory which takes account of the spin flip of conduction electrons. Moreover, it has been assumed earlier [4–8] that the motion of conduction electrons under the MB conditions is semiclassical both in the absence of MB ($w = 0$) and in the case of total breakdown ($w = 1$). In our case this applies only to conduction electrons moving along their own 'legitimate' paths in the $w = 0$ case. If $w = 1$ (and $w^s \neq 0$!), the wave functions of conduction electrons become entangled. We shall show later that this may create states with an effective spin $\frac{1}{2}$ and each of these states represents a mixture of 'prebreakdown' states with opposite spins. This leads to an effective g factor of conduction electrons, which is governed by the 'spin' splitting in a magnetic field [see expressions (12) and (19)].

In the more complex case of advanced MB [$w(1-w)\neq 0$] when spin flip is taken into account ($w^{s}\neq 0$), it is necessary to modify the classification of the states of the MB system. The effect of this is that in calculation of many physical properties of the system it is not possible to separate summation of the spin index. This summation can be carried out only for some special cases such as the case of composite MB orbits which lie entirely within one band and on which there is no spin flip of conduction electrons under the MB conditions. Therefore, in general, there are conduction electron states which are given by the solutions of the dispersion equation (75) and the number of these solutions is *doubled*, compared with the zero spin case. We then cannot identify the spin of each of these states.

It therefore follows that in the case of closed MB configurations and a fixed value of p_z, Eqn (75) gives a discrete set of MB-modified Landau levels:

$$E = E(n, p_z), \tag{76}$$

and in the case of open MB configurations, a spectrum of the magnetic band type [4, 6] is possible:

$$E = E(n, p_z, R), \tag{77}$$

where n is the serial number of the solution of the disperse equation which takes account of the SOC and the continuously variable parameter R is defined by expression (58). Under the advanced MB conditions [$w(1-w)\sim 1$] the energy levels $E(n, p_z)$ and $E(n, p_z, R)$ are distributed at random: their dependence on p_z is a random function. In this case the serial number n of an MB level differs from that obtained in the semiclassical approximation [11, 13], because the number of the magnetic flux quanta, which pass through the area within the classical conduction-electron path, has no simple physical meaning.

We shall consider this in greater detail by deriving the $D(\gamma)$ function for simple MB configurations and we shall take into account the spin degrees of freedom (Fig. 4).

(a) We shall begin with a closed MB configuration with one MB node (Fig. 4a), which subject to the spin splitting can be called the double figure-of-eight. A fourth-order determinant is obtained from expressions (47), (53), (58), (68), and (73). Omission of the phase factor [see expression (74)] and simple transformations yield the dispersion equation

$$D(\{\gamma_i\}) = \cos\Omega - (1-w)^{1/2}\sum_{i=1}^{4}\cos\Omega_i + (1-w)\sum_{i=1}^{3}\cos\Omega_{i,4} + \frac{w}{1+\alpha^2}(\cos\Omega_{2,4} + \alpha^2\cos\Omega_{2,3}) = 0, \tag{78}$$

where

$$\Omega = \frac{1}{2}(\gamma_1+\gamma_2+\gamma_3+\gamma_4),\quad \Omega_i = \Omega-\gamma_i,\quad \Omega_{i,j} = \Omega_i - \gamma_j. \tag{79}$$

In the absence of the SOC ($\alpha = 0$), the dispersion equation (78) can be factorised:

$$D^{0}(\{\gamma_i\}) = 2\left(\cos\frac{\gamma_1+\gamma_3}{2} - \sqrt{1-w}\cos\frac{\gamma_1-\gamma_3}{2}\right) \times\left(\cos\frac{\gamma_2+\gamma_4}{2} - \sqrt{1-w}\cos\frac{\gamma_2-\gamma_4}{2}\right) = 0. \tag{80}$$

If $\gamma_i^{s} = 0$ is substituted in all γ_i [see relationship (60)], which is equivalent to complete neglect of the spin splitting, then each factor in the dispersion equaiton (80) is identical with the function $D(\{\gamma_i\})$ for the simple figure-of-eight given in Ref. [6].

If $w = 0$ (weak fields $H \ll H_0$, no breakdown), the spectrum becomes semiclassical. The dispersion function (78) then splits into factors:

$$D_{w=0}(\{\gamma_i\}) = 8\sin\frac{\gamma_1}{2}\sin\frac{\gamma_2}{2}\sin\frac{\gamma_3}{2}\sin\frac{\gamma_4}{2}. \tag{81}$$

Equating to zero each of them, we obtain the Lifshitz–Onsager condition of the type given by formula (19):

$$S_i(E, p_z) - (-1)^{i}\pi g_i\mu_{\mathrm{B}} m_i H = \frac{2\pi e\hbar H}{c}\left(n+\frac{1}{2}\right) \tag{82}$$

which determines the spectrum of conduction electrons moving along semiclassical paths. Therefore,

$$S_i(E, p_z) = \int^{p_y} p_x^{m(i)}(p_y')\,\mathrm{d}p_y' \tag{83}$$

is the area of a section of the constant-energy surface obtained ignoring the spin splitting (integration is carried out along the whole of a section i) and

$$m_i = \frac{eHT_i}{2\pi c} = \frac{1}{2\pi}\left(\frac{\partial S}{\partial E}\right)_i \tag{84}$$

is the effective cyclotron mass in the same section i (T_i is the time of travel along the section). The following equalities then apply:

$$m_{k-1} = m_k,\quad T_{k-1} = T_k,\quad S_{k-1} = S_k,\qquad g_{k-1} = g_k = g_{m(k)},\quad k = 2l, \tag{85}$$

where l is an integer (in our example, this integer is $l = 1$, 2). Conduction electrons then move along their initial orbits and do not undergo interband transitions.

If $w = 1$ (strong fields $H \gg H_0$, complete breakdown), the motion of conduction electrons considered taking account of the spin degrees of freedom is not fully semiclassical. In this limiting case electrons move without 'noticing' the interband gaps, as in the earlier theory [5, 6]. However, each passage of a conduction electron through an MB node may result in spin flip associated with the SOC. New paths appear and they are composed of sections of the old semiclassical orbits. Mixing of the states with the opposite spins modifies the dispersion function (78) to

$$D_{w=1}(\{\gamma_i\}) = \cos\frac{\gamma_1+\gamma_2+\gamma_3+\gamma_4}{2} + \frac{1}{1+\alpha^2}\left(\cos\frac{\gamma_1-\gamma_2+\gamma_3-\gamma_4}{2} + \alpha^2\cos\frac{\gamma_1-\gamma_2-\gamma_3+\gamma_4}{2}\right). \tag{86}$$

It is clear that quantisation conditions are different for the two limiting cases because the orbit topologies are very different. By analogy with condition (82), subject to relationships (83)–(86), we can write the Lifshitz–Onsager condition for the resultant complete figure-of-eight as follows:

$$S^{(w=1)}(E, p_z) \pm \pi g^{(w=1)}\mu_{\mathrm{B}} m^{(w=1)} H = \frac{2\pi e\hbar H}{c}\left(n+\frac{1}{2}\right), \tag{87}$$

where $S^{(w=1)} = S_1 + S_3$ is the total zero-spin area of this figure and $m^{(w=1)} = m_1 + m_3$. Condition (87) allows us to introduce the effective spin of a conduction electron: the plus (minus) sign then corresponds to an effective spin-up (spin-down) state.

We thus obtain the following very interesting result. In spite of the fact that a conduction electron crosses sections of an MB configuration with *opposite* spins (represented by even and odd numbers), under the complete breakdown conditions a mixture of states degenerates into two (!) effective 'quantum' states which differ in respect of the orientation of the *effective spin*. This gives rise to an effective g factor of the new orbit, which in the case of complete breakdown is

$$g^{(w=1)} = \frac{2}{\pi}\frac{m}{m^{(w=1)}} \arccos\left\{\frac{1}{1+\alpha^2}\cos\left[\frac{\pi}{2m}(g_1 m_1 + g_3 m_3)\right]\right\}. \tag{88}$$

We recall that, as in the Hamiltonian (26a), m denotes the mass of a free electron. The effective g factor of a new orbit can be described in a natural manner in terms of the characteristics of sections (g_i, m_i) and in terms of the SOC parameter α defined by expression (48).

The results obtained can be made clearer by comparison with similar spectral characteristics [see formula (87)] of conduction electrons moving along a simple closed orbit without MB nodes (for example, a circle or an ellipse) with the g factor equal to $g^{(w=1)}$.

If the SOC does not influence MB (i.e. if $\alpha = 0$) the states with opposite spins do not merge: each of the figures-of-eight exists independently of the other. In this situation expression (88) reduces to the fully expected formula for g_{av}, which is the g factor averaged over the new orbits:

$$g_{\mathrm{av}} = g^{(w=1)}_{(\alpha=0)} = \frac{g_1 m_1 + g_3 m_3}{m^{(w=1)}}, \tag{89}$$

which for greater clarity can be rewritten as follows [compare with formula (84)]:

$$g_{\mathrm{av}} = \frac{g_1 T_1 + g_3 T_3}{T_1 + T_3}. \tag{90}$$

It is evident from expressions (89) and (90) that one of the reasons for the change in the g factor of conduction electrons under the conditions of complete breakdown is the difference between the characteristics of the inequivalent sections in an MB configuration. On the other hand, it follows from expression (88) that even if all m_i and g_i are equal, the effective g factor g_{av} is not in general equal to g_i because of the possibility of spin flip of conduction electrons in each passage through an MB node ($\alpha \neq 0$). This conclusion is of fairly general validity and is applicable to different types of MB configurations.

The intermediate case of advanced breakdown [$w(1-w) \sim 1$, $H \sim H_0$], which requires numerical solution of the dispersion equations, is discussed in the next section.

(b) We note that a closed MB configuration (Fig. 4a) transforms topologically into an open MB configuration (Fig. 4c) by the following procedure. Sections 1, 2, and 3, 4 have to be broken and re-joined differently. In this way we obtain the unit cell of an open MB configuration. It is necessary to change then the direction of motion of conduction electrons along the lower branch. This transformation results in the disappearance not only of the turning points on the paths with the phases γ_i, but also of δ_i [see formula (58)]. Therefore the results obtained above and described by expressions (78)–(90) apply also to the MB configuration shown in Fig. 4c, apart from the fact that the phases γ_i must include the terms Rn_i in formula (58), which appear because of the periodicity of the MB configuration: $n_{1,2} = +1$, $n_{3,4} = -1$. This leads, in particular, to a continuous spectrum (lifting of degeneracy of P_x) when $w = 0$ and to a discrete spectrum when $w = 1$. When the breakdown probability $w = 1 - \tau^2$ differs slightly from unity and τ differs slightly from zero [compare with expression (48)], narrow bands appear (they are discussed in the next section).

(c) The MB configurations with two MB nodes, shown in Figs. 4b and 4d, can also be transformed continuously into one another by a similar topological procedure. An open MB configuration (Fig. 4d) is obtained from a close configuration (Fig. 4b) by turning the latter through 90° in the clockwise direction, breaking sections 1, 2 and 7, 8, and re-joining them with equivalent sections which are in the adjacent cells.

In contrast to cases (a) and (b), we shall now consider in greater detail the case of an open MB configuration. In general, MB nodes may be inequivalent, i.e. they may be characterised by different s matrices (identified by I and II in Fig. 4d). However, for the sake of simplicity we shall assume that the MB nodes in a configuration are equivalent, i.e. that $w_{\mathrm{I}} = w_{\mathrm{II}} = w$, $\alpha_{\mathrm{I}} = \alpha_{\mathrm{II}} = \alpha$. This MB configuration consists of eight different sections. The periodicity of p_y in the phases described by expression (58), corresponding to sections 1, 2, 7, and 8 intersecting the boundaries of the cell (Fig. 4d), means that we have to retain terms Rn_i, where $n_i = 1$ for $i = 1, 2$; $n_i = -1$ for $i = 7, 8$; $n_i = 0$ for $i = 3 - 6$.

Application of the rules for the derivation of the dispersion equation yields an eighth-order determinant and expansion of this determinant gives the following expression:

$$\begin{aligned}
D(\{\gamma_i\}) &= \cos\Omega - (1-w)^{1/2}\sum_{i=1,2,7,8}\cos\Omega_i \\
&+(1-w)(\cos\Omega_{1,2} + \cos\Omega_{1,7} + \cos\Omega_{1,8} \\
&+\cos\Omega_{2,7} + \cos\Omega_{2,8} + \cos\Omega_{7,8} - \cos\Omega_{3,5} - \\
&-\cos\Omega_{4,6} - \cos\Omega_{1,2,3,5} - \cos\Omega_{1,2,4,6}) \\
&-(1-w)^{3/2}(\cos\Omega_{1,2,7} + \cos\Omega_{1,2,8} + \cos\Omega_{1,7,8} \\
&+\cos\Omega_{2,7,8}) + (1-w)^{1/2}(1-w^s)(\cos\Omega_{1,3,5} \\
&+\cos\Omega_{3,5,7} + \cos\Omega_{2,4,6} + \cos\Omega_{4,6,8}) \\
&+(1-w)^{1/2}(1-w^0)(\cos\Omega_{2,3,5} \\
&+\cos\Omega_{3,5,8} + \cos\Omega_{1,4,6} + \cos\Omega_{4,6,7}) \\
&+(1-w)^2\cos\Omega_{1,2,7,8} - (1-w^s)^2\cos\Omega_{1,3,5,7} \\
&-(1-w^0)^2\cos\Omega_{1,4,6,7} - (1-w^s)(1-w^0)\times \\
&\times(\cos\Omega_{1,3,5,8} + \cos\Omega_{1,4,6,8}) + w^0 w^s(\cos\Omega_{1,3,6,7} \\
&+\cos\Omega_{1,4,5,7} - \cos\Omega_{1,3,6,8} - \cos\Omega_{1,4,5,8}) = 0,
\end{aligned} \tag{91}$$

where w^0 and w^s are taken from expressions (3) and (53), and expression (91) is simplified by introducing quantities Ω similar to those described by formula (79):

$$\Omega = \frac{1}{2}\sum_{i=1}^{N}\gamma_i, \quad \Omega_j = \Omega - \gamma_j,$$

$$\Omega_{j,k} = \Omega_j - \gamma_k, \quad \Omega_{j,k,l} = \Omega_{j,k} - \gamma_l, \quad \ldots$$

If the influence of the SOC on MB is ignored ($\alpha = 0$), the MB configuration considered here degenerates into two independent MB configurations for each spin orientation. The dispersion function (91) splits into two factors corresponding, under the MB conditions, to spin-up and spin-down conduction electrons:

$$\begin{aligned} D^0(\{\gamma_i\}) = -2\Bigg(&\sin\frac{\gamma_1+\gamma_3+\gamma_5+\gamma_7}{2} \\ &+(1-w)^{1/2}\sin\frac{\gamma_1-\gamma_3-\gamma_5-\gamma_7}{2} \\ &+(1-w)^{1/2}\sin\frac{\gamma_7-\gamma_1-\gamma_3-\gamma_5}{2} \\ &-(1-w)\sin\frac{\gamma_1+\gamma_7-\gamma_3-\gamma_5}{2}\Bigg) \\ \times\Bigg(&\sin\frac{\gamma_2+\gamma_4+\gamma_6+\gamma_8}{2} \\ &+(1-w)^{1/2}\sin\frac{\gamma_2-\gamma_4-\gamma_6-\gamma_8}{2} \\ &+(1-w)^{1/2}\sin\frac{\gamma_8-\gamma_2-\gamma_4-\gamma_6}{2} \\ &-(1-w)\sin\frac{\gamma_2+\gamma_8-\gamma_4-\gamma_6}{2}\Bigg) = 0\,. \end{aligned} \tag{92}$$

If the spin splitting is neglected completely [by assuming that in all γ_i we have $\gamma_i^s = 0$, in accordance with relationship (60)], each factor in the above equation is identical with the dispersion function for the zero-spin MB configuration [6].

By analogy with case (a), we shall now give the dispersion equations for the limiting cases.

If $w = 0$, the dispersion function (91) becomes

$$\begin{aligned} D_{w=0}(\{\gamma_i\}) = -32&\sin\frac{\gamma_1}{2}\sin\frac{\gamma_2}{2}\sin\frac{\gamma_3+\gamma_5}{2} \\ &\times\sin\frac{\gamma_4+\gamma_6}{2}\sin\frac{\gamma_7}{2}\sin\frac{\gamma_8}{2}. \end{aligned} \tag{93}$$

Electrons move along their orbits without transitions from one band to another. If the periodicity is taken into account, the terms Rn_i are retained in the phases, γ_1, γ_2, γ_7, and γ_8. Conduction electrons in the bands to which sections 1, 2, 7, 8 belong move along infinite paths conserving the spin projection along the magnetic field. This gives rise to a continuous spectrum. In the band to which sections 3, 4, 5, and 6 belong the motion of conduction electrons remains finite and the quantisation rules (19) remain valid.

If $w = 1$, closed orbits are formed and they consist of eight sections (1-2)–(3-4)–(7-8)–(5-6) with oppositely oriented spins. The dispersion equation (91) then becomes

$$\begin{aligned} D_{w=1}(\{\gamma_i\}) = \cos\Omega - \frac{1}{(1+\alpha^2)^2}\,&[\cos\Omega_{1,3,5,7} \\ &+\alpha^2(\cos\Omega_{1,3,5,8}+\cos\Omega_{1,4,6,8}) \\ &+\alpha^4(\cos\Omega_{1,4,6,7}-\cos\Omega_{1,3,6,7}+\cos\Omega_{1,3,6,8} \\ &-\cos\Omega_{1,4,5,7}+\cos\Omega_{1,4,5,8})] \end{aligned} \tag{94}$$

We can easily show that the dependence on the continuous parameter R disappears from Eqn (94), because in all the arguments of the cosines the phases corresponding to the different directions of motion of conduction electrons occur in the form of pair sums. Consequently, a discrete spectrum is obtained under complete breakdown conditions ($w = 1$, $H \gg H_0$). As in case (b), narrow bands appear in small values of τ (see next section).

Concluding this section, we note that open MB configurations characterised by $\sum_{i=1}^{N} n_i \neq 0$ are possible. This gives rise to a characteristic spectrum with a nonzero average velocity of conduction electrons participating in MB. We shall not consider this case because it has been discussed sufficiently thoroughly in Ref. [6].

3.3 Phase spectrum of conduction electrons under coherent magnetic breakdown conditions. Problems in calculation of the energy spectrum and the *g* factor of conduction electrons under conditions of advanced magnetic breakdown

Before considering the MB spectrum obtained numerically for a simple MB configuration with one MB node (discussed in the preceding section), we shall discuss briefly the general problems.

The procedure for the derivation of the dispersion functions D [see Eqn (74) or Eqn (75)], the zeros of which govern the MB spectrum, has been developed only for one-dimensional MB configurations [6, 9]. Naturally, in this case the problem can be solved only for periodic MB configurations which appear along specific directions of the magnetic field. Even small deviations of the magnetic field from the relevant crystal axes can alter greatly the properties of the open MB configurations (see, for example, Figs 4c and 4d). This occurs because the areas of the closed loops, which are located in different unit cells in the $\boldsymbol{p}$ space, become incommensurable with one another. Slutskin and Gorelik have shown [47] that the resultant weak aperiodicity of the MB configurations leads to the possibility of quantum localisation of conduction electrons under the MB conditions.

In the case of two-dimensional MB configurations the problem is even more complex. It is more correct to speak now of two-dimensional *MB networks* (see Section 1), because the paths of conduction electrons in *real* space have been considered in the analyses of the spectra of hexagonal (Pippard [4]) and rectangular (Chambers [53]) networks. Even in the case of these symmetric cases there is a problem associated with the fact that the characteristic period of an MB network, formed by circular conduction-electron orbits, is inversely proportional to the magnetic field and becomes commensurable with the spatial period of the crystal lattice only for specific discrete values of the field H. The phase spectrum (discussed below) can be constructed for these values of H and, in general, this spectrum cannot be transformed into the energy spectrum [8], which complicates interpretation of the results.

Let us now turn to the problems relating to inclusion of the spin degrees of freedom of conduction electrons under the MB conditions. Naturally, compared with the zero-spin case the task of calculating the MB spectrum becomes more difficult. This is due to the doubling of the order of the determinant (73), from which the dispersion function is derived, and due to the appearance of a spin contribution to the phase, which is associated with the g factor of conduction electrons.

The MB spectrum can be determined for an arbitrary probability w by a numerical calculation of a set of solutions of the transcendental equations (74) and (75). These solutions are finite trigonometric polynomials representing the phases acquired by conduction electrons in different parts of an MB configuration. In this way the phase spectrum is constructed from the set of solutions

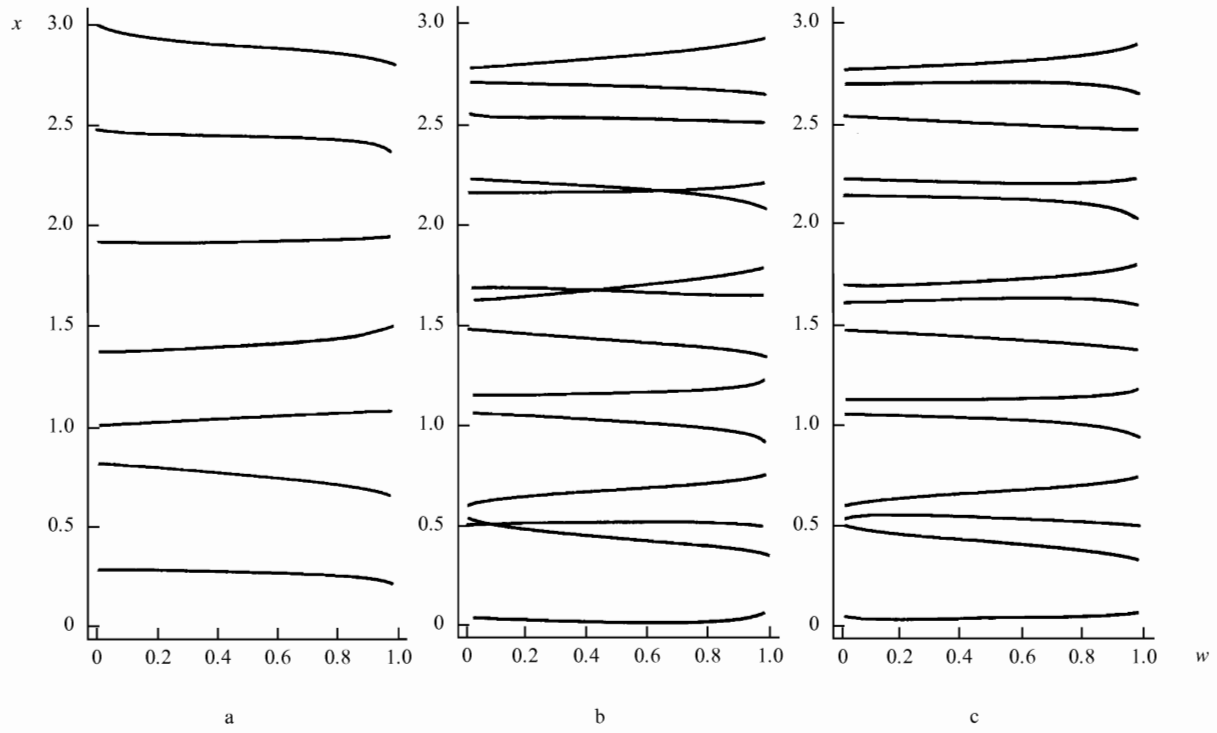

Figure 6. Phase spectrum of the double figure-of-eight type (compare with Fig. 4a): (a) $g_1 = g_2 = 0$, $\alpha = 0$ is the zero-spin case; (b) $g_1^s = \sqrt{2}/3$, $g_3^s = \sqrt{3}/2$, $\alpha = 0$, each zero-spin level splits into two, three ponts of random level crossing can be seen; (c) $g_1^s = \sqrt{2}/3$, $g_3^s = \sqrt{3}/2$, $\alpha = 0.8$, full account of the spin properties, random degeneracy lifted by the SOC.

$\gamma_I(E, p_z)$ obtained for different values of w and p_z. Naturally, the spectra will be different for topologically different (open and closed) MB configurations. Open configurations have a spectrum of the magnetic band type, which increases considerably the volume of calculations.

The next problem is that of finding the energy spectrum from the phase spectrum. The spin splittings which are then obtained should give the g factor of conduction electrons under the MB conditions. Naturally, the g factor is a function of p_z, of the MB probability w, of the SOC parameter α, and of the serial number of the branch of the spectrum. In general, without specifying the dispersion law of conduction electrons in the absence of MB [such as that given by expression (1)], it is possible to determine the phase spectrum of conduction electrons under MB conditions [69–71], which will be discussed below.

We shall now illustrate the results of the preceding section and analyse the MB spectra for MB configurations shown in Fig. 4 on the assumption of a fixed value of p_z. We shall begin by considering an MB configuration of the double figure-of-eight type with one MB node (Fig. 4a). The phase variable is then

$$x = \frac{cS_1}{\pi e\hbar H}, \quad S_3 = \frac{11}{3} S_1 . \tag{95}$$

Here $S_1 = S_2$ is the zero-spin area of the upper branch described by expression (83). The above relationship between the areas of the sections is selected for convenience of comparison with Refs [8, 46], which is discussed below. The g factors are incommensurable when the spin splitting parameters are selected to be

$$g_1^s = g_1 \frac{m_1}{2m} = \frac{\sqrt{2}}{3}, \quad g_3^s = \frac{\sqrt{3}}{2}. \tag{96}$$

The values of the variable x corresponding to $D(\boldsymbol{\gamma}) = D(x) = 0$ give the phase spectrum in accordance with the classification used in Ref. [8]. Fig. 6 shows the dependences of the 'phase' x on the total MB probability w, calculated for different values of α. Here, $w = 1$ corresponds to complete breakdown and $w = 0$ to the absence of breakdown.

Fig. 6a is the spectrum of a completely zero-spin situation when the spin splitting ($g_1^s = g_3^s = 0$) and the SOC ($\alpha = 0$) are ignored. This phase spectrum is formed by any of the factors in the dispersion function (80). Its physical meaning is readily understood by considering the periodicity in simple limiting cases.

In the absence of breakdown there are two sets of equidistant levels ($n = 0, 1, 2, \ldots$):

$$x_{1,n}^{(a)}(w = 0) = \frac{6}{11}\left(n + \frac{1}{2}\right), \quad x_{2,n}^{(a)}(w = 0) = 2\left(n + \frac{1}{2}\right). \tag{97}$$

The first set corresponds to the motion of conduction electrons along the lower zero-spin loop and the second set corresponds to the upper loop (Fig. 4a). It follows from expression (97) that there are $6 + 1 = 7$ branches in the interval $0 \leqslant x \leqslant 3$.

In the case of complete breakdown, an equidistant spectrum corresponding to the total area of the figure-of-eight is obtained ($n = 0, 1, 2, \ldots$):

$$x_n^{(a)}(w = 1) = \frac{3}{7}\left(n + \frac{1}{2}\right). \tag{98}$$

Naturally, inclusion of the spin splitting doubles the number of roots of the dispersion equation $D(x) = 0$ and doubles the number of the branches of the spectrum. This can be seen clearly in Figs 6b and 6c.

When the SOC is ignored and there is no conduction-electron spin flip during crossing of MB nodes [$\alpha = 0$; see

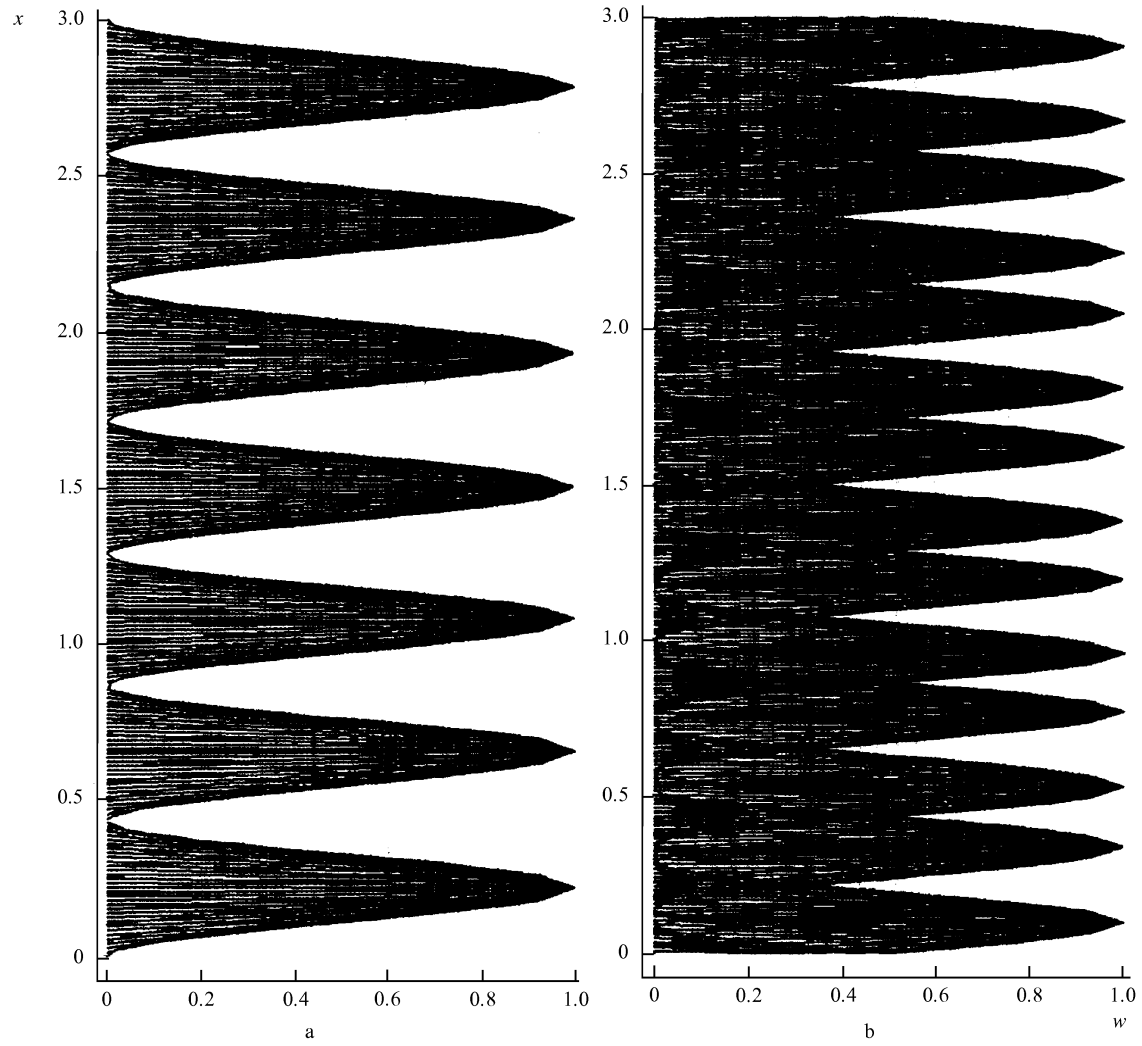

Figure 7. Phase spectrum of an open MB configuration with a single MB node (compare with Fig. 4c): (a) zero-spin case; (b) full account of the spin properties.

the dispersion equation (80)], the spectrum may have points of 'accidental' degeneracy for specific values of w (or H). Fig. 6b demonstrates clearly three regions of such degeneracy. In the limiting cases the sets of levels are described by the following expressions

$$x_{1,n}^{(b)}(w=0)=\frac{6}{11}\left(n+\frac{1}{2}\right)\mp\frac{3}{11}\,g_3^s$$
$$x_{2,n}^{(b)}(w=0)=2\left(n+\frac{1}{2}\right)\mp g_1^s\,. \qquad (99)$$

$$x_n^{(b)}(w=1)=\frac{3}{7}\left(n+\frac{1}{2}\right)\mp\frac{3}{14}\,(g_1^s+g_3^s)\,. \qquad (100)$$

The upper sign (minus) corresponds to the effective down-spin. The last term in expression (100) determines the spin splitting parameter in the case when $w=1$ and corresponds to the average g factor given by formulas (89) and (90).

Finally, the case illustrated in Fig. 6b corresponds to taking the SOC fully into account ($\alpha=0.8$) and is described by the dispersion equation (78). Even a weak SOC lifts the 'accidental' degeneracy of the phase spectrum. It follows from general formulas (81) and (82) that if $w=0$, the spectrum is completely identical with that described by expressions (99) when $\alpha=0$. If $w=1$, two sets of equidistant levels with $\Delta x=\frac{3}{7}$ are formed (as shown in Fig. 6b, but corresponding to opposite orientations of the *effective* spin with even and odd values of n, respectively). The spin splitting is *different* from that given by expression (100): the splitting is approximately 1.3 times stronger. This confirms the conclusion reached in discussing general formula (88) that new effective semiclassical states with up and down spins form in this limiting case.

In the general case of advanced MB [$w(1-w)\neq 0$] it is not possible to select any specific relationship to describe this behaviour of the spin splitting, which begins to depend nonmonotonically also on the serial number of the spectral branch. This is indirect evidence that the total electron g factor of even this simple MB configuration depends in a complex manner on the parameters of the problem. As mentioned earlier, the identification (among the dispersion equation solutions) of those states which correspond to the opposite orientations of the effective spin and, consequently, the direct determination of the effective g factor from the phase spectrum have not yet been carried out for arbitrary values of w and α.

We shall consider a continuous spectrum which appears in the case of a simple open MB configuration (Fig. 4c) discussed in the preceding section as case (b). The phase spectrum is shown in Fig. 7. Case (a) corresponds to a

completely zero-spin situation. In case (b) the spin degrees of freedom are allowed for fully ($\alpha = 0.8$). The phase relationships and the parameters of the spin splitting are described by expressions (95) and (96).

In the limit of strong MB ($w = 1$) it is found that conduction electrons move along closed composite orbits and a discrete spectrum appears. This spectrum is completely identical with that given for $w = 0$ in Figs. 6a and 6c, respectively. This is to be expected because in these limiting cases the areas of the closed figures are identical. The zero-spin spectrum obeys the relationships described by formula (98). The spectrum becomes completely continuous for $w = 0$ (Fig. 7a) and for $w \approx 0.4$ (Fig. 7b). This is due to the superposition, in the latter case, of two sets of magnetic energy bands corresponding to the opposite spin orientations.

We shall consider the simpler example (Fig. 7a) in discussing the behaviour of the spectrum near characteristic instability points $w = 1$ and $w = 0$. This can be done conveniently by introducing the quantity $\tau = \sqrt{1 - w}$. If we assume that the first factor in the dispersion function (80) vanishes and if we use the definition of the phase variable (95), we find that for any value of τ the spectrum is given by the relationship

$$\cos\frac{\tilde{\gamma}_1 + \tilde{\gamma}_3}{2} = \tau\cos\left(\frac{\tilde{\gamma}_1 - \tilde{\gamma}_3}{2} + R\right)$$

$$\Rightarrow -\tau \leqslant \cos\frac{\tilde{\gamma}_1 + \tilde{\gamma}_3}{2} \leqslant \tau. \qquad (101)$$

We have separated here the continuous parameter $R(P_x)$[see expression (58)] and $\tilde{\gamma}_i = \gamma_i - Rn_i$. At low values of τ there are fairly narrow intervals of the permissible values of $\tilde{\gamma}_1 + \tilde{\gamma}_3 = (14/3)x$, repeated at intervals of 3/7 (see expression [98]).

The argument of the cosine, which occurs in expression (108) to the left of the equality sign, can be represented in the form $\pi/2 + \pi n + \delta$, where the first two terms correspond to the position of the level in a discrete spectrum at $\tau = 0$, and $\max|\delta|$, which depends on τ, determines the half-width of a magnetic band. In the limit $\tau \to 0$, the value of δ is also small and, consequently, we have

$$\max|\delta| \approx \tau = \sqrt{1 - w}. \qquad (102)$$

In the other limiting case ($\tau \to 1$) we can readily obtain from expression (101) an estimate for the half-width of the empty bands of the forbidden states which appear in the continuous spectrum and are located near $x_n = (3/7)n$ ($n = 0, 1, 2, \ldots$):

$$\max|\tilde{\delta}| = \arccos\tau \approx \sqrt{2(1 - \tau)} \approx \sqrt{w}.$$

We shall conclude this section by considering the MB spectrum of an open MB configuration with two MB nodes (Fig. 4d), shown in Fig. 8. The special case of the position of an MB network formed by circular orbits was considered by Pippard [46] and is discussed in detail in Ref. [8]. We shall therefore confine ourselves to a computer-calculated illustration and a brief discussion.

In the symmetric zero-spin case, we find that

$$\gamma_{1,7} = \tilde{\gamma}_1 \pm R = \frac{11}{3}\pi x \pm R, \quad \gamma_3 = \gamma_5 = \pi x + \frac{\pi}{2}.$$

The notation used in Ref. [8] is identical with ours apart from taking account of the turning points described by expression (59) on lens-shaped diangular orbits (which account for $\pi/2$ in the above relationship). Consequently, our whole spectrum is shifted along the x axis by $\frac{1}{2}$, compared with the result reported in Ref. [8]: our phase variable x and the quantity τ are identical with ξ and the variable q in Shoenberg's treatment.

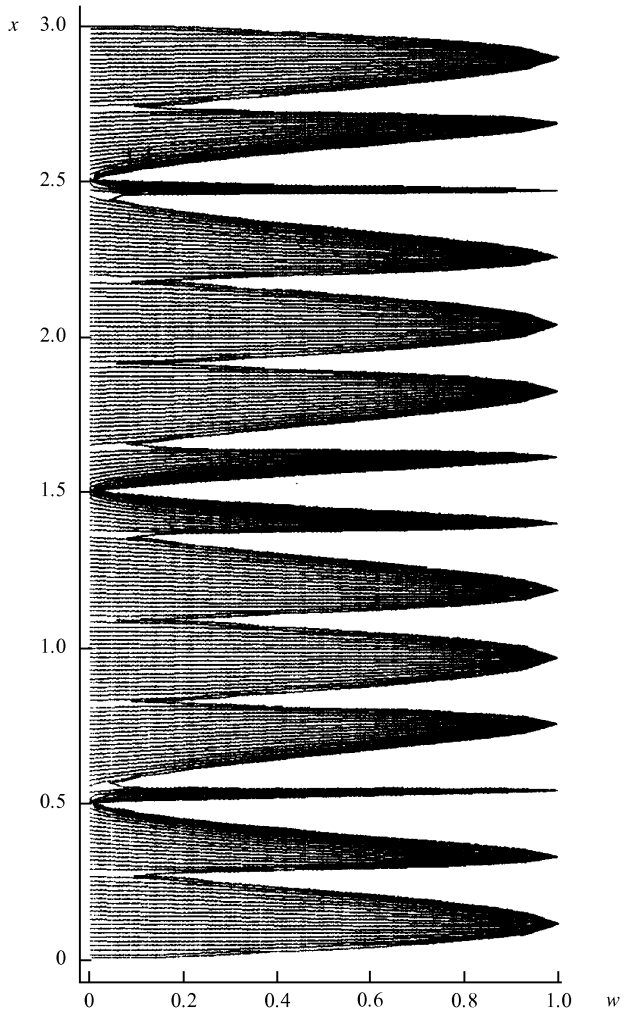

Figure 8. Phase spectrum of an open MB configuration with two MB nodes (compare with Fig. 4d), plotted ignoring the spin degrees of freedom (this is an analogue of the phase diagram given in Refs [4, 8]).

The spectrum of allowed values is readily obtained from the determinant (92):

$$\cos R = \frac{\tau^2\sin(\tilde{\gamma}_1 - \gamma_3) - \sin(\tilde{\gamma}_1 + \gamma_3)}{2\tau\sin\gamma_3}. \qquad (103)$$

If τ is exactly zero, a discrete spectrum is obtained and it corresponds to the motion of conduction electrons along a composite closed orbit 1–3–7–5:

$$x_n(w = 1) = \frac{3}{14}\left(n + \frac{1}{2}\right). \qquad (104)$$

By analogy with the derivation of expression (102), the half-width of the allowed levels, obtained for the case of small values of τ from expression (103), is

$$\max|\delta| = 2\tau|\sin\gamma_3| = 2\tau|\sin(2\pi x)|.$$

This level broadening varies periodically at a frequency $\Delta x = 1$, which corresponds to the area of the lens-shaped

orbit $S_3 + S_5$. Oscillations can be seen clearly in Fig. 8 for $w \to 1$. Naturally, in a Fourier analysis of an MB spectrum, in addition to the component with this frequency a stronger component, described by formula (104) and with the frequency $\Delta x = \frac{3}{14}$, as well as harmonics of this component are obtained [46].

In the opposite limiting case ($\tau \to 1$ or $w \to 0$) there are periodic discontinuities of the spectrum at ($n = 0, 1, 2, ...$)

$$x_n^{(1)}(w = 0) = n + \frac{1}{2}, \tag{105}$$

which correspond to the area of the lens-shaped orbit 3–5. There are discontinuities in the spectrum also if $x_n^{(2)} = (6/7)n$. These discontinuities are weak because in this limiting case the motion of conduction electrons along the large orbit 1–3–7–5 has a very low probability: conduction of electrons must break consecutively through four MB nodes with the probabilities $w \to 0$!

The phase spectrum shown in Fig. 8 is a superposition of the spectra corresponding to 40 different values of the variable R. It is quite clear from this spectrum that the darker regions with a higher density of levels merge at $w = 0$ where they become multiply degenerate levels of expression (105).

3.4 Principal identities in magnetic breakdown theory

In calculation of various macroscopic characteristics of a metal the MB spectra (76) and (77) must be supplemented by formulas which give the matrix elements of the physical quantities in the representation of stationary state vectors $|\eta\rangle$ [6]. The symbol η represents a complete set of quantum numbers representing a stationary state (55): $\eta = (n, p_z, P_y)$. Since conduction electrons spend a very short time at an MB node, we can use the η representation to calculate the matrix elements by extrapolation of expression (55) over the whole of the $\boldsymbol{p}$ space.

The classical physical quantities $\hat{f}$, which are smooth functions of the quasimomentum $\hat{f} = f_i(\hat{\boldsymbol{p}})$, have corresponding analogues in the MB theory. A typical example of a quantity $\hat{f}$ is the electron velocity $v_i(\boldsymbol{p})$ [see Eqn (7) where $\varepsilon_{m\sigma}$ should be replaced with the MB spectrum]. Far from MB nodes the operators $\hat{f}$ are constructed by the correspondence principle, which involves the substitution described by formula (11).

If $f_i(\hat{\boldsymbol{p}})$ is used in the wave function (55) and if expressions (11) and (13) are taken into account, expansion of the difference between the phases of the semiclassical exponential functions in terms of $E_\eta - E_{\eta'}$ yields the matrix elements of the operators:

$$\langle \eta' | \hat{f} | \eta \rangle = \delta_{P_y, P'_y} \delta_{p_z, p'_z} \sum_i^N c_i^*(\eta')\, c_i(\eta) \times \int_0^{T_i} \hat{f}_{m(i)}(t_i, E_\eta, p_z) \exp\left\{ \frac{i}{\hbar} (E_\eta - E_{\eta'}) t_i \right\} \mathrm{d}t_i . \tag{106}$$

The integration variable t_i is the duration of classical motion along a section i when the beginning of the section i corresponds to $t_i = 0$. Expression (106) is derived dropping the cross terms $\langle \Psi_i | \Psi_{i'} \rangle$, which is permissible because of fast oscillations of the semiclassical exponential functions contained in the wave functions (13).

A complete description of the dynamics of conduction electrons under the MB conditions must include the condition of normalisation of the stationary wave function (55) to unity. The normalisation of the wave funcions Ψ_i of the individual sections should be selected so that $\langle \Psi_i | \Psi_{i'} \rangle$ is equal to the time T_i taken by a conduction electron to travel along a section i. We then have

$$\sum_{i=1}^{N} |c_i|^2 T_i = 1 . \tag{107}$$

Therefore, $c_i \sqrt{T_i}$ has the meaning of the amplitude of the probability of detection in a section i of a conduction electron which is in a stationary state Ψ.

Expressions (56), (71), and (106), together with the normalisation condition (107), form a complete set of relationships needed for the calculation of any transport and thermodynamic quantities under the MB conditions. It must be stressed that the amplitudes $c_i(\eta)$ and the energy E_η as well as the matrix elements $\langle \eta' | \hat{f} | \eta \rangle$ vary rapidly and randomly with p_z. This creates a qualitatively new situation in the kinetics of conduction electrons and modifies completely the structure of the transport coefficients, compared with the quasiclassical case such as that described in Ref. [11]. Moreover, an irregular dependence of the matrix elements on η and η', described by expression (106), complicates additionally the task of calculation of these elements. It is not even possible to say in advance whether in this case the transport coefficients are regular functions of the parameters of the problem ($\boldsymbol{H}$, ω, t etc.) or whether they have the same random structure as E_η and the amplitudes $c_i(\eta)$.

However, these difficulties have been overcome because of certain regularities in the quasirandom MB spectrum. These regularities have made it possible to develop a formalism [18, 45, 49] that has led to analytic expressions both for the rapidly oscillating (with $\boldsymbol{H}$) parts of the linear response of the transport coefficients and for the number density of states $\nu(E, p_z)$.

This formalism is based on a circumstance which will be seen to be fundamental later: the random dependence of the amplitudes $c_i(\eta)$ can be expressed directly in terms of the MB spectrum E_η, because it follows from the wave function (55) that these amplitudes are

$$c_i(\eta) = \bar{c}_i[\gamma(E_\eta, p_z)], \tag{108}$$

where $\bar{c}_i(\gamma)$ is a smooth analytic 2π-periodic function of N arguments.

We shall now give an analytic expression for the number density of states $\nu(E, p_z)$ when $w(1 - w) \neq 0$ in the case of an arbitrary closed MB configuration:

$$\nu(E, p_z) = \sum_n \delta[E - E(n, p_z)] . \tag{109}$$

We recall that if the SOC is taken into account, the spin degrees of freedom are hidden in the serial number n of the solution of the dispersion equation.

The familiar equality

$$\delta[f(x)] = \sum_i \frac{\delta(x - x_i)}{|\partial f / \partial x|_{x = x_i}},$$

where x_i are the roots of the equation $f(x) = 0$, leads to

$$\nu(E, p_z) = \left| \frac{\partial D[\gamma(E, p_z)]}{\partial E} \right| \delta\{[D[\gamma(E, p_z)]]\} . \tag{110}$$

Replacing the derivative with respect to energy $\partial D / \partial E$ with the derivative with respect to phases $\partial D / \partial \gamma_i$, we obtain

the following expression for the number density of states in terms of zeros of the dispersion function and its derivatives:

$$\nu(E,p_z)=\sum_{i=1}^{N}\frac{T_i}{\hbar}\left|\frac{\partial D(\boldsymbol{\gamma})}{\partial\gamma_i}\right|\delta[D(\boldsymbol{\gamma})]\,, \tag{111}$$

where T_i is the period of revolution on the ith closed orbit [see the substitution (11)].

The dispersion functions have been found for some specific MB configurations [6, 9, 46, 69–71], discussed in Sections 3.2 and 3.3, both ignoring and taking into account the spin degrees of freedom. However, calculation of the number density of states (111) meets with mathematical difficulties even in the case of a simple MB configuration with one MB node.

The procedure of finding general analytic expressions for the matrix elements of physical quantities can be made easier by the use of two identities which are satisfied [see expressions (108) and (109)] by the number density of states $\nu(E,p_z)$ and by the quadratic combination of the amplitudes $\bar{c}_i^*(\boldsymbol{\gamma})\,\bar{c}_i(\boldsymbol{\gamma})$ [49]:

$$\nu(E,p_z)\equiv\frac{1}{2\pi\hbar}\sum_{i=1}^{N}T_i\,\mathscr{F}_{i,i}[\boldsymbol{\gamma}(E,p_z)]\,, \tag{112}$$

$$\bar{c}_i^*(\boldsymbol{\gamma})\,\bar{c}_{i'}(\boldsymbol{\gamma})\equiv\frac{\mathscr{F}_{i,i'}(\boldsymbol{\gamma})}{\sum_{i=1}^{N}T_i\,\mathscr{F}_{i,i'}(\boldsymbol{\gamma})}, \tag{113}$$

where the matrix $\mathscr{F}_{i,i'}(\gamma)$ represents the following sum of generating functions and a unit matrix:

$$\mathscr{F}_{i,i'}(\boldsymbol{\gamma})=F_{i,i'}(\boldsymbol{\gamma}+\mathrm{i}\mathbf{0})+F^*_{i',i}(\boldsymbol{\gamma}+\mathrm{i}\mathbf{0})+\delta_{i,i'}\,. \tag{114}$$

The appearance of $\mathrm{i}\mathbf{0}$ sets the rule for going around singularities which appear on an N-dimensional D surface, described by expression (75), on which $F_{i,j}(\boldsymbol{\gamma})$ becomes infinite. We shall conclude this section by stressing that, if the spin degrees of freedom of conduction electrons are taken into account, then in all the above expressions the index i not only represents the number of a section but also the spin orientation in this section. Moreover, the phases γ include the spin contribution described by the relationship (60).

4. Magnetic breakdown oscillations of the galvanomagnetic properties of a metal including the spin degrees of freedom

It is well known [6] that quantum oscillations of the transport coefficients (Shubnikov–de Haas effect) originate from the consecutive crossing of discrete quasiclassical levels by the Fermi energy when the applied magnetic field is varied. Asymptotic dependences of the transport coefficients in strong and weak fields are closely related to the nature of motion of conduction electrons. These dependences can be calculated in the semiclassical approximation and the answers can be obtained in the form of integrals over the Fermi surface [11].

It follows from Section 3 that MB contributes much which is new to the nature of the motion of conduction electrons. The energy spectrum becomes much more complex. Hence it follows that the structure of the MB oscillations is much more complex than in the semiclassical case. Moreover, the difference between the semiclassical and MB oscillations cannot be reduced to a more complex structure of the MB levels and of the oscillations of the number density of states. The MB oscillations appear because of interference between semiclassical waves scattered by MB nodes in the $\boldsymbol{p}$ space. Moreover, effects associated with the spin properties of conduction electrons are observed.

The most striking manifestations of the MB effects can be seen in the MB oscillations of the transport coefficients of a number of metals such as Be, Mg, Zn, Al, Sn, etc., which have small closed orbits in their MB configurations (see, for example, the configuration of Zn in Fig. 3b). The linear dimensions of these orbits are much smaller than the reciprocal lattice constants [55] and conduction electrons spend most of their time on large semiclassical sections. This case is interesting because the appearance of small orbits is frequently related to the existence of small Fermi surface sheets the formation of which is usually influenced strongly by the SOC [10, 100]. As pointed out in Section 3.3, this frequently leads to large deviations of the g factor of conduction electrons from its free-electron value and to small cyclotron masses. The latter indicates that the Larmor period T_{cq}, describing the motion of conduction electrons along small orbits, is short compared with the characteristic time spent on large orbits T_c. The index q will be used here and later in this section to denote the quantities which apply to small orbits.

In the case of small orbits the conditions (54a) and (54b) for coherent motion of conduction electrons are satisfied under stringent conditions on the purity of a metal and on temperature, compared with the orbits whose linear dimensions are of the order of the reciprocal lattice vector. One can have here the situation of *intermediate* MB:

$$T_c\gg\tau_{s.a}\gg T_{cq}\,, \tag{115}$$

when the motion of conduction electrons along large orbits shifts the wave function phase (stochastic MB), whereas the motion of these electrons along small orbits is coherent. The intermediate MB regime naturally satisfies the condition $\tau_p\gg T_c$ which is usual in the case of classical galvanomagnetic effects. The smallness of the orbits makes it possible to consider them as special 'quantum switches' controlling the motion of conduction electrons along an MB configuration. They are called the effective MB nodes and the corresponding s matrix is known as effective.

There are metals with MB configurations containing small diangular and triangular orbits [5, 6, 8] (Figs 9a and 9b). We shall find, for these orbits, the effective s matrices and probabilities of crossing effective MB modes P, Q and P_A, P_B, P_C, respectively, deduced taking into account the spin degrees of freedom.

The existence of coherent motion along small orbits under the MB conditions gives rise to oscillations of the transport coefficients and the period of these oscillations corresponds to the area of a small orbit [5–8, 55]. We shall now consider how these oscillations are modified if we include the spin degrees of freedom and the SOC in the analysis, especially as the theory of Falicov, Pippard, and Sievert [55]— which accounts for the existence, profile, and order of magnitude of these oscillations — does not explain correctly the experimentally observed structure of double oscillation peaks of the galvanomagnetic properties of Zn [101].

Before we compare the spin-flip MB theory [65, 66] with the published experimental galvanomagnetic characteristics of a real MB metal, we must apply this theory to a simple

model of a metal [64] illustrated in Fig. 4d. Without taking into account the spin degrees of freedom for circular orbits, this model was used in Stark and Falicov's review [5] and in Shoenberg's book [8] to analyse in detail the galvanomagnetic properties. This will reveal directly the effects of inclusion of the spin of conduction electrons.

We shall begin by discussing the general principles underlying description of the galvanomagnetic properties of metals under the MB conditions.

4.1 Static conductivity tensor under stochastic magnetic breakdown conditions

As noted in Section 3, the nature of motion of conduction electrons under the MB conditions is extremely sensitive to small-angle scattering. It is essential to develop a consistent transport theory which should be based on a quantum transport equation for the nonequilibrium part of the one-electron density matrix [19]. However, in many cases of interest in physics the semiclassical approximation is sufficient. This approximation works not only in the case of stochastic MB, but also for coherent MB when condition (54a) is satisfied [6]. We shall confine ourselves to the derivation of the conductivity tensor $\hat{\sigma}$ for stochastic MB [described by condition (54c)] as a function of the applied magnetic field. We shall base this derivation on the solution of the linearised Boltzmann transport equation.

A specific ergodic distribution of conduction electrons between MB configurations is created under the stochastic MB conditions. The breakdown begins to act as a stochastic factor which mixes conduction electrons over all semiclassical sections. The time interval between two consecutive MB scattering events plays the role of the relaxation time. It is governed by the characteristic cyclotron frequency ω_c and by the corresponding MB probability. The components of the conductivity tensor $\sigma_{\alpha\beta}$ naturally depend on the topology of the MB configuration. In the limiting case $w(1-w) \to 0$ parts of an MB configuration transform into conventional open or closed orbits: the values of $\sigma_{\alpha\beta}$ begin to determine the real time of a free run of conduction electrons between collisions $\tau^* = \tau_p$ [see conditions (54)].

The situation described above corresponds to the Boltzmann transport equation with a linearised collision integral. Its general solution for the stochastic MB case can be sought in the same way as in the semiclassical case (see, for example, Refs [11, 13]):

$$f_m(\boldsymbol{p}) = f_F(\boldsymbol{p}) - \frac{\partial f_F}{\partial E}\, e\boldsymbol{E}\cdot\boldsymbol{\Psi}_m(\boldsymbol{p}), \tag{116}$$

where $f_m(\boldsymbol{p})$ is the conventional distribution function; $f_F(\boldsymbol{p})$ is the equilibrium Fermi–Dirac distribution function; $\boldsymbol{E}$ is the electric field; $\boldsymbol{\Psi}_m(\boldsymbol{p})$ is a vector function with the dimensions of length, which has to be determined. This function is a semiclassical analogue of the operator described by Eqn (106).

The natural variables for the Boltzmann transport equations in the case when static electromagnetic fields are present are E, p_z, t_i [13]. Then, in the lowest order in $\boldsymbol{\Psi}_m(\boldsymbol{p})$, these equations become

$$\frac{\partial \boldsymbol{\Psi}_i}{\partial t_i} + \hat{I}_p\{\boldsymbol{\Psi}_i\} = \boldsymbol{v}_i, \quad \hat{I}_p = \left(\frac{\partial f_F}{\partial E}\right)^{-1} \hat{I}\left(\frac{\partial f_F}{\partial E}\right), \tag{117}$$

where $\boldsymbol{\Psi}_i$ are the values of the functions $\boldsymbol{\Psi}_m(\boldsymbol{p})$ in the parts of an MB network in the r space; $\hat{I}$ is the linear collision operator.

The differential equations (117) in t_i require the boundary conditions. If, for given values of E and p_z, a conduction electron orbit is closed, then obviously the function $\boldsymbol{\Psi}_i$ should depend periodically on t_i. However, if the orbit is open, then the boundary condition states that $\boldsymbol{\Psi}_i$ is finite in the limit $t_i = \pm\infty$. For simplicity, we shall assume that a magnetic field $\boldsymbol{H}$ has a 'good' direction, and the function $\boldsymbol{\Psi}_i$ should be periodic with its period equal to the reciprocal lattice constant [18]. This case differs from the semiclassical situation because under the stochastic MB conditions the functions $\boldsymbol{\Psi}_i$ undergo jumps when crossing MB nodes. This is of fundamental importance in calculation of the conductivity tensor.

It follows that the equations (117) and the usual boundary conditions $\boldsymbol{\Psi}_i$ should be supplemented by stochastic boundary conditions at MB nodes. The latter conditions are derived in accordance with the process of the scattering of a wave packet described in Section 3.1. If the procedure used in the derivation of formula (61) is followed and use is made of the unitarity of the s matrices and of the notation in Fig. 2c, the system of boundary conditions can be written in the form

$$\boldsymbol{\Psi}_{i'} = \sum_{i=1}^{N} w_{i',i}\, \boldsymbol{\Psi}_i, \tag{118}$$

where

$$w_{i',i} = \left|V^{(0)}_{i',i}\right|^2 \tag{119}$$

are the MB probabilities; $\boldsymbol{\Psi}_i = \boldsymbol{\Psi}(T_i)$ are the values of $\boldsymbol{\Psi}_m[\boldsymbol{p}(t_i)]$ at the ends of the sections entering an MB node; $\boldsymbol{\Psi}_{i'} = \boldsymbol{\Psi}(0)$ are the corresponding values at the ends of the sections leaving such a node. The boundary conditions (118) show that the flux of particles leaving an MB node along a given section, for example a section $i' = 1$, is formed from particles moving along incoming sections $i = 1, 3, 4$ with the weights $1-w$, w^0, w^s respectively.

The solution of the equations (117), subject to the boundary conditions (118), makes it possible to find the components of the conductivity tensor $\sigma_{\alpha\beta}$, which are expressed in terms of $\boldsymbol{\Psi}_i$ in accordance with the usual semiclassical formulas:

$$\sigma_{\alpha\beta} = \frac{e^2}{(2\pi\hbar)^3}\frac{eH}{c}\sum_i \int\left(-\frac{\partial f_F}{\partial E}\right) dE \times \int_0^{b_z} dp_z \int_0^{T_i} v_i^{\alpha}(t_i)\, \Psi_i^{\beta}(t_i)\, dt_i . \tag{120}$$

It therefore follows that when the coherence is destroyed by small-angle scattering, MB begins to play the role of a stochastic factor and the small-angle scattering characteristics do not enter the final expressions for $\sigma_{\alpha\beta}$.

4.2 Effective s matrices and effective probabilities of magnetic breakdown for small orbits

The procedures for the calculation of the effective s matrices of diangular and triangular orbits are very similar. This procedure is described in Ref. [6] for the zero-spin case. Therefore, we shall confine ourselves to the derivation of this s matrix for the case of a diangular orbit and in dealing with the triangular case we shall use the expressions for the first column of the matrix [64].

For the sake of clarity we shall go back to explicit inclusion of the spin index in the serial number of the cross

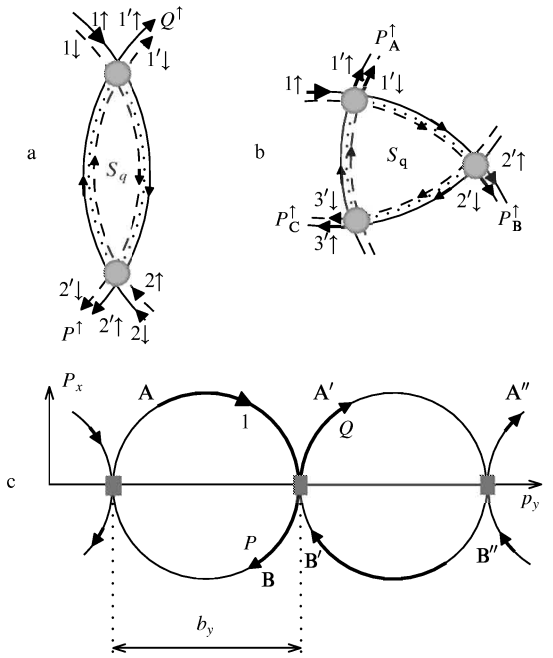

Figure 9. Small orbits: (a) diangular orbit; (b) triangular orbit; (c) reduced MB configuration corresponding to Fig. 4d. Small diangular orbits perform the role of effective MB nodes. The spin splittings are not shown for the sake of clarity.

section, which will become $i_0\sigma$. The expressions for the elements of the effective s matrix can be obtained from the general system of equations (56) by excluding from it the amplitudes $c_{i_0\sigma}$, which apply to inner parts of small orbits (Figs 9a and 9b). The matrix elements $S^{\rm eff}_{i_0\sigma,\,i'_0\sigma'}$ link the initial parts of sections labelled $i_0\sigma$, which enter an effective MB node, to the final parts labelled $i'_0\sigma'$, which leave an effective MB node with identical or opposite spin orientations.

We recall that conduction electrons that have crossed a single MB node and have remained in their own band conserve the spin direction in accordance with the structure of the s matrix (47): $s_{i_0\sigma,\,i'_0\sigma'}=0$ if the band numbers are identical; $m(i_0)=m(i'_0)$, and $\sigma\neq\sigma'$. If MB nodes are equivalent and the spin indices are included explicitly, the matrix element $S^{\rm eff}_{1\sigma,\,1'\sigma'}$ of a diangular orbit (Fig. 9a) is described by the following series:

$$S^{\rm eff}_{1\uparrow,\,1'\uparrow}=\tau\exp(-{\rm i}\Lambda)$$
$$-\left(\frac{\rho}{\beta}\right)^2\left\{\tau\exp[{\rm i}(-\Lambda+\gamma_{{\rm q}\uparrow})]+\tau^3\exp[{\rm i}(-\Lambda+2\gamma_{{\rm q}\uparrow})]+\ldots\right\}$$
$$-\alpha^2\left(\frac{\rho}{\beta}\right)^2\left\{\tau\exp[{\rm i}(-\Lambda+\gamma_{{\rm q}\downarrow})]+\tau^3\exp[{\rm i}(-\Lambda+2\gamma_{{\rm q}\downarrow})]+\ldots\right\}. \tag{121}$$

The first term in the series (121) represents the process in which a conduction electron, which begins to move along a section $i_0=1$, is reflected by an MB node and remains in its own band. The second term represents the tunnelling of a conduction electron without a change in its spin direction. Each component of the expression in the braces differs from the preceding component by one revolution of a conduction electron along a small orbit and two reflections from MB nodes. The third term in the series (121) is similar to the second, except for a change in the spin orientation as a result of MB tunnelling and revolutions along a small orbit with spin down. If $H\neq 0$, the series (121) is readily summed:

$$S^{\rm eff}_{1\uparrow,\,1'\uparrow}=\tau\exp(-{\rm i}\Lambda)\left[1-\frac{\rho^2}{1+\alpha^2}\times\left(\frac{\exp({\rm i}\gamma_{{\rm q}\uparrow})}{1-\tau^2\exp({\rm i}\gamma_{{\rm q}\uparrow})}+\frac{\alpha^2\exp({\rm i}\gamma_{{\rm q}\downarrow})}{1-\tau^2\exp({\rm i}\gamma_{{\rm q}\downarrow})}\right)\right]. \tag{122}$$

The elements of the effective s matrices $S^{\rm eff}_{i_0\sigma,\,i'_0\sigma'}$ can be described more compactly by introducing the notation

$$\Gamma^{\eta}_{i_0,j_0}=\frac{\exp({\rm i}\gamma^{\eta}_{i_0,j_0})}{1-\tau^l\exp({\rm i}\gamma_{{\rm q}\eta})},\quad i_0,j_0=1,2,\ldots,l, \tag{123}$$

where l is the number of sections of a small orbit (in the case of a diangular orbit, this number is $l=2$);

$$\gamma_{{\rm q}\eta}=\frac{cS_{\rm q}}{\hbar eH}+\gamma^{\rm s}_{{\rm q}\eta}+l\Lambda \tag{124}$$

is the phase acquired by conduction electrons in a small orbit [$S_{\rm q}$ is the zero-spin area of a small orbit and $\gamma^{\rm s}_{{\rm q}\eta}$ is the spin contribution described by expression (60)]; $\gamma^{\eta}_{i_0,j_0}$ is the partial phase given by expression (58) and acquired (Fig. 9a) during the motion of conduction electrons in sections of a small orbit.

The subscripts i_0 and j_0 in formula (123) apply to the phase acquired in inner sections of a small orbit along the direction of motion of conduction electrons as it crosses consecutively all the nodes between the sections which enter (i_0) and leave (j_0) an effective MB node. Naturally, if $i_0=j_0$, the phase $\gamma^{\eta}_{i_0,j_0}$ is replaced by the complete phase $\gamma_{{\rm q}\eta}$. The symbol η is used to index the spin state of a small orbit.

The matrix elements $S^{\rm eff}_{1\sigma,\,1'\sigma'}$ for a diangular orbit therefore have the form [64]

$$\begin{aligned}
S^{\rm eff}_{1\uparrow,\,1'\uparrow}&=S^{\rm eff}_{2\uparrow,\,2'\uparrow}\\
&=\tau\exp(-{\rm i}\Lambda)\left[1-\frac{\rho^2}{1+\alpha^2}(\Gamma^{\uparrow}_{1,1}+\alpha^2\Gamma^{\downarrow}_{1,1})\right],\\
S^{\rm eff}_{1\downarrow,\,1'\downarrow}&=S^{\rm eff}_{2\downarrow,\,2'\downarrow}\\
&=\tau\exp(-{\rm i}\Lambda)\left[1-\frac{\rho^2}{1+\alpha^2}(\alpha^2\Gamma^{\uparrow}_{1,1}+\Gamma^{\downarrow}_{1,1})\right],\\
S^{\rm eff}_{1\uparrow,\,1'\downarrow}&=S^{\rm eff}_{2\uparrow,\,2'\downarrow}=S^{\rm eff}_{1\downarrow,\,1'\uparrow}=S^{\rm eff}_{2\downarrow,\,2'\uparrow}\\
&=\tau\exp(-{\rm i}\Lambda)\frac{\rho^2}{1+\alpha^2}(\Gamma^{\uparrow}_{1,1}-\Gamma^{\downarrow}_{1,1}),\\
S^{\rm eff}_{1\uparrow,\,2\uparrow}&=-\frac{\rho^2}{1+\alpha^2}(\Gamma^{\uparrow}_{1,2}+\alpha^2\Gamma^{\downarrow}_{1,2}),\\
S^{\rm eff}_{1\downarrow,\,2'\downarrow}&=-\frac{\rho^2}{1+\alpha^2}(\alpha^2\Gamma^{\uparrow}_{1,2}+\Gamma^{\downarrow}_{1,2}),\\
S^{\rm eff}_{2\uparrow,\,1'\uparrow}&=-\frac{\rho^2}{1+\alpha^2}(\Gamma^{\uparrow}_{2,1}+\alpha^2\Gamma^{\downarrow}_{2,1}),\\
S^{\rm eff}_{2\downarrow,\,1'\downarrow}&=-\frac{\rho^2}{1+\alpha^2}(\alpha^2\Gamma^{\uparrow}_{2,1}+\Gamma^{\downarrow}_{2,1}),\\
S^{\rm eff}_{1\downarrow,\,2'\uparrow}&=S^{\rm eff}_{1\uparrow,\,2'\downarrow}=\frac{\alpha\rho^2}{1+\alpha^2}(\Gamma^{\uparrow}_{1,2}-\Gamma^{\downarrow}_{1,2}),\\
S^{\rm eff}_{2\downarrow,\,1'\uparrow}&=S^{\rm eff}_{2\uparrow,\,1'\downarrow}=\frac{\alpha\rho^2}{1+\alpha^2}(\Gamma^{\uparrow}_{2,1}-\Gamma^{\downarrow}_{2,1}).
\end{aligned} \tag{125}$$

We shall now give the first column in the effective s matrix [64, 66] for a triangular orbit [Fig. 9b, $l = 3$ in the notation of expressions (123) and (124)]:

$$
\begin{aligned}
S^{\mathrm{eff}}_{1\uparrow,1'\uparrow} &= \tau^2 \exp(-\mathrm{i}\Lambda)\left[\frac{1}{\tau} - \frac{\rho^2}{1+\alpha^2}(\Gamma^{\uparrow}_{1,1} + \alpha^2\Gamma^{\downarrow}_{1,1})\right],\\
S^{\mathrm{eff}}_{1\uparrow,1'\downarrow} &= \tau \exp(-\mathrm{i}\Lambda)\frac{\alpha\rho^2}{1+\alpha^2}(\Gamma^{\uparrow}_{1,1} - \Gamma^{\downarrow}_{1,1}),\\
S^{\mathrm{eff}}_{1\uparrow,2'\uparrow} &= -\frac{\rho^2}{1+\alpha^2}(\Gamma^{\uparrow}_{1,2} + \alpha^2\Gamma^{\downarrow}_{1,2}),\\
S^{\mathrm{eff}}_{1\uparrow,2'\uparrow} &= \frac{\alpha\rho^2}{1+\alpha^2}(\Gamma^{\uparrow}_{1,2} - \Gamma^{\downarrow}_{1,2})\\
S^{\mathrm{eff}}_{1\uparrow,3'\uparrow} &= -\tau \exp(\mathrm{i}\Lambda)\frac{\rho^2}{1+\alpha^2}(\Gamma^{\uparrow}_{1,3} + \alpha^2\Gamma^{\downarrow}_{1,3}),\\
S^{\mathrm{eff}}_{1\uparrow,3'\downarrow} &= \tau \exp(\mathrm{i}\Lambda)\frac{\alpha\rho^2}{1+\alpha^2}(\Gamma^{\uparrow}_{1,3} - \Gamma^{\downarrow}_{1,3}).
\end{aligned}
\tag{126}
$$

In the limiting case of the absence of the SOC the matrix elements (125) and (126) simplify greatly and they describe two independent types of conduction electron motion: with spin up and spin down. For each spin direction they are formally identical with the results reported in Ref. [6], but the spin term $\gamma^{\mathrm{s}}_{\mathrm{q}\eta}$ is retained in the phases described by expression (124).

However, if $\gamma^{\mathrm{s}}_{\mathrm{q}\eta}$ assumes a value πr ($r = 0, 1, 2, \ldots$), we can see from expression (123) that $\Gamma^{\uparrow}_{i_0,j_0} = \Gamma^{\downarrow}_{i_0,j_0}$. In this case the parameter α disappears from the matrix elements (125) and (126), and we once again obtain the results of Ref. [6]. The only difference is that the SOC parameter α still occurs in expression (50) which gives the renormalised breakdown field H_0.

When we know the elements of the effective s matrix (125), we can find the effective probabilities that conduction electrons follow a diangular orbit with different spin rotations:

$$
W^{\mathrm{eff}}_{1\sigma,1'\sigma'} = \left|S^{\mathrm{eff}}_{1\sigma,1'\sigma'}\right|^2, \tag{127}
$$

which can be utilised directly to calculate the magnetoresistance in a simple model of a metal which has a periodic MB network (Fig. 4d).

We recall that within the limits of a small orbit the motion of conduction electrons is coherent and over large parts of the orbits the phase coherence is destroyed completely by small-angle scattering. This transforms the motion of conduction electrons into a random walk. In calculation of the conductivity the spin of conduction electrons appears only in the expression for the acquired phase (60), which is different for different spin orientations. In the case of stochastic motion in large orbits the process of small-angle scattering causes phase shifts. Therefore, the spin orientation of conduction electrons moving along large parts is unimportant in the processes of *charge transport under intermediate MB conditions*. In this case the total probabilities of passing along small orbits or of reflection from these orbits are important.

In the case of a diangular orbit when the spin degrees of freedom are taken into account the effective probabilities will be denoted by P^{σ} and Q^{σ}, respectively ($\sigma = \uparrow\downarrow$). Then, in the case of a conduction electron approaching an effective MB node with spin up (Fig. 9a, $i_0\sigma = 1\uparrow$), the probabilities are

$$
\begin{aligned}
P^{\uparrow} &= W^{\mathrm{eff}}_{1\uparrow,2'\uparrow} + W^{\mathrm{eff}}_{1\uparrow,2'\downarrow}\\
&= \frac{w^2}{1+\alpha^2}\left(\frac{1}{|1-\tau^2\exp(\mathrm{i}\gamma_{\mathrm{q}\uparrow})|^2} + \frac{\alpha^2}{|1-\tau^2\exp(\mathrm{i}\gamma_{\mathrm{q}\downarrow})|^2}\right),\\
Q^{\uparrow} &= W^{\mathrm{eff}}_{1\uparrow,1'\uparrow} + W^{\mathrm{eff}}_{1\uparrow,1'\downarrow} = 1 - P^{\uparrow}.
\end{aligned}
\tag{128}
$$

Similarly, in the case of a conduction electron approaching an effective MB node with spin down (Fig. 9, $i_0\sigma = 1\downarrow$), we find that

$$
\begin{aligned}
P^{\downarrow} &= W^{\mathrm{eff}}_{1\downarrow,2'\uparrow} + W^{\mathrm{eff}}_{1\downarrow,2'\downarrow}\\
&= \frac{w^2}{1+\alpha^2}\left(\frac{\alpha^2}{|1-\tau^2\exp(\mathrm{i}\gamma_{q\uparrow})|^2} + \frac{1}{|1-\tau^2\exp(\mathrm{i}\gamma_{\mathrm{q}\downarrow})|^2}\right),\\
Q^{\downarrow} &= W^{\mathrm{eff}}_{1\downarrow,1'\uparrow} + W^{\mathrm{eff}}_{1\downarrow,1'\downarrow} = 1 - P^{\downarrow},
\end{aligned}
\tag{129}
$$

where w is the total MB probability, described by expression (2) for equivalent small-orbit nodes.

The matrix elements (126) can be used to find three pairs of probabilities P^{σ}_A, P^{σ}_B, and P^{σ}_C (Fig. 9b) for a triangular orbit:

$$
\begin{aligned}
P^{\uparrow}_B &= W^{\mathrm{eff}}_{1\uparrow,2'\uparrow} + W^{\mathrm{eff}}_{1\uparrow,2'\downarrow}\\
&= \frac{w^2}{1+\alpha^2}\left(\frac{1}{|1-\tau^3\exp(\mathrm{i}\gamma_{\mathrm{q}\uparrow})|^2} + \frac{\alpha^2}{|1-\tau^3\exp(\mathrm{i}\gamma_{\mathrm{q}\downarrow})|^2}\right),\\
P^{\uparrow}_C &= W^{\mathrm{eff}}_{1\uparrow,3'\uparrow} + W^{\mathrm{eff}}_{1\uparrow,3'\downarrow} = \tau^2 P^{\uparrow}_B
\end{aligned}
\tag{130}
$$

$$
\begin{aligned}
P^{\uparrow}_A &= W^{\mathrm{eff}}_{1\uparrow,1'\uparrow} + W^{\mathrm{eff}}_{1\uparrow,1'\downarrow} = 1 - P^{\uparrow}_B - P^{\uparrow}_C,\\
P^{\downarrow}_B &= W^{\mathrm{eff}}_{1\downarrow,2'\uparrow} + W^{\mathrm{eff}}_{1\downarrow,2'\downarrow}\\
&= \frac{w^2}{1+\alpha^2}\left(\frac{\alpha^2}{|1-\tau^3\exp(\mathrm{i}\gamma_{\mathrm{q}\uparrow})|^2} + \frac{1}{|1-\tau^3\exp(\mathrm{i}\gamma_{\mathrm{q}\downarrow})|^2}\right),\\
P^{\downarrow}_C &= W^{\mathrm{eff}}_{1\downarrow,3'\uparrow} + W^{\mathrm{eff}}_{1\downarrow,3'\downarrow} = \tau^2 P^{\downarrow}_B,\\
P^{\downarrow}_A &= W^{\mathrm{eff}}_{1\downarrow,1'\uparrow} + W^{\mathrm{eff}}_{1\downarrow,1'\downarrow} = 1 - P^{\downarrow}_B - P^{\downarrow}_C.
\end{aligned}
\tag{131}
$$

An important result is that, for arbitrary values of g_{q} and $\alpha \neq 0$, the probabilities (127) for each spin orientation oscillate in very different ways with the magnetic field. We can see that the total effective probabilities (128), (129) and (130), (131) for each spin orientation are periodic functions of two phases (124), which differ by an amount $2\gamma^{\mathrm{s}}_{\mathrm{q}} = \pi g_{\mathrm{q}} m_{\mathrm{q}}/m$, where g_{q} is the electron g factor for a small orbit and m_{q} is the cyclotron mass.

If the SOC and the spin are ignored, a small diangular orbit may 'switch off and on' the motion of a conduction electron in an MB configuration. If the SOC is taken into account, it is difficult to satisfy the condition of complete transparency which applies to a zero-spin diangular orbit. In addition to the condition, which resembles the Lifshitz–Onsager quantitation rule for a small orbit [6]

$$
S_{\mathrm{q}}(E, p_z) = \frac{2\pi e\hbar H}{c}\left(n - \frac{\Lambda}{\pi}\right), \tag{132}
$$

it is now necessary to make sure that $\gamma^{\mathrm{s}}_{\mathrm{q}}$ is equal to $2\pi r$ (where r is an integer) or $g_{\mathrm{q}} = 4m_{\mathrm{q}}r/m$, for which there is no justification at all.

Expressions (128)–(131) for the probabilities are relatively clear. This is because we have been considering a fairly simple case of small symmetric orbits and equivalent MB nodes on these orbits. In other cases the elements of the effective s matrix and, consequently, the probabilities are described by fairly cumbersome and asymmetric expressions for the dependences on the phases [102]. This is true, for example, of Al [103] when what are called the β orbits are considered.

4.3 Resistance oscillations in a simple model of a metal

We shall consider the magnetoresistance in a simple model of a metal with a periodic MB configuration, which has small closed diangular orbits (Fig. 4d). We shall ignore the time spent by conduction electrons in small orbits and replace them by effective MB nodes (points). The result is a reduced MB configuration which is shown schematically in Fig. 9c.

In the zero-spin model this example is considered in greater detail in Shoenberg's book [8] where the effective path method proposed by Pippard [4, 46, 104] is used. Similar expressions can be derived starting from the transport equations (117) [6]. We shall obtain an expression for the resistance on the basis of the theory developed above and we shall show that if the SOC is included, the resistance oscillations have the structure of double peaks.

We shall begin with a qualitative explanation of the dependences of the conductivity σ on the effective probabilities P and Q ignoring the spin degrees of freedom. Let us turn to Fig. 9c. Starting from a point A and moving along an MB configuration characterised by $P = 0$ ($Q = 1$), a conduction electron is in *infinite* motion along the upper path. A small orbit does not transmit this electron. When high fields ($H \gg H_0$) are applied or when $P = 1$ ($Q = 0$), a conduction electron moves only along a closed circular path. The total transparency of the small orbit (in the absence of the spin degrees of freedom!) leads to *finite* motion of the electron.

Under advanced breakdown conditions ($PQ \neq 0$) we can expect features typical of these two types of motion. Expressions obtained from the semiclassical theory [11–13] of the galvanomagnetic properties of a metal are quite different in the case of closed and open paths.

We shall assume that in the case of advanced breakdown a conduction electron moves along an open path. Under the intermediate MB conditions the role of the effective electron-scattering time τ^* is played by the scattering time for MB nodes. It is the MB scattering that disturbs infinite motion of conduction electrons in this case. The frequency of such scattering can be easily estimated. The frequency is proportional to $\omega_c P$, where P is the probability of the escape of a conduction electron from an *open* orbit to a *closed* one. It follows from semiclassical concepts [11, 13] that the motion along an open path resembles the motion of a conduction electron in the absence of a magnetic field. If the open direction coincides with p_y, then

$$\sigma_{xx} \approx \sigma_0 = \frac{ne^2\tau^*}{m^*} \tag{133}$$

Here σ_0 is the conductivity when $H = 0$; n is the number of electrons per unit volume, m^* is the effective mass. Since $\omega_c = eH/m^*c$, we can rewrite the conductivity (133) thus:

$$\sigma_{xx} \approx \frac{nec}{H}\frac{1}{P}. \tag{134}$$

Let us now assume that the same conduction electron moves along a closed orbit. In this case the role of τ^* is played by the effective time spent on closed orbits, such that $\tau^{*-1} \approx \omega_c Q$, where Q is the probability of the escape of a conduction electron from a *closed* orbit to an *open* one. In the case of closed orbits [11–13] the motion in a plane perpendicular to the applied magnetic field resembles a diffusion walk. A conduction electron moves for a long time along a closed orbit and the longitudinal conductivity component decreases inversely proportional to the square of the magnetic field:

$$\sigma_{xx} \approx \frac{\sigma_0}{(\omega_c\tau^*)^2}. \tag{135}$$

Substitution of the expression for the conductivity (133) and of τ^* in expression (135) gives

$$\sigma_{xx} \approx \frac{nec}{H}\,Q\,. \tag{136}$$

Therefore, σ_{xx} is on the one hand proportional to Q [as in the above expression] and, on the other, it is inversely proportional to P [as in expression (134)]. Consequently, the total conductivity should be

$$\sigma_{xx} \approx \frac{nec}{H}\frac{Q}{P}. \tag{137}$$

It should be noted that in the case of small values of the products such that $PQ \to 0$ the collision frequency is again determined by the real scattering time $\tau^* = \tau_p$ [defined by inequalities (54)].

We shall now derive an expression for the conductivity tensor which takes account of the spin degrees of freedom and we shall do this on the basis of the transport equations (117)–(120). This can be done if we find the dependence of $\boldsymbol{\Psi}_i$ on the effective probabilities P^σ and Q^σ. If the collision integral in the Boltzmann equation (117) is ignored, the x component of $\boldsymbol{\Psi}_i^x$ is

$$\Psi_i^x(t_i) = \Psi_i^x(0) - \frac{c}{eH}\left[p_y^i(t_i) - p_y^i(0)\right]. \tag{138}$$

Here $\Psi_i^x(0)$ is the value of the distribution function at the beginning of the ith section and the second term in the above expression follows from Eqn (7).

If $t_i = T_i$, then expression (138) becomes

$$\Psi_i^x(T_i) = \Psi_i^x(0) + \frac{c}{eH}\,\Delta_i\,, \tag{139}$$

where $\Delta_i = n_i b_y$ represents an increment in the coordinate p_y due to the passage of a conduction electron along the ith section [the definition of n_i is given in the text following expression (59)]. It is important to note that the open periodic MB configuration shown in Fig. 9c has the property

$$\sum_i^N \Delta_i = b_y \sum_i^N n_i = 0\,. \tag{140}$$

It follows from the system of equations (117) and from formula (120) that if $\hat{I} = 0$ the component σ_{xx} is given by

$$\sigma_{xx} = \frac{e^2}{(2\pi\hbar)^3}\frac{eH}{c} \times \sum_i \int_0^{b_z} \mathrm{d}p_z \int_0^{T_i} \frac{\partial\Psi_i^x(t_i)}{\partial t_i}\,\Psi_i^x(t_i)\,\mathrm{d}t_i\,, \tag{141}$$

where the integral with respect to time is

$$\frac{1}{2}\left[\Psi_i^{x2}(T_i) - \Psi_i^{x2}(0)\right]. \tag{142}$$

The boundary conditions (118) for the reduced MB configuration (Fig. 9c) in the case of stochastic motion of conduction electrons along large sections [condition (115)] become

$$\begin{aligned}\Psi^x_{A'\sigma}(0) &= Q^\sigma\,\Psi^x_{A\sigma}(T_A) + P^\sigma\,\Psi^x_{B'\sigma}(T_{B'}),\\ \Psi^x_{B'\sigma}(0) &= P^\sigma\,\Psi^x_{A'\sigma}(T_{A'}) + Q^\sigma\,\Psi^x_{B''\sigma}(T_{B''}).\end{aligned} \tag{143}$$

The spin index is included explicitly above, although earlier it has been incorporated in i. The condition of periodicity of the function $\Psi_i^x(\boldsymbol{p})$ in terms of p_y leads to

$$\Psi^x_{A\sigma} = \Psi^x_{A'\sigma}, \quad \Psi^x_{B\sigma} = \Psi^x_{B'\sigma} = \Psi^x_{B''\sigma}.$$

It therefore follows that formulas (143) can be rewritten in the form

$$\begin{aligned}\Psi^x_{A\sigma}(0) &= Q^\sigma\,\Psi^x_{A\sigma}(T_A) + P^\sigma\,\Psi^x_{B\sigma}(T_B),\\ \Psi^x_{B\sigma}(0) &= P^\sigma\,\Psi^x_{A\sigma}(T_A) + Q^\sigma\,\Psi^x_{B\sigma}(T_B)\end{aligned} \tag{144}$$

Substitution of formulas (144) and (142) in expression (141) yields the following expression for a component of the conductivity tensor:

$$\sigma_{xx} = \sum_\sigma \sigma^\sigma_{xx} = \sum_\sigma \frac{e^2}{(2\pi\hbar)^3}\frac{eH}{c} \times \int_0^{b_z} \mathrm{d}p_z\, Q^\sigma P^\sigma \left[\Psi^x_{A\sigma}(T_A) - \Psi^x_{B\sigma}(T_B)\right]^2. \tag{145}$$

The symmetry of the MB configuration (Fig. 9c) and the property (140) give

$$\Psi^x_{A\sigma} + \Psi^x_{B\sigma} = 0, \quad \Delta_A + \delta_B = 0. \tag{146}$$

Substitution of expression (139) in expression (145), subject to the equalities (146), gives σ^σ_{xx}

$$\sigma^\sigma_{xx} = \frac{e^2}{(2\pi\hbar)^3}\frac{eH}{c} \times \int_0^{b_z} \mathrm{d}p_z \cdot 4Q^\sigma P^\sigma \left(\Psi^x_{A\sigma}(0) + \frac{c}{eH}\Delta_A\right)^2. \tag{147}$$

We can determine the quantity $\Psi^x_{A\sigma}(0)$ if in the boundary conditions (144) we replace $\Psi^x_{A\sigma}(T_A)$ and $\Psi^x_{B\sigma}(T_B)$ with the values of the function (139). The qualities (146) give

$$\Psi^x_{A\sigma}(0) = \frac{c}{eH}\Delta_A\frac{Q^\sigma - P^\sigma}{2P^\sigma}. \tag{148}$$

Substitution of the function (148) in expression (147) subject to property (140) gives the expression

$$\sigma^\sigma_{xx} = \frac{ecb_y^2}{(2\pi\hbar)^3 H}\int_0^{b_z} \mathrm{d}p_z\,\frac{Q^\sigma(p_z)}{P^\sigma(p_z)}. \tag{149}$$

We shall obtain the results specifically for circular orbits (Fig. 9c). For simplicity, we shall also assume that the Fermi surface is cylindrical. Then Q and P are independent of p_z and $b_y = 2p_\perp$, where $p_\perp$ is the radius of the circle. Since $2V_p/(2\pi\hbar)^3 = n$, where $V_p = b_z\pi(p_\perp)^2$ is the volume occupied by a conduction electron, we finally obtain

$$\sigma^\sigma_{xx} = \frac{nec}{H}\frac{2Q^\sigma}{\pi P^\sigma}. \tag{150}$$

The remaining components of the conductivity tensor can be found by the conventional semiclassical approach [11–13] when the average of the velocities along closed orbits is zero.

The conductivity tensor then looks as follows:

$$\sigma^\sigma = \frac{nec}{H}\begin{bmatrix}\dfrac{2Q^\sigma}{\pi P^\sigma} & -\dfrac{1}{2}\\ \dfrac{1}{2} & 0\end{bmatrix}. \tag{151}$$

This expression agrees with the qualitative estimate (137) and it is easy to understand from the physics point of view. If $Q^\sigma = 0$, conduction electrons move along closed orbits and the conductivity σ_{xx} along an MB network is zero. If $Q^\sigma = 1$, and $P^\sigma = 0$, a conduction electron can escape to infinity, so that 'superconductivity' appears. We have mentioned earlier that in these limiting cases we should use the real momentum relaxation time τ_p, which leads to finite values of the conductivity. In the collision-free case, conduction electrons cannot move along the y axis (transversely relative to the open direction), which is understandable. This is why in the adopted approximation the component σ_{yy} also vanishes.

Therefore, inclusion of the spin degrees of freedom gives rise to the conductivities $\sigma^\uparrow_{xx}$, and $\sigma^\downarrow_{xx}$, which oscillate together with the effective MB probabilities. Summation over the spin index in Eqn (145) can yield an expression for the resistivity tensor $\rho_{\alpha\beta} = \sigma^{-1}_{\alpha\beta}$. The expression for the component ρ_{yy} is:

$$\rho_{yy} = \frac{2H}{\pi nec}\left[(P^\uparrow)^{-1} + (P^\downarrow)^{-1} - 2\right], \tag{152}$$

where use is made of $P^\sigma + Q^\sigma = 1$. Expressions (151) and (152) are fully identical with the results obtained by the effective path method taking the spin into account [66].

The above expression for the resistivity can be presented graphically. In the limit of strong fields $H \gg H_0$ the resistivity ρ_{yy} oscillates (Fig. 10) approaching the value ρ_{sat}. Here, $\rho_{\mathrm{sat}} = 8H_0/\pi nec$ is the saturation value of the resistivity calculated ignoring the coherent small-orbit effects, i.e. assum-ing completely stochastic MB. This result can be obtained formally by averaging expression (152) over the phase (dotted curve in Fig. 10b).

In the limiting case when the spin degrees of freedom are ignored, i.e. when $\gamma^s_q = 2\pi r$ (r is an integer) but for any value of α, we obtain the zero-spin results from expression (152) [5, 8]. This result is represented by the continuous curve in Fig. 10b. We can see that, for specific magnetic fields, defined by the relationship (132) the resistance of a linear MB network falls to zero. This corresponds to complete inter-ference transparency of small diangular orbits [see also the discussion following relationship (132)].

In general, the behaviour of the transverse resistivity curve $\rho_{yy}/\rho_{\mathrm{sat}}$ in intermediate fields depends on the small-orbit g factor g_q and on the SOC parameter α. In the case of coherent motion of conduction electrons along a diangular orbit when possible spin flip ($\alpha \neq 0$) is taken into account, the number of the oscillation peaks is doubled. The relative amplitudes of two peaks from one zero spin parent depends

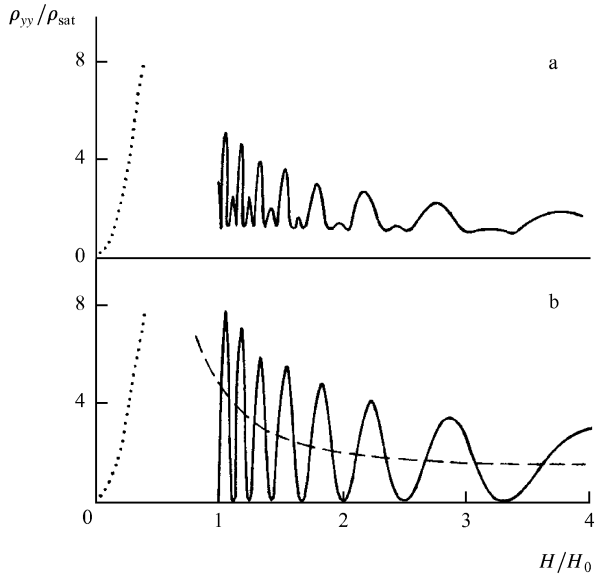

Figure 10. MB oscillations of the transverse magnetoresistance ρ_{yy}/ρ_{sat} plotted for the MB configuration shown in Fig. 4d: (a) totally coherent motion of conduction electrons along a diangular orbit ($\alpha = 0.4$ and and $\gamma_m^s = 0.4\pi$); (b) continuous curve represents the results of Refs [4, 8] for any value of α and $\gamma_m^s = 2\pi r$ ($r = 0, 1, 2, \ldots$); the dashed curve corresponds to stochastic motion of conduction electrons in a small orbit. In plotting these curves the area S_m of the small orbit is assumed to be $(2\pi\hbar e/c) \times 10H_0$.

on g_q. This is shown in Figs 10a and 11a. Fig. 11b illustrates the fact that if the SOC is ignored, the inclusion of g_q in expressions (151) and (152) alters the oscillation amplitudes, but does not double the number of peaks.

It therefore follows that the adopted model makes it possible to account consistently for the appearance of a complex structure of the MB oscillation peaks by the SOC and by the spin splitting of the Landau levels. It should be noted that similar splitting of the peaks was observed by Stark [101] for Zn (this is discussed in detail later).

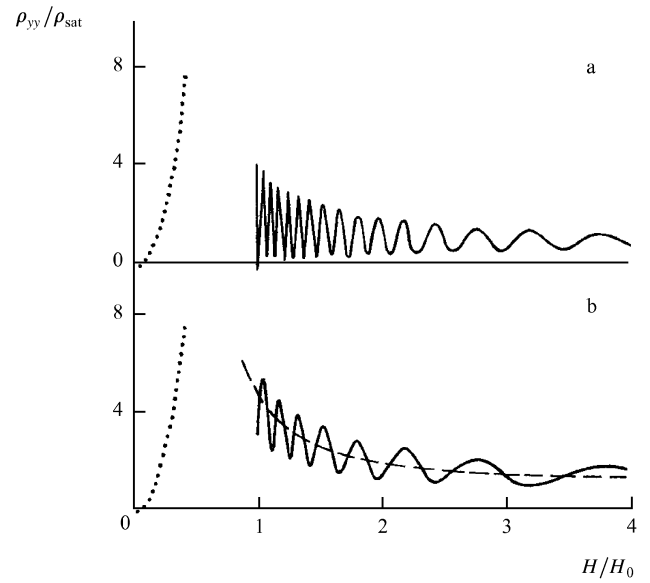

Figure 11. MB oscillations of the transverse magnetoresistance ρ_{yy}/ρ_{sat}: (a) $\alpha = 1$, $\gamma_m^s = 0.5\pi$; (b) SOC is ignored ($\alpha = 0$), continuous curve $\gamma_m^s = 0.4\pi$, and the dashed curve to $\gamma_m^s = 0.5\pi$. The values of S_m used in plotting these curves are the same as in Fig. 10.

It should also be noted that Sowa and Falicov investigated [57] the influence of small-angle scattering on the MB oscillations in a metal described by the same model. A similar double-peak structure is predicted there and the stronger the small-angle scattering, the flatter are the oscillation peaks. Peak doubling reported in Ref. [57] originates from the assumption of the authors about the bimodal nature of the distribution of the small-orbit areas, which leads to the possibility of the existence of conduction electrons with two different phases in the course of different passages through a section *i*. The results reported in this review allow us to conclude that among possible reasons for the appearance of a bimodal distribution are the spin splitting of the Landau levels, [described by relationship (60)] in a magnetic field and the spin flip of conduction electrons under the MB conditions because of the SOC.

4.4 Galvanomagnetic properties of zinc: theory and experiment

We shall now adopt a model which corresponds more closely to reality. In the case of hcp metals (Be [7], Mg, and Zn [5, 55, 101]) a hexagonal two-dimensional MB configuration appears if the field $\boldsymbol{H}$ is parallel to the hexagonal axis of a crystal (Fig. 3). The Fermi surfaces of these metals are well known (Fig. 3a) [90]. In our analysis the important parts are those associated with MB: a 'hole' monster, which lies in the second band and whose characteristic dimensions are comparable with the dimensions of the Brillouin zone, and six small electron sheets in the form of cigars or needles, which are in the third band and are located on the vertical edges of the Brillouin zone.

If $H \ll H_0$, the numbers of electrons and holes are equal. All the orbits are in this case closed and, in the absence of MB, the resistance rises proportionately to H^2, which is typical of compensated metals [11]. However, MB disturbs the exact compensation and open as well as closed orbits appear. If $H \gg H_0$, all the charge carriers (both those which move along giant orbits in the course of breakdown and those which move along an inner belt of the monster) have an electron spectrum and, therefore, the magnetoresistance saturates. If a sample is of sufficiently high quality so that the motion of conduction electrons along a small triangular orbit is coherent the resistance oscillations appear and they correspond to the area of a small triangular orbit which may be the area of a needle in the case of Zn [101] or a cigar in the case of Mg [5] and Be [7]. These are the orbits which can be regarded as effective MB nodes [5, 6], which are only slightly more complex than diangular orbits (Fig. 9b).

The effective MB probabilities (130) and (131) oscillate if the phase coherence is conserved in the course of motion of conduction electrons along these small orbits. It is obvious that the characteristic cyclotron frequency of a small triangular orbit ω_c^θ is much greater than the cyclotron frequency of a large hexagonal orbit ω_c^χ [5, 8], i.e. conduction electrons move stochastically over large sections of an MB network (the phase of their wave function is lost!) and they move coherently along small orbits.† This corresponds to the real situation of the *intermediate* MB regime described by inequalities (115).

† Here and in Section 5, the index θ indicates a small orbit of the triangular type and the index χ refers to a hexagonal orbit.

Since the dimensions of the needles are much less than those of the monster, such an MB network can be replaced by a reduced network in which all small triangular orbits are replaced by effective MB nodes described by the effective s matrices $\hat{S}^{\text{eff}}$. In our case, when the spin degrees of freedom are taken into account, the unitary matrix $\hat{S}^{\text{eff}}$ is of sixth rank. The expressions for some of its matrix elements are given in Section 4.2 [see set of expressions (126)].

In calculation of the galvanomagnetic properties of Zn which has a two-dimensional MB network with small orbits, it is convenient to use the 'effective path' method [104]. This method is applied to hcp metals (Zn and Mg) in Refs [4, 55] and it is given in a sufficiently detailed form in Ref. [8]. A more general approach [18], based on consistent derivation of the transport equation, unfortunately has not yet been developed for quantitative analysis of two-dimensional MB networks [6].

Generalisation of the effective path method to the case of existence of a probability of spin-flip MB in the intermediate MB regime, which is defined by condition (115), can be found in Refs [64–66]. Our analysis will be based on Ref. [66], where the galvanomagnetic properties of Zn are considered.

The results obtained by the effective path method can be written down conveniently in terms of a complex variable $x + iy$. In this case the conductivity becomes

$$\hat{\sigma} = \sigma_{xx}^{\sigma} - i\sigma_{yx}^{\sigma} . \tag{153}$$

In contrast to the preceding section, we have to bear in mind that a layer of MB configurations in terms of p_z has a finite thickness $2p_{zm}$ and the MB parameters (τ and α), as well as the cross-sectional area of a small orbit $S_q = S_\theta$, are functions of p_z.

Averaging over the initial spin orientations (a similar averaging procedure is used in calculations dealing with the Kondo effect), we obtain

$$\hat{\sigma} = \frac{1}{2}\sum_{\sigma} \hat{\sigma}^{\sigma},$$

and, omitting the intermediate steps given in Ref. [66], we find the expression for the total conductivity tensor $\hat{\sigma}$ is

$$\hat{\sigma} = \frac{b}{Hp_{zm}} \int_0^{p_{zm}} \hat{D}(p_z)\, dp_z + \frac{a}{H^2}. \tag{154}$$

The components of the tensor $\hat{D}$ are

$$D_{xx} = \frac{1}{4}\sum_{\eta} \frac{1 + 3|\Gamma_\eta|^2\tau^2}{1 - 3|\Gamma_\eta|^2 + 3|\Gamma_\eta|^4(1 + \tau^2 + \tau^4)} - \frac{1}{2},$$
$$D_{xy} = -\frac{\sqrt{3}}{4}\sum_{\eta} \frac{1 - |\Gamma_\eta|^2(2 + \tau^2)}{1 - 3|\Gamma_\eta|^2 + 3|\Gamma_\eta|^4(1 + \tau^2 + \tau^4)} + \frac{\sqrt{3}}{2}. \tag{155}$$

The summation is carried out over the small-orbit spin index η:

$$|\Gamma_\eta|^2 = |\Gamma_{i,j}^{\eta}|^2 \frac{1}{1 + \tau^6 - 2\tau^3 \cos\gamma_{\theta\eta}}. \tag{156}$$

The second term in Eqn (154) describes the contribution made to the conduction process by all the closed orbits that do not participate in MB. In this sense the quantity a is a fitting parameter in the theory [8, 55, 66]. In the absence of MB, all the electron orbits are in this case closed and if $\omega_c\tau^* \gg 1$, they make the usual contribution to $\sigma_{xx} \approx a/H^2$ [11–13]. The resultant narrow layer of open (because of MB) orbits (for zinc, we have $p_{zm} \approx 0.04p_F$ [105]) is represented by the first term in expression (154). It is this term that dominates the galvanomagnetic properties under advanced MB conditions (when $(H \geqslant H_0)$.

In the limiting case when there is no MB, the whole component of the conductivity tends to zero ($\sigma_{xy} \propto H^{-2}$), as expected [11–13], because a metal is completely compensated in fields $H \ll H_0$. The quantity b, which represents the imbalance between electrons and holes which appears as a result of MB, can be estimated from the integral

$$b = \int_0^{p_{zm}} \frac{6nec}{\pi}\, dp_z . \tag{157}$$

Here, $n(p_z)\, dp_z$ determines the number of conduction electrons per unit volume in an elementary section of the Fermi surface.

Eqns (154) and (157) are written down on the assumption that $n(p_z)$ varies smoothly with p_z, in contrast to $\hat{D}(p_z)$ which varies periodically with the phase $\gamma_{\theta\eta}(p_z)$. This phase is given by expression (124) except that the notation is altered: $q \to \theta$. If a conduction electron moves stochastically over small-orbit sections ($\omega_c^{\theta} < \tau_{s.a}^{-1}$), the result should be stochastisation of the phase $\gamma_{\theta\eta}$ in Eqn (156). Consequently, the results can be obtained in the limit of stochastic MB if Eqns (154) and (155) are averaged over this phase (see Refs [57, 58, 66]).

In general, the conductivity of Eqn (154) depends on the magnetic field H, on the microscopic parameters of MB nodes, on the thickness $2p_{zm}$ of an MB layer, and on the fitting parameter α. The strongest dependence on p_z in the integrand applies to the area of a triangular orbit [55]

$$S(p_z) = S_0 + \zeta p_z^2, \tag{158}$$

where S_0 is the extremal section of a needle ($p_z = 0$). The needle narrowing parameter

$$\zeta = \frac{1}{2}\left(\frac{\partial^2 S}{\partial p_z^2}\right)_{p_z=0}$$

has been estimated on the basis of various theoretical models. In particular, the following estimates of ξ are given in Refs [5, 55]: $\zeta_1 = -1.13 \times 10^{-2}$ a.u. and $\zeta_2 = -1.77 \times 10^{-2}$ a.u. The components of the resistivity tensor are related to $\hat{\sigma}$ by the expressions

$$\rho_{xx} = \frac{\sigma_{xx}}{\sigma_{xx}^2 + \sigma_{xy}^2}, \quad \rho_{xy} = \frac{\sigma_{xy}}{\sigma_{xx}^2 + \sigma_{xy}^2}. \tag{159}$$

We shall now discuss the results obtained and then compare them with the published experimental data of Stark [101] and Falicov, Pippard, and Sievert (FPS) [55]. The theoretical dependences were fitted to the experimental data by the least-squares method in a wide range of values of H_0^0 (2–6 kG). The optimal values of the parameters were found by the simplex method [66]. The results of this procedure are plotted in Figs 12 and 13, and the parameters found are compared with the known values in Table 1. The following quantity is used in this table:

$$g_{\theta}^{s} = g_{\theta}\frac{m_{\theta}}{2m}. \tag{160}$$

The value of b lies within the limits $(0.67–0.695) \times 10^8$ kG Ω^{-1} m^{-1}. This value can be used together with

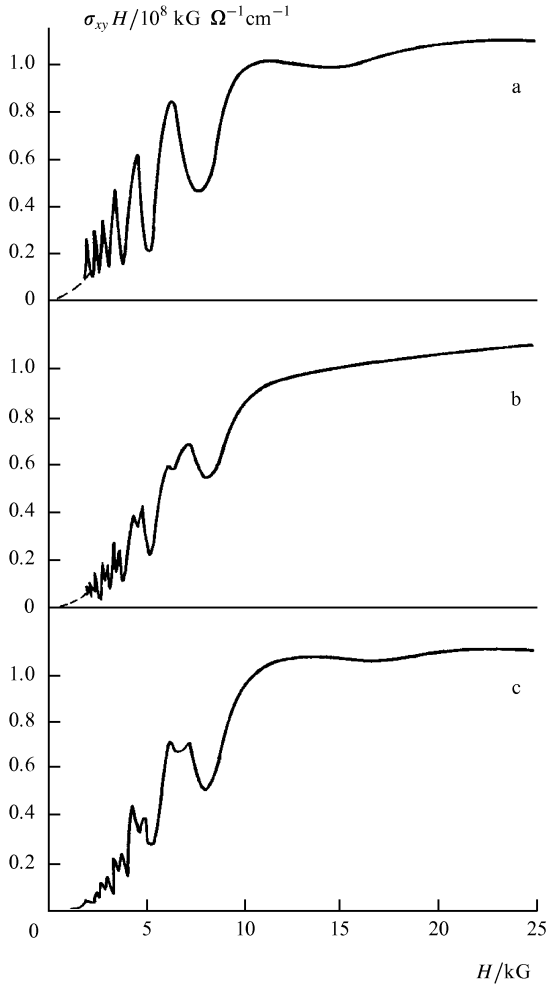

Figure 12. Oscillations of the off-diagonal component of the conductivity tensor $\sigma_{xy}H$: (a) theoretical results [55]; (b) theoretical results taking account of the SOC [66]; (c) experimental curves [101] taken from [55]. The parameters used in calculation of the theoretical curves are listed in Table 1.

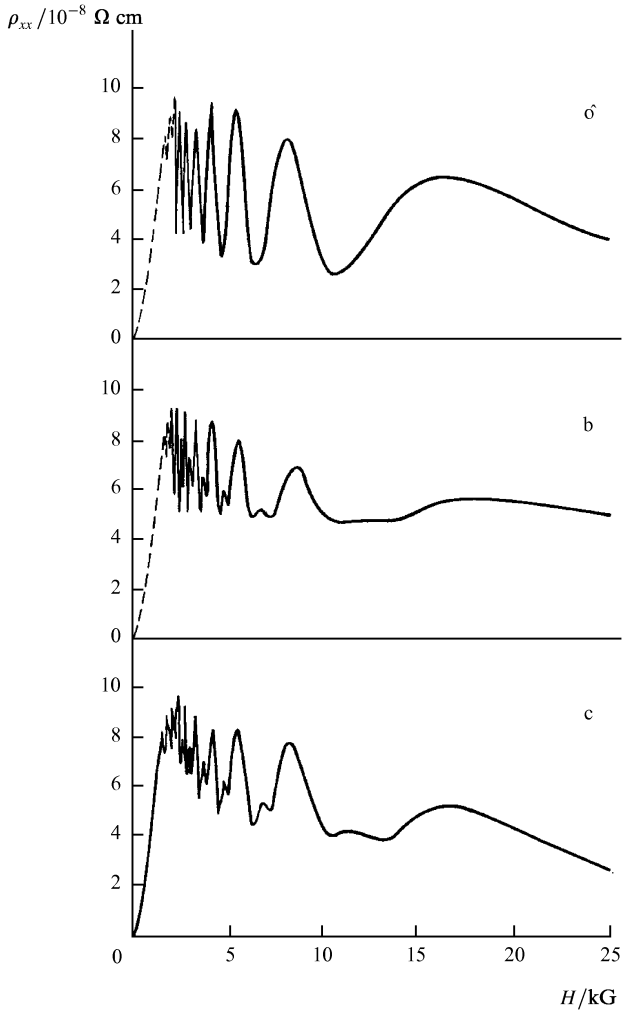

Figure 13. Oscillations of the field dependence of the magnetoresistance ρ_{xx}: (a) theoretical results [55]; (b) theoretical results taking account of the SOC [66]; (c) experimental curves [101] taken from [55]. The parameters used in calculation of the theoretical curves are listed in Table 1.

the integral (157) to find the 'experimental' estimate of the half-width of an MB belt on the needles: $p_{zm}^{\exp} \approx (1.8 - 1.9) \times 10^{-2}$ a.u., which is close to the theoretical estimate of the half-width of the belt on the monster, $p_{zm}^{\text{theor}} = 1.95 \times 10^{-2}$ a.u. [55]. This agreement supports the adopted model.

It should be noted that the integral with respect to p_z, encountered in the calculation of $\hat{\sigma}H$, was calculated in Ref. [55] by simple summation. The interval $0 < p_z < p_{zm}$ was split into 20 layers equidistant from one another. It follows from our calculations [66] that the adoption of this procedure in the calculation of an integral of the type described by Eqn (154) leads to errors of the order of 20% – 40%.

We carried out numerical integration by adopting one of the modifications of the Simpson method (the relative error did not exceed 1% and the number of layers in weak fields $H \leqslant H_0$ reached 320).

Naturally, the FPS results [55] can be obtained also from our formulas if the following changes are made:

(1) it is assumed that $\alpha = 0$, i.e. that the SOC does not affect MB;

(2) if the dependence on the spin of conduction electrons is removed from all formulas, i.e. if the spin index is dropped and no summation over the spin is carried out; the conductivity can then be calculated from an expression which differs only slightly from the integral (154);

(3) if the phase acquired by a conduction electron in a revolution around a small orbit is altered:

$$\gamma_{\theta\eta} \to \gamma_\theta^{\text{FPS}} = \frac{c\hbar}{eH} S_\theta(p_z) + \gamma_0 ,$$

Table 1.Parameters of theoretical curves plotted in Figs 12 and 13, compared with the results reported in Ref. [55].

Calculation parameters	Ref. [55]	Ref. [66]
$a/10^8$ kG^2 Ω^{-1} cm^{-1}	0.17	0.17
$b/10^8$ kG^2 Ω^{-1} cm^{-1}	0.67	0.67
H_0 (H_0^0)/kG	2.7 (–)	3.0 (3.7)
$S_0/10^{-5}$ a.u.	4.24	4.05
$p_{zm}^{\exp}/10^{-2}$ a.u.	2.0	1.83
$\zeta/10^{-2}$ a.u.	–1.77	–1.13
$g_\theta^s = g_\theta m_\theta/2m$	–1.22	0.41
α	–	0.75

where $\gamma_0 = -3.84$ is a parameter introduced in the theory and independent of the magnetic field; in the FPS theory [55] this parameter is needed to improve the agreement with the experimental results and to estimate the value of the g factor of conduction electrons in a needle.

Since the spin contribution to the phase, given by expression (124), is determined to within $2\pi r$ (r is an integer), our value of g^s can be used, in combination with $m_\theta/m_0 = 0.0075$ [8], to estimate the g factor of conduction electrons in a needle: $g_\theta \approx 109 + 642r$. In view of the theoretical restriction on this value, $g_\theta < 266$ [91, 105], we obtain $g_\theta \approx 109$, in agreement with the estimates given in Ref. [91].

The value of the SOC parameter $\alpha = 0.75$ confirms that in the case of Zn the SOC has a strong influence on the spectrum in MB regions. In this sense this metal can be regarded as a test ground for checking the theory of spin-flip MB (see Sections 5 and 6, where we shall consider the de Haas–van Alphen effect and conduction-electron spin resonance). It is evident from expression (50) that inclusion of the SOC increases somewhat the interband gap Δ: the increase is by a factor of $(1+\alpha^2)^{1/4} \approx 1.1$, compared with the estimates based on the breakdown field H_0^0 in the absence of the SOC. The value of the breakdown field H_0, which depends on the SOC parameter α is given in Table 1 and is in agreement with the experimental data [106].

The proposed theory, like the FPS theory [55], agrees poorly with experiments carried out in low fields ($H \leqslant H_0$). This is manifested by the appearance of hf oscillations with a considerable amplitude, which does fall when the field is reduced but not as fast as in the experiments. However, this is associated with the limited nature of the adopted model of intermediate MB and of the effective path method. The role of small-angle scattering may increase in weak fields. In fact, even partial stochastisation of the motion of conduction electrons along small orbits should result in flattening of the sharp peaks of the MB oscillations [57, 58]. Naturally, in the case of completely stochastic MB, the oscillations disappear completely, as demonstrated by the simple model (Fig. 10). The theoretical curves plotted in Figs 12 and 13 for weak fields ($H \leqslant 2$ kG) are based on the experimental dependences. These weak-field parts of the theoretical curves are shown dashed in the figures.

It follows from Figs 12 and 13 that a consistent theory of MB which takes account of spin flip explains much better not only the nature of the behaviour of the experimental curves (appearance of a fine structure in the form of double peaks), but also ensures a satisfactory quantitative agreement with experiments in the case of such complex oscillations. Hence, it follows that under the experimental conditions described in Ref. [101] the intermediate MB regime is observed.

5. The de Haas – van Alphen effect under spin-flip magnetic breakdown conditions

5.1 Fundamentals of the theory of the de Haas – van Alphen effect

Oscillations of the thermodynamic potential and of its derivatives in a magnetic field, i.e. the de Haas–van Alphen (dHvA) effect, provide reliable information on the energy structure of metals and Fermi surfaces [8, 11–13]. These oscillations appear because discrete quasiequidistant energy levels cross consecutively the Fermi energy ϵ_F when the magnetic field is varied. This is possible only in the presence of closed electron orbits on the Fermi surface and in the semiclassical approximation these orbits should satisfy expressions (1) and (8).

Let us recall the main principles of the theory of the dHvA effect in its general form. It is well known (see, for example, Refs 11, 13]) that, in the case of a system which obeys the Fermi–Dirac statistics and has states with an energy E, the thermodynamic potential is given by the expression

$$\Omega = -k_B T \sum \ln\left(1 + \exp\frac{\mu - E}{k_B T}\right). \tag{161}$$

Here and later in this section the quantity μ is the chemical potential equivalent to ε_F. The summation in expression (161) is carried out over all possible states. The energy $E = E(n, p_z, \sigma)$ is defined as the solution which satisfies the implicit equation (19) with the quantum number n.

The oscillatory part of the thermodynamic potential (161) is calculated in the standard way [11, 13, 74]. As usual, fast oscillations of the cosines that contain the semiclassical phases described by formula (15) have the effect of selecting the values of $S^\xi(E, p_z)$ which are extremal in terms of p_z when $E = \varepsilon_F$ (the index ξ identifies the extremal sections).

The expression for the oscillatory part $\tilde{\Omega}$ of the thermodynamic potential per unit volume of a metal is

$$\begin{aligned}
&\tilde{\Omega} = \sum_\xi \tilde{\Omega}_\xi, \\
&\tilde{\Omega}_\xi = \left(\frac{e}{2\pi c\hbar}\right)^{3/2} \frac{e\hbar H^{5/2}}{\pi^2 c m_\xi} \left|\frac{\mathrm{d}^2 S^\xi}{\mathrm{d}p_z^2}\right|^{-1/2} \\
&\quad \times \sum_{r=1}^{\infty} \frac{R_T R_D R_s}{r^{5/2}} \cos\left[2\pi r\left(\frac{F_\xi(E, p_z)}{H} + \frac{1}{2}\right) \pm \frac{\pi}{4}\right],
\end{aligned} \tag{162}$$

where

$$F_\xi = \frac{c S^\xi(E, p_z)}{2\pi e\hbar} \tag{163}$$

is the frequency of the dHvA oscillations [8] which can be expressed in terms of the area S^ξ of an extremal section of the Fermi surface described by formula (158),

$$R_T = \frac{rTa_\xi/H}{\sinh(rTa_\xi/H)} \tag{164a}$$

is the temperature factor, and

$$R_D = \exp\left(-\frac{r x_D a_\xi}{H}\right) \tag{164b}$$

is the Dingle factor [8].

The quantity x_D in expression (164b) is known as the Dingle temperature, which is governed by the average scattering time of conduction electrons. Expressions (164a) and (164b) contain the coefficient

$$a_\xi = \frac{2\pi^2 k_B c m_\xi}{\hbar e} = 1.47\,\frac{m_\xi}{m} \times 10^5\ \mathrm{GK}^{-1}. \tag{165}$$

In formula (162) the quantity

$$R_s = \cos\left(\frac{\pi}{2} r g_\xi \frac{m_\xi}{m}\right) = \cos(\pi r g_\xi^s) \tag{166}$$

is the spin factor which appears as a result of superposition of oscillations of conduction electrons with two spin

orientations [8, 11, 13, 74]. As in the preceding sections, the quantity

$$g_\xi^s = g_\xi \frac{m_\xi}{2m} \tag{167}$$

represents the spin splitting parameter.

It should be pointed out that in the case of free conduction electrons ($g_\xi = 2$, $m_\xi = m$) the factor described by expression (166) is simply $(-1)^r$. The spin splitting is exactly equal to the separation between the Landau levels. This remains approximately true also of bands which are characterised by $m_\xi/m \ll 1$, because of the strong SOC, since in this case the relative deviation of the g factor is $\Delta g_\xi/g_0 \approx m/m_\xi$ (see Section 2.3 and Ref. [10]) and, therefore, we have $g_\xi^s \approx 1$. However, even a relatively small deviation of g^s from unity can alter quite strongly the amplitude of the dHvA oscillations.

Expression (162), apart from the Dingle factor (164b), was first derived by I M Lifshitz and A M Kosevich [107] and we shall refer to this expression as the LK formula. As pointed out earlier, in general, the Fermi surface is complex and has several extremal cross sections [represented by the sum over ξ in expression (162)] along a selected direction of the magnetic field and, consequently, several sets of values of F_ξ, m_ξ, and g_ξ. Therefore, the oscillatory quantity consists of the sum with several contributions and each of them is described by the LK formula, but with different values of the parameters.

The LK formula accounts satisfactorily for the experimental results on the dHvA effect. Essentially, it is the main working formula used in determination of the Fermi surfaces of various metals [8, 11, 12]. However, the LK formula ignores the role of MB.†

Under the MB conditions the harmonics of the dHvA effect may include the frequencies F_ξ, which correspond to areas that exceed the dimensions of a section of the Brillouin zone even in the case of metals with a closed Fermi surface. The MB spectrum of conduction electrons is known only for specific directions of the magnetic field and for the symmetric MB configurations (see Sections 3.2 and 3.3). In spite of this, the current ideas on the motion of conduction electrons in a magnetic feld have proved sufficient to develop a theory of the oscillatory effects under the MB conditions [5, 6, 8]. The main feature of the dHvA effect under the MB conditions is a reduction in the amplitude of isolated orbits and an increase in the amplitude of composite orbits as the breakdown probability increases.

An expression for the oscillatory part of the potential $\tilde{\Omega}$ is obtained in Ref. [108] for a simple MB configuration which has two equivalent MB nodes. It is shown there that the LK formula has an additional factor which is due to MB. It should be pointed out that the treatments given by Kochkin [108], in Shoenberg's monograph [8] for Mg, and by Lonzarich and Holtham [103] for Al take into account the influence of the SOC on the dHvA effect, but they ignore spin flip of conduction electrons under the MB conditions. Belokolos [94] deals with MB in Tl and calculates the dHvA effect due to composite orbits.

In general, an oscillatory correction to the thermodynamic quantity under the MB conditions can be calculated by two methods proposed in Refs [6, 56]. They are based on a calculation of the oscillatory part of the number density of states $\tilde{\nu} = \tilde{\nu}(E, p_z)$ of a system with given values of E and p_z.

Falicov and Stachowiak [56] use a theorem relating the number density of states to the Fourier transformations of the Green function. This function corresponds to the sum of semiclassical wave packets which return to a given point of an MB coupled-orbit network following all possible paths. Their amplitudes then decrease in accordance with the number of the MB nodes crossed. The phases are determined by the areas of the sectors bounded by these paths. The method proposed in Ref. [56] yields expressions similar to the LK formula in the case of a one-dimensional MB network (as shown in Fig. 4d, but for circular orbits and ignoring the spin splitting) [5, 8], which are also valid in the case of a more complex real situation of a two-dimensional MB network observed under the MB conditions in Mg (Fig. 3) [5, 8, 56].

The results given in Ref. [56] can be stated as follows: the oscillatory part of the free energy is determined similarly to the sum in expression (162) over all the closed orbits, which are possible in an MB network, except that each term is multiplied by the 'MB weakening' factor

$$R_b = (\mathrm{i}\rho)^{n_1}(\tau)^{n_2}, \tag{168}$$

where n_1 and n_2 are the numbers of the branching points of a given orbit at which respectively breakdown and reflection can be expected. It is assumed that all MB nodes are equivalent. The appearance of the imaginary unity i in expression (168) follows from the condition of conservation of the number of particles in the semiclassical Pippard model [4, 104]. We have seen that in the microscopic theory the breakdown gives rise, in the phase of the wave function of conduction electrons, not to $\pi/2$, which corresponds to i in expression (168), but to a quantity Λ which depends in a complex manner on H_0/H [compare with expression (49)]. In the course of motion along open orbits the phase acquires a correction Rn_i [see formula (58)].

The most consistent derivation of the oscillatory part $\tilde{\Omega}$ of the thermodynamic potential without limitations on the nature and connectivity of MB configurations is given in Refs [6, 49]. The Slutskin method involves representation of the oscillatory part of the number density of states $\tilde{\nu}(E, p_z)$ as a sum of multiple Fourier series (112). The coefficients in this series are expressed in terms of the products of the s-matrix elements for a given MB configuration and the phases are proportional to the areas of closed orbits composed of semiclassical sections.

However, these theories (see also Refs [5–8]) deal with the phenomena associated solely with the orbital motion of conduction electrons under the MB conditions and the spin properties of conduction electrons are included only in the formal sense: the SOC is assumed to alter the value of the g factor of conduction electrons [see expressions (166) and (167)]. In this connection it would be undoubtedly of interest to analyse theoretically the influence of the SOC on the oscillations of the number density of states under the coherent MB conditions, since spin flip of conduction electrons associated with MB leads to interference between semiclassical conduction-electron states with different spin orientations, which influences the dHvA effect.

† The LK formula ignores also the magnetic interaction [8], which is outside the scope of the present review.

5.2 Magnetic breakdown oscillations of the number of states density including the spin degrees of freedom

If we use the definition (112) of the number density of states $\nu(E,p_z)$ under the MB conditions and expand the exponential function [see formula (70)] occurring in $F_{i,i}(\boldsymbol{\gamma}+\mathrm{i}\boldsymbol{0})$ [given by expression (114)] as a Fourier series, we obtain the oscillatory part of the number density of states

$$\tilde{\nu}(E,p_z)=\frac{1}{\pi\hbar}\sum_{i}^{N}T_i\sum_{\boldsymbol{L}}{}'\bar{A}_{i,i}(\boldsymbol{L})'\cos(\boldsymbol{L}\cdot\boldsymbol{\gamma})\,. \tag{169}$$

The Fourier coefficients [representing the smooth part of the probability amplitude, which is discussed after formula (70)]

$$\bar{A}_{i,i}(\boldsymbol{L})=\langle F_{i,i}(\boldsymbol{\gamma}+\mathrm{i}\boldsymbol{0})\exp(-\mathrm{i}\boldsymbol{L}\cdot\boldsymbol{\gamma})\rangle$$

are real because $V^{(0)}_{i,i'}$ are real and unitary. According to expression (69), they represent the product of the s-matrix elements with $\Lambda=0$ for each specific value of $\boldsymbol{L}$. It should be pointed out that, in contrast to formula (4.2.3) given in Ref. [6], expression (169) cannot be summed explicitly over the spin of σ because of the inclusion of the SOC. We recall that in our case the spin index is 'hidden' in the serial number i of a section [see discussion following formula (61)].

In the sum over $\boldsymbol{L}$ in expression (169) the only nonzero amplitudes $\bar{A}_{i,i}(\boldsymbol{L})$ are those with such values of $\boldsymbol{L}$ which generate closed orbits that pass through a section i. All the closed orbits that begin and end in the section i create all possible closed j paths. Each jth path passes l_k times along the kth section of a closed orbit ($k=1,\ 2,\ \ldots,\ N$). For a given $\boldsymbol{L}$, these jth paths differ from one another by the sequence of passing along semiclassical sections of an MB network. The sequence in which the jth path is traversed corresponds to a specific sequence of the serial numbers of the sections $[i,\ \ldots,\ i]$. The serial numbers of the first and last terms in the sequence are identical with the first and second subscripts in $\bar{A}_{i,i}(\boldsymbol{L})$.

Writing down the given values of $\boldsymbol{L}$ in the form $\boldsymbol{L}=r\boldsymbol{j}$, we obtain the following expression for the amplitude $\bar{A}_{i,i}(\boldsymbol{L})$.

$$\bar{A}_{i,i}(\boldsymbol{L})=j_iR_b(r\boldsymbol{j})\,, \tag{170}$$

where $\boldsymbol{j}$ are the N vectors with the relatively prime integer components that have no common divisors; r gives the number of revolutions along the jth path; $R_b(r\boldsymbol{j})$ is a quantity independent of the section number i, but defined uniquely by the N vector $\boldsymbol{L}=r\boldsymbol{j}$. It should also be mentioned that the quantity $R_b(r\boldsymbol{j})$ is equal to the product of the s-matrix elements which are complex amplitudes of the probability of a transition between adjacent parts of the jth path. The number of times that each s-matrix element occurs in $R_b(r\boldsymbol{j})$ is the same as the number of times that the jth path crosses a given MB node. Formula (170) states that the closed j paths $[i,\ldots i',\ldots,i]$, differing in respect of cyclic transposition of the terms in the sequence $[i',\ldots,i,\ldots,i']$, correspond to the same amplitude $\bar{A}_{i,i}(\boldsymbol{L})$. Since there are sequences $[i,\ldots,i]$, invariant under the cyclic transposition ($i'=i$), it follows that the quantities $R_b(r\boldsymbol{j})$ are the same for all such transpositions and that formula (170) contains the number of such sequences j_i.

Therefore, the sum

$$\sum_{l_1,l_2,\ldots,l_N\geqslant 0}{}'\bar{A}_{i,i}(l_1,l_2,\ldots,l_N)$$

with N vectors $\boldsymbol{L}$, which give rise to closed orbits, can be represented as the sum over j paths. It follows from formulas (169) and (170) that

$$\tilde{\nu}(E,p_z)=\frac{1}{\pi\hbar}\sum_{j}\boldsymbol{T}\cdot\boldsymbol{j}\sum_{r=1}^{\infty}R_b(r\boldsymbol{j})\cos(r\boldsymbol{j}\cdot\boldsymbol{\gamma})\,, \tag{171}$$

where the scalar products of the vectors $\boldsymbol{T}\cdot\boldsymbol{j}=T_j$ and $\boldsymbol{j}\cdot\boldsymbol{\gamma}=\gamma_j$ give, respectively, the cyclotron period and the quasiclassical phase acquired by a conduction electron on a closed orbit when this electron begins its motion with one spin orientation and after a time T_j returns to the same point with the unaltered spin orientation.

Summation in expression (171) is carried out over all possible values of j, which generate closed j paths. Following [6], we shall use the term j orbit for all the j paths corresponding to the N vector $\boldsymbol{j}$. The vector $\boldsymbol{j}$ in expression (171) carries information also about the orientations of the spin of conduction electrons on all possible closed orbits.

5.3 Oscillatory part of the thermodynamic potential

It is well known that in the absence of MB the quantum oscillations of the thermodynamic quantities with the magnetic field can be expressed in terms of the oscillatory part of the number density of states $\tilde{\nu}(E,p_z)$ with given values of E and p_z.

The oscillatory part of the thermodynamic potential $\tilde{\Omega}$ is calculated from the number density of states (171) in a manner similar to that used in the standard derivation of expressions (161) and (162). Therefore, we shall give directly the final expression for $\tilde{\Omega}$ per unit volume of a metal [67, 102]. It should be stressed, in general, that it is not possible to sum explicitly over the spin projections:

$$\begin{aligned}\tilde{\Omega}=&\left(\frac{e}{2\pi c\hbar}\right)^{3/2}\frac{e\hbar H^{5/2}}{2\pi^2c}\\&\times\sum_{j,\xi}\left|\frac{\mathrm{d}^2S_j^{\xi}}{\mathrm{d}p_z^2}\right|^{-1/2}\frac{1}{m_{\xi j}}\sum_{r=1}^{\infty}\frac{R_TR_b(r\boldsymbol{j})}{r^{5/2}}\\&\times\cos\left[r\left(\frac{cS_j^{\xi}(E,p_z)}{e\hbar H}+\gamma_j^{\mathrm{s}}+\Lambda_j-2\pi\gamma\right)\pm\frac{\pi}{4}\right].\end{aligned} \tag{172}$$

Here $S_j^{\xi}(E,p_z)$ is the zero-spin area of a closed jth orbit; $2\pi\gamma$ is the constant phase,† which is independent of MB; R_T is the temperature factor identical with that given by formula (164a), except for the following substitutions that represent new summation over all the j orbits:

$$\xi\to\xi\boldsymbol{j}\colon\quad a_{\xi}\to a_{\xi j},\quad m_{\xi}\to m_{\xi j},\quad S^{\xi}\to S_j^{\xi}\,. \tag{173}$$

All the quantities in expressions (172) and (173) dependent on E and p_z are taken to correspond to $E=\varepsilon_{\mathrm{F}}$ and $p_z=p_z^{\xi}$, where the index ξ labels the extremal areas of the j orbits. In the case of closed composite orbits (for example, orbits that do not fit within the first Brillouin zone), exactly as in Ref. [6], all the quantities with the index $\boldsymbol{j}$ are composite MB analogues of the corresponding semiclassical quantities. In particular, γ_j^{s} and Λ_j are given by the relevant sums of the spin contribution (60) and of the phase shifts (49) of the wave function of conduction

† The sum of parameters γ and Λ_j give a quantum correction to the $\frac{1}{2}$ usually employed in the Lifshitz–Onsager formula [8, 11].

electrons which occur along the jth orbit under the MB conditions.

In the case of the j orbits which are in the same zone and for which there is no spin flip of conduction electrons for $\alpha \neq 0$ (as is true, for example, of the triangular orbits on the needles of Zn), it is possible to sum in expression (172) over the spin projections.† When this is done, the expression for $\tilde{\Omega}$ acquires the standard spin factor $R_s(j) = \cos(r\pi g_j^s)$, where g_j^s is the spin splitting parameter of the jth orbit (167) modified by the substitutions (173). In the case of these orbits, expression (172) is identical, apart from the notation, with the formula for $\tilde{\Omega}$ derived in Ref. [6]. Naturally, in the absence of the SOC and spin flip of conduction electrons under the MB conditions ($\alpha = 0$), a similar result is obtained if the spin states are taken into account.

We shall conclude this section by noting that expression (172) ignores the dissipative processes in the electron system. A reduction in the oscillation amplitude, associated with the scattering of conduction electrons, is taken into account by introducing the Dingle factor. It is shown in Ref. [49] that inclusion of the Dingle factor under the MB conditions gives rise to an additional factor in expression (172) and this factor is similar to that given by formula (164b).

5.4 Amplitudes of the de Haas – van Alphen effect for the principal orbits in zinc

We have shown in Section 4 that the SOC has a significant influence on the galvanomagnetic properties of Zn. Therefore, it would be of interest to apply the theory developed above in order to calculate the absolute values of the amplitudes of the dHvA effect contributed by the four main orbits that appear in the central section (summation over ξ will now be ignored) of the hexagonal MB network of Zn (Fig. 3b). The MB factor $R_b(r\boldsymbol{j})$ with $r = 1$ in expression (172) can be calculated by a combinatorial procedure as the sum over j orbits. A simple illustration of this method, applied to several orbits that appear as a result of MB in Mg, is given in Shoenberg's book [8]. For large values of r such a combinatorial calculation of $R_b(r\boldsymbol{j})$ becomes very cumbersome even if the SOC is ignored. It is then more convenient to employ the integral representation of $R_b(r\boldsymbol{j})$ [6].

In dealing with the influence of the SOC on the amplitude of the dHvA effect under the MB conditions from the fundamental point of view one can use a clearer combinatorial method when $r = 1$. This makes it possible to deduce relatively simply the MB factor $R_b(r\boldsymbol{j})$ and to carry out the summation over the spin in expression (172).

Expression (172) for the first harmonic ($r = 1$) but without the Dingle factor gives the magnetic susceptibility of the jth orbit:‡

$$\frac{d\tilde{M}_j}{dH} = \left(\frac{e}{c\hbar}\right)^{3/2}\left(\frac{m}{m_j}\right)^{1/2}\frac{k_B T F_j^2}{H^{5/2}\sinh(a_j T/H)} \times \sum_{\sigma}\dot{R}_b(\boldsymbol{j})\cos\left(\frac{2\pi F_j}{H} + \gamma_j^s + \varphi\right), \quad (174)$$

where F_j is the frequency (163) of the dHvA oscillations for the jth orbit and φ is a constant (for a fixed field H) phase, the value of which is unimportant.

The mass ratio m_j/m in the susceptibility (174) follows from the factor $|\partial^2 S_j/\partial p_z^2|$ in expression (172) for circular orbits and those formed from arcs of a circle (see, for example, the results reported for Mg in Ref. [8], chapter 7), which is true also of Zn (Fig. 3b).

The susceptibility expression (174) is derived ignoring the difference in respect of the spin§ in all the composite MB quantities [apart from the spin contribution to the phase γ_j^s and the MB factor $R_b(r\boldsymbol{j})$, which governs the amplitude $\tilde{\Omega}$]. Moreover, the index j is treated as a scalar quantity, i.e. these MB quantities are replaced with their semiclassical analogues.

The scalar symbol j in expression (174) applies to a set of j orbits of one type, which enclose the same zero-spin area, but differ from one another in respect of the spin orientation in at least one of the sections. Partial summation over $\boldsymbol{j}$ has to be carried out over sets of such orbits and this effectively represents spin averaging.

Since a semiclassical packet crossing MB nodes splits into three [see formula (61)], it follows from the structure of the s matrix (47), where we should substitute $\Lambda = 0$ [6, 9], that $R_b(r\boldsymbol{j})$ for a closed jth orbit is given by

$$R_b(r\boldsymbol{j}) = \left(\pm\frac{\rho}{\beta}\right)^{n_{1j}}\tau^{n_{2j}}\left(\pm\frac{\alpha\rho}{\beta}\right)^{n_{3j}}, \quad (175)$$

where n_{1j} is the number of breakdowns without spin flip; n_{2j} is the number of reflections; n_{3j} is the number of breakdowns with spin flip on the jth orbit; the plus and minus signs for each MB node are defined in accordance with rule (51). For simplicity, we shall assume that all MB nodes are equivalent. The main difference between the above expression and the semiclassical formula (168) is — apart from the difference between the phases discussed earlier — the occurrence of breakdowns with spin flip.

The identical MB factors in expression (175) and the different signs in front of γ_j^s in expression (174) for the phase yield, after averaging over spin, a factor $R_s(j) = \cos(\pi g_j^s)$ for any pair of two j orbits which are of the same type. In the final analysis, the field dependence of the amplitude $d\tilde{M}/dH$ for the jth orbit is governed by the sum over all the orbits which are of the same type, subject to the difference between the spin orientations, and each term in the sum should be multiplied by its own MB factor (175) and also by the factor $R_s(j)$ which appears as a result of spin averaging. Moreover, some paths are characterised by an additional weighting factor C_j, which is related to the symmetry and is equal to the number of ways which can be used to construct a given orbit j [8, 56].

We shall consider a hexagonal MB network of Zn and we shall take account of the doubling of the number of sections because of the SOC (Fig. 3b). As in the case of Mg [8], we shall identify four main types of orbit (Fig. 14): $\odot$ is a giant circular orbit which appears because of MB; θ is a triangular orbit associated with needles; λ is a diangular orbit combining large sections of the monster with small sections of the needles; χ is a hexagonal orbit associated with the monster. The cross-sectional area of the monster is assumed to be negative, i.e. it is assumed that a conduction

† This is true also of closed loops, which may possibly occur in the j orbit and which belong to the same band.

‡ Only the longitudinal component of the magnetic susceptibility $d\tilde{M}/dH = -(\partial^2\tilde{\Omega}/\partial H^2)_\mu$ is considered; here, μ is the chemical potential [see formula (161)].

§ This is usually done in the derivation of the formula for $\tilde{\Omega}$, because $g\mu_B H \ll \mu$.

electron follows a whole orbit opposite to the directions of revolution along electron orbits $\odot$, θ and λ. Some of the orbit characteristics are listed in Table 2.

The circular orbit $\odot$ has twelve MB nodes and it splits into six pairs of large sections and six pairs of small sections, identified by the symbols L (large) and S (small), respectively. It is clear that the remaining orbits can be composed of L and S sections. This splitting makes it possible to determine the spin contributions γ_j^s of all possible orbits shown in Fig. 14 and to calculate directly the product of the factors

$$C_j R_b(j) R_s(j) \tag{176}$$

by the procedure described above.

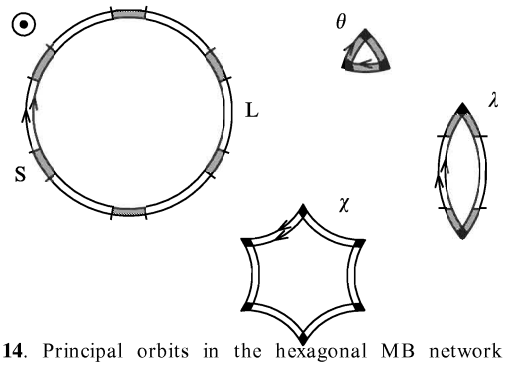

Figure 14. Principal orbits in the hexagonal MB network of Zn calculated taking into account the spin degrees of freedom. The black areas are the points of reflection of conduction of electrons from MB nodes and the shaded regions are MB positions. The characteristics of the orbits of conduction electrons in the absence of spin flip are given in Table 2.

Table 2. Characteristics of the orbits shown in Fig. 14.

Orbit type	$\frac{m_i}{m}$	Weighting factor C_j	No. of breakdowns $n_1 j + n_{3j}$	No. of reflections n_{2j}	dHvA frequency F_j/MHz
$\odot$	1	1*	12	0	831.26 [85]
θ	0.0075 [85]	2	0	3	0.0158 [109]
λ	0.337 [8]	3*	4	2	47.179 [110]
χ	0.0986 [8]	1	0	6	543.31 [110]

* The weighting factor is given for just one orbit ($n_{3j} = 0$).

Calculation of the total amplitudes (176) for the triangular and hexagonal orbits presents no difficulties because there is no spin flip on these orbits. For example, the phases in expression (174) corresponding to such orbits with opposite spins are $\gamma_\theta \pm 3\gamma_S$ and $\gamma_\chi \pm 6\gamma_L$, where $\gamma_j = 2\pi F_j/H + \varphi$ is the phase acquired by a conduction electron when spin is ignored ($j = \theta, \chi$): γ_L and γ_S are the spin contributions to the phase in the large and small sections, respectively. When these phases and the data of Table 2 are used in spin summation, the result is

$$C_\theta R_b(\theta) R_s(\theta) = 2(1-w)\cos(3\gamma_S), \tag{177}$$

$$C_\chi R_b(\chi) R_s(\chi) = (1-w)^3 \cos(6\gamma_L) \tag{178}$$

for the triangular and hexagonal orbits, respectively.

The total amplitude, consisting of the contributions described by formula (176), can be determined for the diangular orbit λ taking account of the spin orientation in each of the sections (Fig. 14). In general, there are five orbit pairs which are of the diangular type. For example, the motion of a conduction electron without spin flip corresponds to the pair of phases

$$\gamma_\lambda \pm 2(\gamma_L + 2\gamma_S).$$

The phase with the plus sign corresponds to the motion of a conduction electron along external spin-up sections without spin flip, whereas the phase with the minus sign represents the motion of such an electron along internal spin-down sections. For this pair expression (176) is of the form

$$3(w^0)^2 (1-w)\cos[2(\gamma_L + 2\gamma_S)].$$

Inclusion of the remaining orbits of this type leads to the following total MB amplitude, which appears in expression (174) and in which the SOC ($\alpha \neq 0$) and the spin contributions of the phase are taken into account:

$$\sum_\lambda C_\lambda R_b(\lambda) R_s(\lambda) = 3(w^0)^2(1-w)\Big\{\cos[2(\gamma_L + 2\gamma_S)] + 4\alpha^2[\cos(\gamma_L + 2\gamma_S)\cos(2\gamma_S - \gamma_L) - 1] + \alpha^4 \cos[2(2\gamma_S - \gamma_L)]\Big\}. \tag{179}$$

In the case of the circular $\odot$ orbit, if spin flip is taken into account in each 12 MB nodes (Fig. 14), the result is 25 orbit pairs differing in respect of the spin orientation in the large and small sections. Inclusion of the symmetry of these orbits in this analysis gives 57 products described by expression (176) with different weighting factors $C_\odot$, even powers of the numbers $n_{1\odot}$ and $n_{3\odot}$, and combinations of the phases γ_S and γ_L.

By way of example, we shall show how to derive some of these products. For example, in the case of motion of conduction electrons without spin flip along the circular orbit $\odot$ (Fig. 14), it is found that the phases, described by expression (174) and corresponding to orbits with opposite spins, are

$$\gamma_\odot \pm \pi g_0^s = \gamma_\odot \pm 6(\gamma_L + \gamma_S),$$

where g_0^s is the spin splitting parameter of the circular orbit. The pair of phases

$$\gamma_\odot \pm 6(6\gamma_S - 2\gamma_L)$$

corresponds to one pair of orbits, which differ symmetrically in respect of the spin orientations. The sign which occurs in the phase in front of γ_L (γ_S) determines the spin orientation in a large L (or small S) section. It is clear that the replacement of the up spin ($\uparrow$) with the down spin ($\downarrow$) transforms one of these orbits into the other. In this case we have $n_{3\odot} = 8$. If all possible orbits on which a conduction electron acquires this phase are included, spin averaging yields

$$15(w^0)^2 (w^s)^4 \cos(2\gamma_S - 6\gamma_L).$$

Another pair of phases $\gamma_\odot \pm 4(\gamma_S + \gamma_L)$ corresponds to two pairs of orbits with different serial numbers of spin-flip breakdowns. The spin orientations in one small and one large section are then opposite to the orientations in the other sections. If all possible orbits are included and the sequence in which conduction electrons cross all MB nodes

is taken into account, spin averaging gives the following expression for these orbit pairs:

$$-12(w^0)^5 w^s \cos[4(\gamma_S+\gamma_L)],\quad 24w^0(w^s)^5\cos[4(\gamma_S+\gamma_L)]$$

respectively.

The contributions of the remaining orbits are found similarly. The final expression for the total MB amplitude of the circular orbit, which appears in expresison (174) after spin averaging, is

$$\sum_{\odot} C_{\odot} R_b(\odot) R_s(\odot) = (w^0)^6 [\cos(6\gamma_+) + \alpha^2\Sigma(1) + \alpha^4\Sigma(2) + \alpha^6\Sigma(3) + \alpha^8\Sigma(4) + \alpha^{10}\Sigma(5) + \alpha^{12}\cos(6\gamma_-)], \quad (180)$$

where the following notation is used to simplify the above expression:

$$\gamma_+ = \gamma_S + \gamma_L,\quad \gamma_- = \gamma_S - \gamma_L,$$

$$\Sigma(1) = 12\{\cos\gamma_-[\cos(5\gamma_+) + \cos(3\gamma_+) + \cos\gamma_+] - [\cos(4\gamma_+) + \cos(2\gamma_+) + 1]\},$$

$$\Sigma(2) = \cos(4\gamma_+)[30\cos(2\gamma_-) + 24] - 48\cos\gamma_-[2\cos(3\gamma_+) + 3\cos\gamma_+] + 24\cos(2\gamma_+)[2\cos(2\gamma_-) + 3] + 27\cos(2\gamma_-) + 96,$$

$$\Sigma(3) = 18\cos(3\gamma_+)[\cos(3\gamma_-) + 4\cos\gamma_-] + 18\cos(3\gamma_-)[\cos(3\gamma_+) + 4\cos\gamma_+] - 36\cos(2\gamma_+)[2\cos(2\gamma_-) + 3] - 36\cos(2\gamma_-)[2\cos(2\gamma_+) + 3] + 288\cos\gamma_+\cos\gamma_- + 4\cos(3\gamma_+)\cos(3\gamma_-) - 184,$$

$$\Sigma(2) \to \Sigma(4),\quad \Sigma(1) \to \Sigma(5)$$

in the substitution $\gamma_+ \to \gamma_-$, $\gamma_- \to \gamma_+$.

In determination of the spin corrections γ_L and γ_S it is natural to assume that the cyclotron mass $m_\odot$ and the g factor $g_\odot$ of the circular orbit $\odot$ are equal to the mass m and to the g factor $g = 2$ of a free electron, since this orbit corresponds to a section of the Fermi sphere in the model of almost-free electrons. The spin splitting parameter for the circular orbit is then unity, i.e. $6(\gamma_L + \gamma_S) = \pi$. In our analysis of the galvanomagnetic properties of Zn (Section 4.4) we derived the spin splitting parameter g^s_θ for a needle, which is 0.41 [see formula (160) and Table 1]. If the spin contribution $3\gamma_S$ in expression (177) for a triangular orbit is πg^s_θ, we obtain

$$\gamma_S = \frac{\pi}{3} g^s_\theta,\quad \gamma_L = \frac{\pi}{6}(1 - 2g^s_\theta). \quad (181)$$

Substitution of expressions (181) into formulas (176)–(180) and substitution of the cyclotron masses and dHvA frequencies listed in Table 2, as well as of the parameters $H_0 = 3.0$ kG and $\alpha = 0.75$ from Table 1, gives the resultant oscillation amplitudes $d\tilde{M}_j/dH$ for each orbit. Fig. 15 shows field dependences of the amplitudes $|d\tilde{M}_j/dH|$ calculated for the four orbits discussed above. The temperature factor R_T, where it is assumed that $T = 1$ K, is included to ensure a closer approach to reality.

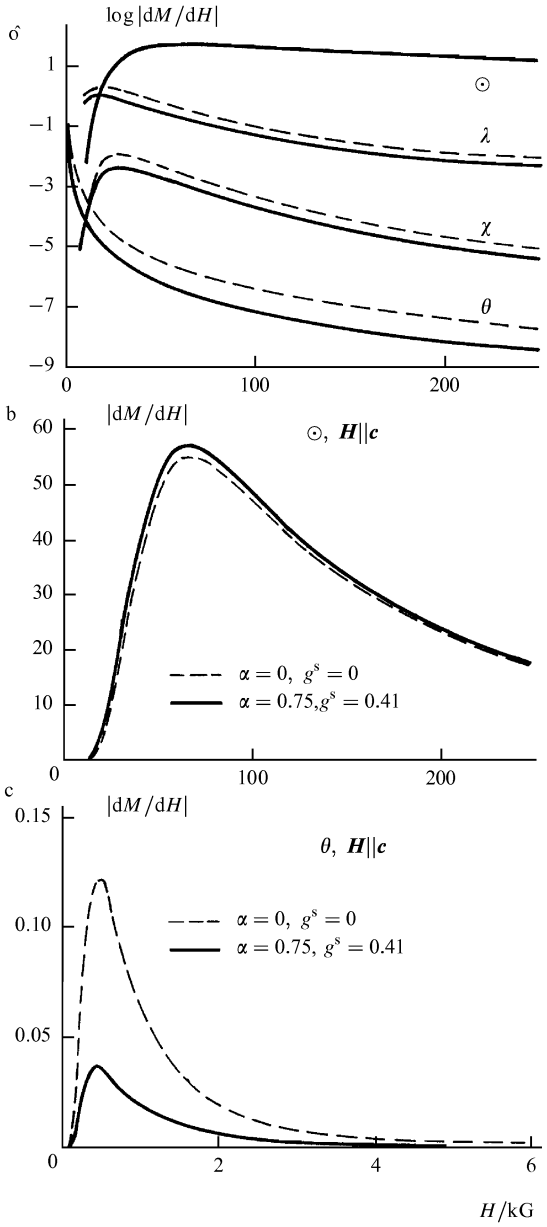

Figure 15. Magnetic-field dependences of the dHvA amplitudes obtained at 1 K for the principal orbits in Zn in the presence (continuous curves) and absence (dashed curves) of the spin degrees of freedom: (a) logarithmic field dependence for all types of orbits; (b) dependence for a circular orbit; (c) dependence for a triangular orbit. The graphs are plotted ignoring the Dingle factor. The parameters used in the calculation of the curves are listed in Tables 1 and 2.

As in the case of the theory of MB without spin flip, developed for Mg [8, 56], an increase in the field reduces the oscillations of the χ and θ orbits, so that the oscillations of the composite $\odot$ and λ orbits become dominant as the role of MB increases. Inclusion of the spin degrees of freedom of conduction electrons and of the SOC reduces significantly the amplitudes of the dHvA oscillations for all the orbits except for the circular one. This is due to the fact that the orbit $\odot$ crosses a large number of MB nodes and at each MB node we can expect spin flip of conduction electrons. This increases the number of possible paths each of which is determined by its own MB amplitude.

It therefore follows that the probability of finding conduction electrons of the opposite spins on this orbit increases. This probability depends in a complex manner [see expression (180)] on the SOC parameter α and on the g factors of different sections.

The behaviour of the oscillations associated with the θ orbit, which passes along a needle in Zn, has been used as one of the early proofs of the existence of MB [3, 4]. If spin is included, the maximum amplitude (Fig. 15c) is more than halved. The appearance of the factor $R_s = \cos(\pi g_\theta^s)$ in expression (174) does indeed account satisfactorily for the experi-mentally observed [105] strong dependence of the amplitude of the dHvA oscillations on the g factor of the needles.

We can summarise by saying that, in general, MB amplitudes depend in a complex manner on the SOC parameter α and on the g factor.

5.5. Oscillations of the de Haas – van Alphen effect in the case of magnetic breakdown and spin splitting of the Landau levels at 'needles' in zinc

It would be of interest to substitute the characteristics of an MB system (in particular, the parameters of the needles), obtained by comparing the theoretical and experimental galvanomagnetic properties of Zn (Section 4.4), in the theoretical expressions for the dHvA effect and to compare them with the familiar experimental results. We are aware of just one investigation in which the spin splitting of the energy levels in a magnetic field under the MB conditions has been detected in the dHvA oscillations representing the needles in Zn at $T = 1.2$ K [105].

This comparison of the theory and experiment is more of illustrative nature, because in this case of a triangular orbit the SOC does not play such an important role as in the case of diangular or circular orbits, because there is no conduction-electron spin flip during motion along these orbits. Fig. 16a give the experimental dependence of the second derivative of the magnetisation with respect to the magnetic field.

Generalisation of the theory of the dHvA effect under the MB conditions to include the SOC, which is done in the preceding section, makes it possible to determine $d^2\tilde{M}(H, T)/dH^2$ for the triangular θ orbit of Zn (Figs 3b and 14) in a more consistent manner than is done in Ref. [105]. The field derivative of expression (174) containing the Dingle factor yields [67]

$$\frac{d^2\tilde{M}_\theta(H, T)}{dH^2} = \left(\frac{e}{c\hbar}\right)^{3/2}\left(\frac{m}{m_\theta}\right)^{1/2}\frac{4\pi k_B T F_\theta^3}{H^{9/2}} \times \sum_{r=1}^{\infty} r^{3/2}\,\frac{\exp(-a_\theta r x_D/H)}{\sinh(a_\theta r T/H)}\,C_\theta \tau^{3r}\cos(\pi r g_\theta^s) \times \sin\left[r\left(\frac{2\pi F_\theta}{H} + 3\Lambda - 2\pi\gamma\right) - \frac{\pi}{4}\right], \qquad (182)$$

where x_D is the Dingle temperature [see formula (164b); 3Λ is the sum of the phase shifts contributed by three MB nodes [formulas (49)]; $a_\theta$is defined by expression (165) subject to substitutions (173); $g_\theta^s = 0.41$ (Table 1). The other parameters which occur in expression (182) have the values used in plotting the graphs in Figs. 12, 13, and 15 ($H_0 = 3$ kG, $\alpha = 0.75$, $F_\theta = 15.8$ kG).

The theoretical curve obtained for $T = 1.2$ K, assuming that the Dingle temperature is $x_D = 1.5$ [105] and that

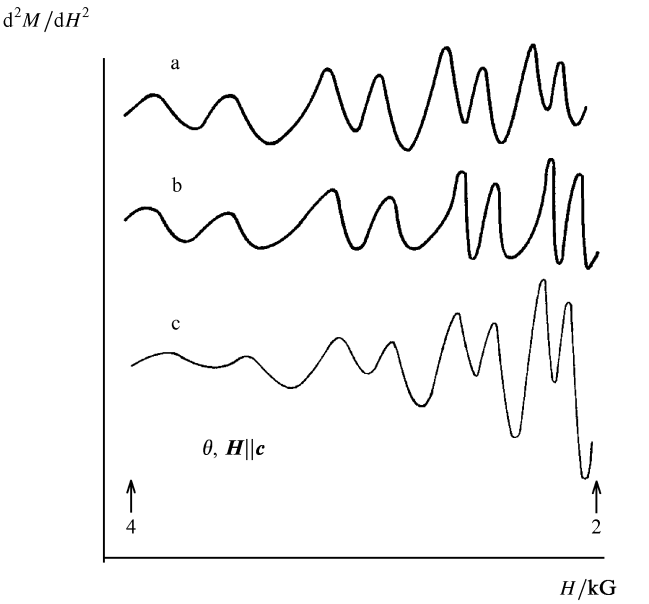

Figure 16. Oscillations of d^2M/dH^2 for needles of Zn at $T = 1.2$ K. The experimental (a) and theoretical (b) curves are reproduced from Ref. [105]. The values of the parameters used in the calculation of curve (c) are given in the text.

$\gamma = 0.21$, is plotted in Fig. 16c. It is quite clear from Figs 16a and 16c that the theoretical and experimental curves behave in the same way, that the frequency dependences are the same, and that both curves include strongly split peaks. We are of the opinion that this is evidence of a qualitative agreement between the results, supporting further the estimates obtained in Section 4.

Since there is no spin of conduction electrons during their motion along a triangular orbit, the curve in Fig. 16c does not differ significantly from the theoretical curve in Fig. 16b, which is taken from Ref. [105]. However, there is an important difference between the approaches used there and here: the results of Ref. [67] are derived consistently from the MB theory which takes into account the spin degrees of freedom from the microscopic point of view (this applies in particular to γ_s and α) [9], whereas in Ref. [105] the phenomenological parameters, describing the spin splitting of the peaks, are found by fitting the theoretical curve to the experimental results. O'Sullivan and Schirber [105] were forced to use the characteristic breakdown field $H_0 = 5$ kG in order to achieve a better agreement with the experimental results. However, this value differs from $H_0 \approx 3$ kG found from other experiments [5, 8]. In our analysis [67] we used the parameters (dHvA frequency, H_0, α, and the g factor of conduction electrons on a needle) deduced by an independent method in Ref. [66] from the galvanomagnetic properties of Zn, which were in good agreement with the published data.

It should also be noted that the phase in the expression (182) includes the quantity Λ [formula (49)], which depends in a complex manner on the field H and on the breakdown field H_0 renormalised by the SOC. The MB shift of the phase Λ follows from the solution of the quantum Schrodinger equation in the MB regions and this shift depends strongly on the ratio H_0/H. In our case the value of 3Λ ranges from -0.49 for $H = 1.67$ kG to -1.02 for $H = 4$ kG when the SOC parameter is $a = 0.75$. Only the

constant phase shift $2\pi\gamma$ is considered by O'Sullivan and Schirber [105]; the parameter γ should then assume one of two values (0.32 or 0.82) in order to describe the positions of the spin-split peaks.

When this difference between the phases is included, we find that the dips between the peaks, which correspond to different spin states, are less pronounced (Fig. 16c) than those predicted by the old theory (Fig. 16b), which in our opinion agrees better with the experiments (Fig. 16a). However, as in Ref. [105], there remains a fairly large dis-crepancy between the experiment and theory in the position of the maximum of the oscillation amplitude, which in the case of the theoretical curve is shifted towards weaker fields:

$$H_{\max}^{\text{theor}} = 0.75 < H_{\max}^{\text{exp}} \approx 2.2 \text{ kG}.$$

Unfortunately, we were unable to compare the amplitude characteristics more rigorously, since the experimental results were plotted in arbitary units and we did not know at what intervals of the field H the measurements were made.

The discrepancies between our theory (describing the dHvA effect under the MB conditions, taking account of the SOC) and experiments may also be related to such phenomena as the magnetic interaction or may be associated with the inhomogeneities of a sample ignored in the theory. The inhomogeneities may lead, as pointed out earlier, to an increase in the role of low-angle scattering in the course of motion of conduction electrons along a small triangular orbit, partial loss of coherence, and consequent smoothing out of the oscillation peaks.

6. Influence of magnetic breakdown on conduction-electron spin resonance in pure metals (Zn and Mg)

In the preceding sections we have considered the phenomena associated with the orbital motion of conduction electrons under the MB conditions. We demonstrated that the spin of conduction electrons and the SOC alter considerably the main dynamic characteristic of MB, which is the s matrix, and complicate considerably the spectrum of conduction electrons under the MB conditions including a change in the electron g factor.

In this connection it would undoubtedly be of interest to consider the influence of MB on such purely spin phenomena as conduction electron-spin resonance [98, 99, 111, 112]. This resonance was first studied experimentally by Stesmans and Witters [16]: they explained the low intensity of the resonance signal obtained for Zn by the occurrence of MB. Theoretical estimates of the influence of stochastic MB on conduction-electron spin resonance in Zn and Mg were given in Refs [17, 68].

Before discussing this resonance under the MB conditions, it is useful to consider qualitatively the influence of the Fermi surface anisotropy on the main characteristics of the resonance.

6.1 Conduction-electron spin resonance in metals with a complex Fermi surface. 'Motional narrowing'

The first theory of conduction-electron spin resonance in metals was put forward by Dyson [98], who took account of the diffusion of conduction electrons out of a skin layer on the basis of a model of quasifree electrons, i.e. by regarding these electrons as a gas of noninteracting quasiparticles with the dispersion law

$$\varepsilon(\boldsymbol{p}) = \frac{p^2}{2m^*}, \tag{183}$$

where m^* is the effective mass of conduction electrons. Dyson's theory is in good agreement with the experimental results, particularly those obtained for alkali metals (see, for example, Refs [111, 112]).

However, as is well known, the majority of metals have anisotropic and very complex Fermi surfaces [11, 12, 90]. These are the metals that have been investigated intensively in the last 20–25 years by the methods of conduction-electron spin resonance. The specific dependences of the signal intensity, and of the width, profile, and position of a resonance line on the frequency and temperature do not fit the framework of Dyson's theory.

The influence of motion of conduction electrons with an *arbitrary dispersion law* on the conduction-electron spin resonance spectrum of metals was first considered by I M Lifshitz and his colleagues [99, 113–115]. They developed a theory of this resonance on the basis of the solution of the transport equation for the density operators. They demonstrated that this affects the results only quantitatively (with the exception of one special case†): the change from one dispersion law to another alters only slightly a numerical factor representing the dimensionless component of the velocity of conduction electrons on the Fermi surface along a static magnetic field [113].

The resonance in question is therefore an integral effect. There are no special Fermi surface sections, belts, or points with 'effective' conduction electrons. The contribution to the resonant absorption is made by all the conduction electrons which are near the Fermi surface ($\Delta\varepsilon \ll \varepsilon_F$: the definition of $\Delta\varepsilon$ is given in the footnote discussing the diffusion of conduction electrons).

The g factor of conduction electrons and the spin relaxation time τ_s are regarded as parameters in Refs [98, 99, 113–115]. Therefore, there is only one way of taking into account the influence of the Fermi surface anisotropy on conduction-electron spin resonance; it is related to identifying the g factor and the lifetime of the spin state of each conduction electron, both of which depend on the position of the Fermi surface: $g(\boldsymbol{p})$ and $\tau_s(\boldsymbol{p})$. The dependence on the quasimomentum of conduction electrons appears as the result of influence of the SOC, which couples the orbital motion and the spin degrees of freedom of conduction electrons, manifested directly in conduction-electron spin resonance (see Section 2.1).

† If the applied magnetic field is sufficiently strong ($\omega_c\tau^* \gg 1$, where τ^* is the mean free time of conduction electrons), the coefficients representing the diffusion of conduction electrons along and across the field are different. The transverse diffusion length decreases with the mean free path until it becomes equal to the cyclotron orbit radius [11–13] (see also Section 4.3). Only the diffusion perpendicular to the face of a sample is effective in conduction-electron spin resonance. Therefore, if in the interval $\Delta\varepsilon \geqslant \max\{k_BT,\ g\mu_BH\}$ (T is the absolute temperature) near ε_F there are only open constant-energy surfaces of conduction electrons and their open directions are perpendicular to the boundary of a sample, a change in the magnetic field direction does not alter the effective coefficient of diffusion in such a metal [114] (see also [111]). However, this combination of conditions is not encountered in any of the metals in which conduction-electron spin resonance has been observed!

The difference $\Delta g(\boldsymbol{p}) = g(\boldsymbol{p}) - g_0$ (see Section 2.3) and the lifetime $\tau_s(\boldsymbol{p})$ (see, for example, Ref. [10]) depend on the ratio of the SOC energy to the energy parameters of the band structure of a specific metal, and they vary from one point on the Fermi surface to another. Following the majority of the previous treatments, we shall discuss qualitatively the influence of the anisotropic (dependent on $\boldsymbol{p}$) g factor of conduction electrons on the investigated resonance and we shall regard τ_s as constant for all the conduction electrons on the Fermi surface (see, however, Refs [116, 117]).

A common feature of all the experiments on spin resonance is the presence of a static magnetic field $\boldsymbol{H}$, which splits the spin levels of each conduction electron by $g(\boldsymbol{p})\mu_B H$, and of a weak alternating field $\tilde{\boldsymbol{H}}$, which is perpendicular to $\boldsymbol{H}$ ($\tilde{H} \ll H$). Then the field $\tilde{\boldsymbol{H}}$ induces transitions between the spin levels of conduction electrons when a quantum $\hbar\omega$ of the alternating field is equal to the Zeeman splitting: $\hbar\omega = g(\boldsymbol{p})\mu_B H$. When this condition is satisfied by the majority of conduction electrons, i.e. when†

$$\hbar\omega_s = \langle g(\boldsymbol{p})\rangle \mu_B H\,, \tag{184}$$

the absorption of the microwave power of the field $\tilde{\boldsymbol{H}}$ increases strongly (this happens in what are known as the reflection experiments).

Another method for the observation of conduction-electron spin resonance in metals (transmission experiments [112]) is based on selective transparency of metal plates, predicted theoretically a long time ago [99, 113, 115]. This phenomenon occurs because the spin diffusion length δ_s, traversed by a conduction electron without spin flip, is usually much greater than the depth of the skin layer δ. In fact, since the spin relaxation time τ_s is practically always much longer than the mean free time τ^* of conduction electrons, it follows that

$$\delta_s \sim (D\tau_s)^{1/2} \sim (v_0^2\tau^*\tau_s)^{1/2} \sim l\,\frac{\tau_s}{\tau^*} \gg \delta\,, \tag{185}$$

where v_0 is a typical velocity of conduction electrons; l is the mean free path of these electrons; $D \sim v_0^2\tau^*$ is the diffusion coefficient (when the field $\boldsymbol{H}$ is perpendicular to the boundary).

In the transmission experiments the microwave power of the field is applied to one side of a sample and the induced transverse magnetisation is measured on the other side. The thickness of the sample d should be less than δ_s. Under resonance conditions the microwave field creates a non-equilibrium magnetisation of conduction electrons in the skin layer. These electrons diffuse across the sample and transport the magnetisation to the other side of the sample where the power stored in the spins of conduction electrons in the skin layer is emitted as radiation (for details see Refs [112, 118]).

We shall now consider the relationship between the distribution of $g(\boldsymbol{p})$ on the Fermi surface and the observed characteristics of conduction-electron spin resonance. We shall consider particularly the relationship between this distribution and the experimental g factor $g^{\exp}$, deduced from the position of the centre of the resonance line, and also the relationship with the profile and width of this line. We shall find the contribution of the g-factor anisotropy ignoring the factors which reduce the spin lifetime τ_s because of the scattering of conduction electrons by phonons, boundaries, other electrons, impurities, dislocations, and various inhomogeneities (for details see Ref. [88]) and which lead to the homogeneous width of the resonance line.

The simplest interpretation of the observed line width is as follows. Conduction electrons with different quasimomenta (and g factors) resonate in different fields. Had this been possible, an experiment would have revealed a spin resonance line whose inhomogeneous width represents the real scatter of the electron g factor over the Fermi surface (continuous curve in Fig. 17), given by

$$\Delta\omega_g \approx \frac{1}{\hbar}\,\sigma_g \mu_B H\,. \tag{186}$$

Here, $\sigma_g = \langle [g(\boldsymbol{p}) - \langle g(\boldsymbol{p})\rangle]^2\rangle^{1/2}$ is the rms deviation of the g factor varying over the Fermi surface and $\Delta\omega_g$ is the width of a spin resonance line contributed by the gth factor anisotropy.

In fact, such an inhomogeneously broadened line is not observed because conduction electrons do not stand still on the Fermi surface. In a magnetic field a conduction electron moves along the Fermi surface either along orbits described by expression (8) ($\omega_c\tau^* \gg 1$, which is obeyed in strong fields at low temperatures and by pure metals) or they diffuse because of various types of scattering ($\omega_c\tau^* \ll 1$; the range in which such scattering predominates will be called arbitrarily the 'high-temperature' range). This topic is discussed in Refs [88, 97]. In the latter case the influence of the applied magnetic field on the motion of conduction electrons over the Fermi surface is essentially negligible [12].

At 'high temperatures' a conduction electron visits many points on the Fermi surface in the time τ_s ($\tau_s \gg \tau$). These points are characterised by different values of $g(\boldsymbol{p})$ and, consequently, by different resonance fields H (spectrometers for the investigation of conduction-electron spin resonance operate at a fixed frequency ω). Consequently, conduction electrons 'feel' a certain average field, the resonance line becomes narrower, and the contribution of the g-factor anisotropy to the observed line width is then [10]

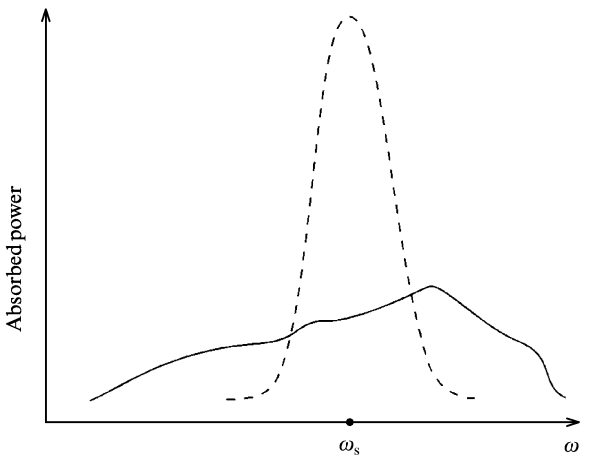

Figure 17. Schematic representation of the absorption spectrum in the case of conduction-electron spin resonance [79]. The continuous curve corresponds to a hypothetical g distribution and the dashed curve represents a resonance signal which is motionally narrowed.

† Here, $\langle ... \rangle = (2/v)\int_{FS} ... \,dS/v(\boldsymbol{p})$ represents averaging over the Fermi surface [11, 12] and $v = \int_{FS} dS/v$ is the number density of states on this surface.

$$\Delta\omega \sim (\Delta\omega_g)^2\tau \sim \frac{\sigma_g^2}{\langle g\rangle^2}\,\omega_s^2\,\tau\,, \tag{187}$$

where the resonance frequency ω_s [see formula (184)] determines the position of the resonance line.

This effect has been understood and explained first in the case of nuclear magnetic resonance in liquids and it has been called 'motional narrowing' [119]. Therefore, at 'high temperatures' one narrow spin resonance line† is observed for metals with the g-factor anisotropy. The width of this line is $\Delta\omega$ and it is centred at the frequency ω_s determined by the weighted average over the distribution of the g factors over the Fermi surface (dashed curve in Fig. 17). It should be pointed out that $g^{\exp} = \langle g\rangle$, and that $\Delta\omega$ in formula (187) depends on the square of the frequency at which the experiment is carried out.

Cooling increases the momentum relaxation time τ^* of conduction electrons when a metal is sufficiently pure. Consequently, cooling also increases the contribution made to the line width by the narrowing mechanism described by formula (187). This increase continues until $\hbar/\tau^*$ becomes of the order of $\sigma_g\mu_B H$. At this stage one can expect complete disappearance of motional narrowing of the line [120]. However, motion of conduction electrons along cyclotron orbits begins earlier, before the scattering electrons manage to complete several revolutions around the Fermi surface (in this case we have $\hbar\omega_c \geqslant \hbar/\tau^*$). The g factor is then first averaged along the cyclotron orbits.

In the case of each orbit represented by its own value of p_z the change in the g factor is [79, 81]

$$\Delta g(p_z) = \langle g(p)\rangle_{p_z=\text{const}} - \langle g(p)\rangle\,, \tag{188}$$

which reduces significantly the rms scatter σ_g of the g factor and we then have $\langle[\Delta g(p_z)]^2\rangle^{1/2}$. For example, in the case of Al the averaging by the diffusion of conduction electrons gives $\sigma_g = 0.469$ and the initial averaging over the cyclotron orbits gives $\sigma_g = 0.67$ [81]. In the intermediate case ($\omega_c\tau^* \sim 1$) the averaging procedure is highly specific [81, 82] and it is associated with the mixed nature of the motion of conduction electrons in a magnetic field (this point is discussed later).

It should also be pointed out that the existence of the scatter of the g factors of conduction electrons on the Fermi surface gives rise to a parameter of the transmission resonance: this parameter has the dimensions of length and it limits the depth of penetration of the nonequilibrium magnetisation [118]. The parameter δ_c represents the distance to which the spins of conduction electrons diffuse without loss of coherence:

$$\delta_c^2 = \frac{\langle v_z^2\rangle}{(\Delta\omega_g)^2}\,. \tag{189}$$

In this case the propagation of a signal across a metal plate is limited by the shorter of the two characteristic lengths δ_s and δ_c. It should be noted that if $\sigma_g \to 0$, then $\delta_c \to \infty$ and the results of Ref. [118] are identical with the conclusions reached in Refs [99, 113].

It therefore follows that $g^{\exp}$ is obtained from the distributed $g(\boldsymbol{p})$ by averaging over the whole Fermi surface. However, the averaging procedure varies somewhat depending on the nature of the motion of conduction electrons on the Fermi surface. There is a change also in the important parameter σ_g, which represents the rms scatter of the g factor. In contrast to conduction-electron spin resonance, the dHvA effect can be used to find the g factors of the extremal orbits (see Section 5) and, consequently, $g^{\exp} = g(p_z^{\xi})$ from the experimental results; here ξ is the serial number of the extremal section.

6.2 Models of the Fermi surface with g anisotropy

In calculation of the g factor of conduction electrons in metals it is natural to use the real Fermi surface and the real band structure of a metal. However, we shall consider here the model Fermi surfaces used in the theory of conduciton-electron spin resonance. The simplest model, frequently used for calculations based on this theory [11, 98, 111–112], is that of an electron gas described by expression (183) characterised by $g(\boldsymbol{p}) \approx g_0$. In this case the Fermi surface is a sphere. The model agrees best with experiments carried out on univalent metals. Calculations have shown (see Ref. [121]) that in the case of alkali metals we have $|\Delta g(p)| < 0.1$, and the experimental value $\Delta g^{\exp}$ varies from 10^{-5} (for Li) to 10^{-2} (for Cs, which is the alkali metal with the strongest SOC) [122].

In the case of polyvalent metals the model Fermi surface can also be a sphere. (This sphere can be used to plot the Fermi surface of a metal in the approximation of almost-free electrons [92]). The g factor of conduction electrons, dependent on $\boldsymbol{p}$, is distributed on the sphere and the sphere extends over several Brillouin zones. the spherical model has been applied most frequently to Al. This model of the Fermi surface with a hypothetical distribution of the g factor has been found to account for the increase in the width and for the shift of a resonance line as the frequency ω is increased in the case of Al, Cu, and Ag: these effects are attributed to the simultaneous influence of the g-factor anisotropy and of the Fermi-liquid interaction (first experiments were reported in Ref. [123] and the theory was given in Ref. [79]). This has made it possible to find the value of the spin parameter B_0 of the Fermi-liquid interaction from the shift of the resonance line in the case of Al.

The spherical model has been developed further by including the results of a calculation of the g factors of conduction electrons in Al reported in [81]. It has been found that in the second and third Brillouin zones near 24 W points‡ the g factor of conduction electrons $g(\boldsymbol{p})$ can reach values of the order of hundreds [in this case the energy gap $\Delta(\boldsymbol{p})$ is small near the W points!]. This circumstance is taken into account as follows [82]. There are 48 (24×2) small regions scattered over the Fermi surface and they correspond to the vicinities of the real W points. Each such region is characterised by a large and constant shift of the g factor $|\Delta g_W| \sim 10^3$, and the average over the Fermi surface is $\langle \delta g_W(\boldsymbol{p})\rangle = 0$. Outside these regions we have $\Delta g = 0$. This simple model can account by the 'motional narrowing' for the linear frequency dependence of the width of a spin resonance line at moderate temperatures ($\omega_c\tau^* \sim 1$).

As a rule, the Fermi surface of polyvalent metals consists of several disconnected sheets, which are located

† In the case of thin samples, of thickness $d \ll \delta_s$, the profile of the spin resonance line of conduction electrons is Lorentzian, but for thick samples the line has the Dyson profile [118].

‡ Aluminium is an hcp metal and its Brillouin zone is a cubo-octahedron. The W points are located at the intersections of this zone with quadrilateral and hexagonal faces [90].

in different zones. If we assume that small-angle scattering of conduction electrons predominates, we find that this leads to the establishment of an equilibrium on each Fermi surface sheet separately. This happens if the characteristic time of the scattering of conduction electrons, which is not accompanied by the transfer of the electrons from one sheet to the other, is less than the characteristic intersheet scattering time. Under these conditions it is useful to employ a model of a metal postulating the existence of several conduction electron groups.

Each group can be assigned its own average characteristics such as the g factor (g_i), the spin (τ_{si}) and momentum (τ_{pi}) relaxation times, etc., depending on the complexity of the model. For example, such a model has been proposed for Al [77] and the coupling between the conduction electrons belonging to the different groups is provided by three mechanisms: intergroup scattering of conduction electrons at a frequency $1/\tau_{ij}$, exchange interaction, and diffuse reflection of conduction electrons at a boundary. It should be noted that experiments [16] on conduction-electron spin resonance in Zn have revealed a possible coupling between such groups by MB.

The proposed model predicts changes in the observed g factor as a result of cooling because of reduction of the coupling between two groups of spins, and also because of the absence of the Fermi-liquid interaction (discussed above). In the limit of low temperatures a spin resonance line can have a structure because of the difference between the g factors of two conduction-electron groups. (This has probably been observed in the experiments on Mg [16, 124]; see below.) Moreover, it has been shown that diffuse (multichannel) reflection from a boundary without spin flip influences the spectrum even in the case of relatively thick samples: it transfers spin excitation from a weakly damped mode (when σ_{gi} is small) to a strongly damped mode (large σ_{gi}).

In concluding this section we note that attempts have been made [75, 76] to utilise the real structure of the Fermi surface of Ag and Cu in a qualitative explanation of the angular dependences of the spin resonance spectrum. A quantitative analysis can be found in Ref. [125]. The real Fermi surface has also been used in considering conduction-electron spin resonance in Refs [16, 81, 126, 127].

6.3 Discussion of the model. The Hamiltonian of the problem

Among all the metals that have an anisotropic and complex Fermi surface and which exhibit conduction-electron spin resonance, the properties of Zn and Mg are best suited to the study of the influence of MB on this resonance. This is due to the fairly low breakdown fields of these metals. The experimental estimates for Zn gives values of H_0 ranging from 2.7 kG [5] to 3.5 kG [106] (in Section 4 we gave 3.0 kG for Zn); the corresponding value for Mg is 5.85 kG [5]. Magnetic fields used in studies of this resonance are limited to the range $H \leqslant 10$ kG, since only a certain range of frequencies ($\nu < 10^{10}$ Hz) is technically attainable in the existing spectrometers [16, 111].

Both Zn and Mg are divalent metals with the hcp lattice. In the system of double bands typical of these metals, the Brillouin zone represents a straight hexagonal prism. These two metals have complex Fermi surfaces consisting of unconnected sheets. The part of the Fermi surface important in our discussion is shown in Fig. 3a.

The application of a sufficiently strong magnetic field directed along the sixfold axis gives rise to MB which couples conduction electrons in the monster and cigars. The role played by MB in conduction-electron spin resonance can be made clear on the basis of a simple model postulating predominance of small-angle scattering of conduction electrons and establishment of an equilibrium within each Fermi surface sheet: MB is made stochastic by this scattering. Such strong small-angle scattering may be on thermal phonons since the temperatures at which the resonance is observed in these metals are fairly high: $T = 40$ K for Mg [16]. Therefore, three groups of conduction electrons with parameters averaged in each group are present. Each group has its own g factor and these factors are not in general equal.

In the adopted model in the absence of MB each group of conduction electrons should give rise to its own resonance line, provided this is possible, and each group should have its own line width, inversely proportional to the group relaxation time of the transverse magnetisation. The line intensity should depend on the number of conduction electrons on the relevant sheets: the strongest signal should come from the conduction electrons on the large monster, a weak signal is expected from the electrons on a lens, and a practically undetectable signal should originate from the cigars. MB should result in exchange of conduction electrons and, consequently, it should alter the magnetisation and broaden the resonance lines of two electron groups: those belonging to the monster and the cigars. For simplicity, we shall assume that MB acts independently of all the factors that might broaden and shift the resonance line and, therefore, it makes an additive contribution to the total line width. This assumption will make possible to ignore, in our subsequent calculations, all possible mechanisms of broadening of the resonance line, apart from that under consideration.

We should bear in mind that in the adopted model the approximation of 'instantaneous' establishment of an intragroup equilibrium is fairly rough and it is most likely to overestimate somewhat the contribution of MB to the resonance line width.

Since in our model the conduction-electron lenses interact with external magnetic fields independently of the other electron groups, the model Hamiltonian of two coupled electron groups subjected to an external static field $\boldsymbol{H} \| Oz$ and to an alternating field $\tilde{\boldsymbol{H}}$ ($\tilde{\boldsymbol{H}} \ll H$), perpendicular to the static field, is [17]:

$$\hat{H} = \hat{H}_0(t) + \hat{H}_{\mathrm{MB}}, \quad \hat{H}_0(t) = \hat{H}_{\mathrm{kin}} + \hat{H}_{\mathrm{Z}}(t). \tag{190}$$

Here

$$\hat{H}_{\mathrm{kin}} = \sum_{n,\boldsymbol{p},\sigma} [\varepsilon_n(\boldsymbol{p}) - \varepsilon_{\mathrm{F}}]\, \hat{a}^{+}_{n,\boldsymbol{p},\sigma}\, \hat{a}_{n,\boldsymbol{p},\sigma} \tag{191}$$

is the kinetic energy operator;

$$\begin{aligned} \hat{H}_{\mathrm{Z}}(t) &= \hat{H}^0_{\mathrm{Z}}(t) + \hat{H}'_{\mathrm{Z}}(t) \\ &= -\boldsymbol{H}\cdot(\hat{\boldsymbol{M}}_1 + \hat{\boldsymbol{M}}_2) - \tilde{\boldsymbol{H}}(t)\cdot(\hat{\boldsymbol{M}}_1 + \hat{\boldsymbol{M}}_2) \end{aligned} \tag{192}$$

is the Zeeman Hamiltonian; $\tilde{\boldsymbol{H}}(t)$ varies at a frequency ω;

$$\hat{M}^{\alpha}_{n} = \frac{g_m \mu_{\mathrm{B}}}{2} \sum_{\boldsymbol{p},\sigma,\sigma'} \hat{a}^{+}_{n\boldsymbol{p}\sigma}\, \hat{\sigma}^{\alpha}_{\sigma\sigma'}\, \hat{a}_{n\boldsymbol{p}\sigma'} \tag{193}$$

is the operator of projection of the magnetic moment of the nth group of conduction electrons ($\alpha = x, y, z$ identifies the component);

$$\hat{H}_{\mathrm{MB}} = \sum_{p_0, q_0, \sigma, \sigma'} (V_{12}^{\sigma\sigma'}\, \hat{a}_{1p\sigma}^{+}\, \hat{a}_{2p\sigma'} + \mathrm{H.c.}) \qquad (194)$$

is the tunnelling Hamiltonian of MB.

Here, $n = 1$ and 2 for the monster and cigars (needles), respectively; $\hat{a}_{1p\sigma}^{+}$ and $\hat{a}_{2p\sigma}$ are the creation and annihilation operators for conduction electrons belonging to the nth group; $\boldsymbol{p}$ and $\boldsymbol{q}$ describe the quasimomentum spaces of the bands 1–2 and 3–4, respectively; $\hat{\sigma}_{\sigma\sigma'}^{\alpha}$ are the Pauli matrix elements; $V_{12}^{\sigma\sigma'}$ is the tunnelling parameter selected so that the tunnelling probabilities, proportional to $|V_{12}^{\sigma\sigma'}|^2$, are equal to the corresponding MB probabilities w^0 and w^s [see expression (52)]; $\{\boldsymbol{p}_0\}$ and $\{\boldsymbol{q}_0\}$ are the MB regions on the monster and cigars (needles), respectively.

The rates of relaxation of the transverse magnetisation of the monster conduction electrons have been calculated by the nonequilibrium density matrix methods [128]. In accordance with the adopted model, it has been assumed that their resonance is far from saturation and the temperatures of the kinetic ($\hat{H}_{\mathrm{kin}}$) and Zeeman ($\hat{H}_{\mathrm{Z}}$) 'baths' have been selected to be equal to the thermostat temperature T, which corresponds to the 'instantaneous' establishment of an equilibrium in each of the conduction electron groups. A nonequilibrium state then appears as a result of the absorption of energy from the alternating field by the conduction electron spins.

6.4 Discussion of the experiments and evaluation of the theoretical results

Calculations which are standard in the nonequilibrium density matrix method [128] have been used to show [17] that the contribution of MB to the line width of conduction-electron spin resonance is proportional to the MB probabilities. The probabilities are known to depend on the law of inclination of the magnetic field [see expression (50)]. (Experimental data on the dependence of the breakdown field on the angle θ between the field $\boldsymbol{H}$ and the sixfold crystallographic axis $\boldsymbol{c}$ are reported for Mg in Ref. [91] and for Zn in Ref. [106]. Consequently, the total *experimental* resonance line width can be represented as the following sum of two components: the 'residual' width a independent of MB and the MB contribution

$$\left(\frac{1}{T_2}\right)^{\mathrm{exp}} = a + b \exp\left(-\frac{H_0^{(\theta=0^\circ)}}{H \cos\theta}\right), \qquad (195)$$

where b is a phenomenological parameter.

The theory should be checked by selecting those experiments on the spin resonance in Mg and Zn which have been carried out on single crystals or on polycrystalline samples but with the $\boldsymbol{c}$ axis orientation. In the case of Mg these are the experiments reported in Refs [16, 124, 129], whereas for Zn we are aware of only one investigation [16].

Before actual comparison with experiments, we shall give the estimates reported in Ref. [17]. In our case, when 'tracking' the response from the conduction-electron monster ($n = 1$), theoretical estimates of the MB contribution to the resonance line width can be obtained from the simple and physically clear formula

$$\left(\frac{1}{T_2^{\mathrm{MB}}}\right)_1^{\mathrm{theor}} \approx N \frac{p_z^{\mathrm{MB}}}{p_{z1}} \frac{\omega_{c1}}{2\pi}\, w, \qquad (196)$$

where p_{z1} is the longitudinal dimension of the monster; p_z^{MB} is the thickness of the MB layer; ω_{c1} is the cyclotron frequency of the monster; $N = 6$ is the number of the MB regions; w is the total MB probability given by expression (2).

We shall now discuss the experimental results for these two metals and use expression (196) to estimate the effect of MB on conduction-electron spin resonance. The experiments on Mg reveal a wide resonance line with a strong angular dependence. The line width is maximal at $\theta = 0^\circ$ and it decreases monotonically with increase in the angle up to $\theta = 90^\circ$. The experimental points taken from Ref. [129] are reproduced in Fig. 18.

It therefore follows that the resonance signal can be regarded as the response of the monster conduction electrons and the θ-dependent contribution to the line width can be attributed to the influence of MB described by expression (195). It is evident from Fig. 18 that the resonance line width attributed to MB varies from $(3 \pm 1) \times 10^8$ s^{-1} to zero. The parameters of the phenomenological *experimental* curve, described by expression (195) and plotted in Fig. 18,

$$a = 6.2 \times 10^8 \text{ s}^{-1}, \quad b \exp\left(-\frac{H_0^{(\theta=0^\circ)}}{H}\right) = 2.9 \times 10^8 \text{ s}^{-1}$$

were found by the least-squares method in Ref. [17] on the assumption that $H = 3.3$ kG [124, 129].

On the other hand, expression (196) gives the following theoretical estimate of the contribution

$$\left(\frac{1}{T_2^{\mathrm{MB}}}\right)_1^{\mathrm{theor}} (\theta = 0^\circ) = (9-15) \times 10^8 \text{ s}^{-1}, \qquad (197)$$

where the following values are assumed: the static MB field $H_0 = 5.85$ kG [5], the alternating resonance field $H = 3.3$ kG [124, 129], and the parameters of the monster $\omega_1 = (4.2 - 6.8) \times 10^{10}$ s^{-1} [5, 8] and $p_z^{\mathrm{MB}}/p_{z1} = 0.14$ [5].

We can see that the calculated contribution of MB to the width of the resonance line of conduction electrons on

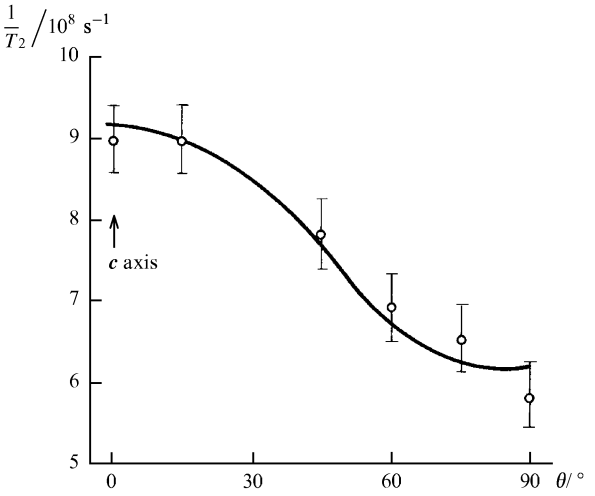

Figure 18. Dependence of the total width of a conduction-electron spin resonance line on the angle of inclination of a magnetic field applied to pure Mg. The experimental points are taken from Ref. [129]: $T = 40$ K, resonance frequency 9.2 GHz, $g = 2.00 \pm 0.01$. The position of the phenomenological curve, described by expression (195), was determined by the least squares method.

the monster of Mg is in qualitative agreement with the experimental results. As expected on the basis of the adopted model, it exceeds the experimental value by an order of magnitude. An additional confirmation of the correctness of this theoretical model is the observation of a weaker and narrower signal of the conduction-electron lens against the background of the wide spin resonance line of Mg [16].

The resonance in Zn generates only a weak and narrow signal of the conduction-electron lens. The spin resonance line of the monster conduction electrons has not been observed becaue, as postulated, of its large width. According to Ref. [16], the failure to observe the monster line should be attributed to the influence of MB.

We shall estimate the contribution of MB to the total width of the resonance representing the monster conduction electrons on the basis of expression (196):

$$\left(\frac{1}{T_2^{\mathrm{MB}}}\right)_1^{\mathrm{theor}} (\theta = 0^\circ) \approx 3 \times 10^8 \ \mathrm{s}^{-1}, \tag{198}$$

where $H_0 = 2.7$ kG, $p_z^{\mathrm{MB}}/p_{z1} = 0.05$ [5], the alternating resonance field is $H = 6.5$ kG [16], and $\omega_{\mathrm{cl}} = 9 \times 10^9 \ \mathrm{s}^{-1}$ [16, 91].

This estimate is considerably larger than the resonance line width ($6 \times 10^7 \ \mathrm{s}^{-1}$) reported for the lens conduction electrons in Ref. [16]. Hence, it follows from our model that MB does indeed broaden the resonance line due to the monster conduction electrons. However, it is evident from the above results and from Fig. 18 that there is an order-of-magnitude agreement between this result and the experimental width of the resonance line of Mg. Consequently, without other factors, the effect of MB alone cannot suppress the line in question, especially as at $\theta = 90^\circ$ there should be no influence of MB at all on the resonance of the monster. (This possibility is not discussed in Ref. [16], although the direction of the magnetic field has been varied.)

It should also be pointed out that in the adopted model a similar contribution (but independent of θ!) to the resonance line width can be made by the transfer of conduction electrons from the monster to the cigars (needles) because of the scattering on phonons [97, 88]. Estimates show that the wave vector of thermal phonons $k_{\mathrm{ph}} = k_{\mathrm{B}}T/\hbar s$ (s is the velocity of sound) remains less than $\Delta k = \delta p/\hbar$ (which is the minimum separation between the parts of the Fermi surface of interest to us) right down to temperatures T_{ph}.

In the case of Zn, this temperature is $T_{\mathrm{ph}} = 20$ K and for Mg it is $T_{\mathrm{ph}} = 45-50$ K. The velocity of sound is assumed to be $s_{\mathrm{Zn}} = 4 \times 10^4 \ \mathrm{m \ s}^{-1}$ and $s_{\mathrm{Mg}} = 6 \times 10^3 \ \mathrm{m \ s}^{-1}$. In the case of Zn it is found that $\Delta k = 0.04$ a.u.$^{-1}$. Since the interband gap in Mg is twice as large, it follows that $\Delta k_{\mathrm{Mg}} = 2\Delta k_{\mathrm{Zn}}$. Consequently, thermal phonons can only participate in the effective intragroup mixing (in agreement with the adopted model) and cannot compete with MB at temperatures $T \leqslant T_{\mathrm{ph}}$.

7. Conclusions

We shall now summarise our results. From the formal point of view the mathematical formalism of the MB theory [6] can be generalised quite simply to the case in which the SOC is taken into account. It is then necessary to consider the following points:

—the SOC modifies considerably the conduction-electron spectrum in the regions of anomalous approach of the bands;

—the main dynamic parameter of MB is the 4×4 s matrix, which determines the *three-channel* MB scattering of conduction electrons; spin-flip MB becomes probable;

—the SOC alters fundamentally the classification of the states of conduction electrons under the MB conditions; it is not in general possible to separate the spin and orbital degrees of freedom;

—there is a considerable change in the MB spectrum of conduction electrons; in particular, complete breakdown (when the total MB probability is unity) *does not reduce* to the semiclassical case: the wave functions of conduction electrons with oppositely oriented spins become intermingled and states with an effective spin are formed.

The theory of spin-flip MB is supported by the experimental results on the galvanomagnetic properties and on the dHvA effect in Zn. This is manifested by the doublet structure of the MB oscillation peaks. The splitting in terms of the magnetic field can be used to find the microscopic characteristics of conduction electrons in a metal, such as the g factor, the effective mass of electrons, and the SOC parameter in the MB theory.

MB acts as an additional mechanism of spin relaxation of conduction electrons. In the case of conduction-electron spin resonance this may give rise to a characteristic angular dependence of the resonance line width, which is most likely in the case in Mg.

The relatively simple examples, with calculations continued until numerical values have been obtained, thus show that inclusion of the degrees of freedom in the MB theory does not reduce to simple summation (multiplication by 2 in the final expressions). It has recently been concluded that the consequences of the spin flip of conduction electrons under the MB conditions have been observed for some pure metals back in the sixties.

We have deliberately limited our discussion to normal metals. In systems with a known strong SOC (transition metals, ferromagnetic compounds) it is essential to take into account the spin degrees of freedom. However, the theoretical picture of MB in this case is far from complete and not so clear. It is necessary to take into account the collective properties of the spin system, which requires a separate discussion.

In recent years the interest in MB has extended to an unexpected, from the point of view of the theory of metals, direction of organic compounds which become superconducting at temperatures of about 10 K. A study of the Fermi surfaces of these organic semiconductors is developing rapidly and MB can provide much useful and accurate information on the energy spectra of these materials.

Not everything is clear in the case of simple metals. We have discussed above the problem of finding the energy spectrum (and the g factor) of conduction electrons under the MB conditions. The characteristics of the MB spectrum play an important role in the description of the effects due to coherent MB [6]. Consequently, the spin degrees of freedom should affect also the completely coherent motion of conduction electrons under the MB conditions. It is interesting to consider the problem of the spin characteristics of the system under the conditions of quantum MB localisation of conduction electrons.

We hope that the above discussion not only will stimulate further theoretical studies of spin dynamics of conduction electrons under the MB conditions, but will also draw the attention of experimentalists to the unusual and fine phenomenon of magnetic breakdown.

Acknowledgements. We are grateful to M I Kaganov for his very helpful interest in our work over a period of many years. We are also grateful to B I Kochelaev for the above work. One of us (Yu N P) is grateful to A A Slutskin for valuable discussions, which helped to confirm the correctness of the selected approach.

References

1. Cohen M H, Falicov L M *Phys. Rev. Lett.* **7** 231 (1961)
2. Priestley M G *Proc. R. Soc. London Ser. A* **276** 256 (1963); Priestley M G, Falicov L M, Weisz G *Phys. Rev.* **131** 617 (1963)
3. Dhillon J S, Shoenberg D *Philos. Trans. R. Soc. London Ser. A* **248** 1 (1955)
4. Pippard A B *Philos. Trans. R. Soc. London Ser. A* **256** 317 (1964)
5. Stark R W, Falicov L M *Prog. Low Temp. Phys.* **5** 235 (1967)
6. Kaganov M I, Slutskin A A, in *Elektrony Provodimosti* (Conduction Electrons) (Moscow: Nauka, 1985) p. 101; Kaganov M I, Slutskin A A *Phys. Rep.* **98** 187 (1983)
7. Alekseevskii N E, Nizhankovskii V I, in *Elektrony Provodimosti* (Conduction Electrons) (Moscow: Nauka, 1985) p. 197
8. Shoenberg D *Magnetic Oscillations in Metals* (Cambridge: Cambridge University Press, 1984)
9. Proshin Yu N *Zh. Eksp. Teor. Fiz.* **93** 1356 (1987) [*Sov. Phys. JETP* **66** 770 (1987)]
10. Jafet J *Solid State Phys.* **14** 1 (1963)
11. Lifshitz I M, Azbel' M Ya, Kaganov M I *Electron Theory of Metals* (New York: Consultants Bureau, 1973)
12. Kaganov M I, Lifshitz I M *Usp. Fiz. Nauk* **129** 487 (1979) [*Sov. Phys. Usp.* **22** 904 (1979)]
13. Abrikosov A A *Fundamentals of the Theory of Metals* (Amsterdam: North-Holland, 1988)
14. Blount E I *Phys. Rev.* **126** 1636 (1962)
15. Tselfes W, Flouda E, Boukos N, et al. *Physica B* **172** 405 (1991)
16. Stesmans A, Witters J *Phys. Rev. B* **23** 3159 (1981)
17. Kochelaev B I, Proshin Yu N *Fiz. Tverd. Tela (Leningrad)* **27** 265 (1985) [*Sov. Phys. Solid State* **27** 161 (1985)]
18. Slutskin A A *Zh. Eksp. Teor. Fiz.* **58** 1098 (1970) [*Sov. Phys. JETP* **31** 589 (1970)]; Slutskin A A *Pis'ma Zh. Eksp. Teor. Fiz.* **18** 587 (1973) [*JETP Lett.* **18** 346 (1973)]
19. Slutskin A A *Zh. Eksp. Teor. Fiz.* **65** 2114 (1973) [*Sov. Phys. JETP* **38** 1057 (1974)]
20. Slutskin A A, Kadigrobov A M *Fiz. Nizk. Temp.* **4** 536 (1978) [*Sov. J. Low. Temp. Phys.* **4** 262 (1978)]
21. Stark R W, Friedberg C B *J. Low Temp Phys.* **26** 763 (1977)
22. Gorelik L Yu, Kovtun E A *Fiz. Nizk. Temp.* **19** 395 (1993) [*Low Temp. Phys.* **19** (1993)]
23. Walker I R *J. Low Temp. Phys.* **90** 205 (1993)
24. Lonzarich G G, in *Electrons at Fermi Surfaces* (Ed. M Springford) (Cambridge: Cambridge University Press, 1980) Chap. 6
25. Kumin P R, Dyakina V P, Startsev V E, Cherepanov A N *Fiz. Met. Metalloved.* **12** 39 (1990)
26. McMullan G J, Pilgram D D, Marshall A A *Phys. Rev. B* **46** 3789 (1992)
27. Liu C T, Tsui D C, Shayegan M, Ismail K, Antoniadis D A, Smith H I *Appl. Phys. Lett.* **58** 2945 (1991)
28. Beton P H, Dellow M W, Main P C, et al. *Phys. Rev. B* **43** 9980 (1991)
29. Hu J, MacDonald A H *Phys. Rev. B* **46** 12554 (1992)
30. Behler S, Winzer K *Z. Phys. B* **82** 355 (1991)
31. Audouard A, Richard J, Dubois S, et al. *Synth. Met.* **56** 2629 (1993); Henriques A B, Morgoon V N, de Souza P L, et al. *Phys. Rev. B* **49** 11248 (1994)
32. Williams J M, Schultz A J, Geiser U, et al. *Science* **252** 1501 (1991)
33. Sasaki T, Sato H, Toyota N *Solid State Commun.* **76** 507 (1990)
34. Sasaki T, Sato H, Toyota N *Physica C* **185–189** 2687 (1991)
35. Wosnitza J, Crabtree G W, Wang H H, et al., in *Physical Phenomena at High Magnetic Fields* (Reading, MA: Addison-Wesley, 1991) pp 1–11
36. Kartsovnik M V, Kovalev A E, Kushch N D *J. Phys. I* **3** 1187 (1993)
37. Sasaki T, Toyota N *Synth Met.* **56** 2303 (1993)
38. Uji S, Aoki H, Tokumoto M, et al. *Phys. Rev. B* **49** 732 (1994)
39. Caulfield J, et al. *Synth. Met.* **61** 63 (1993)
40. Uji S, Aoki H, Brooks J S, et al. *Solid State Commun.* **88** 683 (1993)
41. Kanoda K, Kato K, Kawamoto A, et al. *Synth. Met.* **56** 2309 (1993)
42. Kartsovnik M V, Laukhin V N, Pesotskii S I *Usp. Fiz. Nauk* **162** (10) 183 (1992) [*Sov. Phys. Usp.* **35** (1992)]
43. Tamura M, Kuroda H, Uji S, et al. *J. Phys. Soc. Jpn.* **63** 615 (1994)
44. Alekseevskii N E, Bazan C, Glinski M, et al. *J. Phys. E* **12** 648 (1979)
45. Slutskin A A *Zh. Eksp. Teor. Fiz.* **53** 767 (1967) [*Sov. Phys. JETP* **26** 474 (1968)]
46. Pippard A B *Proc. R. Soc. London Ser. A* **270** 1 (1962)
47. Slutskin A A, Gorelik L Yu *Solid State Commun.* **46** 601 (1983)
48. Sandesara N B, Stark R W *Phys. Rev. Lett.* **53** 1681 (1984)
49. Slutskin A A, Author's Thesis for Doctorate of Physico-mathematical Sciences (Khar'kov: Physicotechnical Institute of Low Temperatures, 1980)
50. Pippard A B, in *Physics of Metals,* Vol. 1: *Electrons* (Ed. J M Ziman) (Cambridge: Cambridge University Press, 1969)
51. Chambers R G *Proc. Phys. Soc. London* **88** 701 (1966)
52. Chambers R G *Proc. Phys. Soc. London* **89** 695 (1966)
53. Chambers W G *Phys. Rev.* **140** A 135 (1965)
54. Falicov L M, Sievert P R *Phys. Rev.* **138** A88 (1965)
55. Falicov L M, Pippard A B, Sievert P R *Phys. Rev.* **151** 498 (1966)
56. Falicov L M, Stachowiak H *Phys. Rev.* **147** 505 (1966)
57. Sowa E C, Falicov L M *Phys. Rev. B* **32** 755 (1985)
58. Freericks J K, Falicov L M *Phys. Rev. B* **39** 5678 (1989)
59. Bir G L, Pikus G E *Symmetry and Strain-Induced Effects in Semiconductors* (New York: Wiley, 1975)
60. Kaganov M I, Proshin Yu N *Fiz. Tverd. Tela (Leningrad)* **28** 1226 (1986) [*Sov. Phys. Solid State* **28** 689 (1986)]
61. Slutskin A A, Kadigrobov A M *Pis'ma Zh. Eksp. Teor. Fiz.* **32** 363 (1980) [*JETP Lett.* **32** 338 (1980)]
62. Slutskin A A, Manzhelii E V *Fiz. Nizk. Temp.* **19** 86 (1993) [*Low Temp. Phys.* **19** (1993)]
63. Slutskin A A, Manzhelii E V *Fiz. Nizk. Temp.* **19** 824 (1993) [*Low Temp. Phys.* **19** (1993)]
64. Proshin Yu N, Useinov N Kh *Phys. Status Solidi B* **166** 173 (1991)
65. Proshin Yu N, Useinov N Kh *Physica B* **173** 386 (1991)
66. Proshin Yu N, Useinov N Kh *Zh. Eksp. Teor. Fiz.* **100** 1088 (1991) [*Sov. Phys. JETP* **73** 602 (1991)]
67. Proshin Yu N, Useinov N Kh *Zh. Eksp. Teor. Fiz.* **105** 139 (1994) [*Sov. Phys. JETP* **78** 73 (1994)]
68. Proshin Yu N, Author's Thesis for Doctorate of Physico-mathematical Sciences (Kazan: Kazan State University, 1987)
69. Proshin Yu N, Noskova T L *XXIX Soveshch. po Fizike Nizkikh Temperatur: Tez. Dokl., Kazan, 1992* (Abstracts of Papers presented at Twenty-Ninth Conference on Low Temperature Physics, Kazan, 1992) Part 2, p. 353
70. Proshin Yu N, in *Program of Sixth Joint Magnetism and Magnetic Materials International Conference, Albuquerque, NM, 1994,* p. 131

71. Proshin Yu N, in *Magnetic Resonance and Related Phenomena Extended Abstracts of Twenty-Eighth Ampere Congress, Kazan, 1994*) p. 256
72. Landau L D *Zh. Eksp. Teor. Fiz.* **30** 1058 (1956) [*Sov. Phys. JETP* **3** 920 (1956)]
73. Gorbovitskii B M, Perel' V I *Zh. Eksp. Teor. Fiz.* **85** 1812 (1983) [*Sov. Phys. JETP* **58** 1054 (1983)]
74. Lifshitz E M, Pitaevskii L P *Statistical Physics* Vol. 2, 3rd edition (Oxford: Pergamon Press, 1980)
75. Walker M B *Phys. Rev. Lett.* **33** 406 (1974)
76. Walker M B *Can J. Phys.* **53** 165 (1975)
77. Silsbee R H, Long J P *Phys. Rev. B* **27** 5374 (1983)
78. Zil'berman G E *Zh. Eksp. Teor. Fiz.* **30** 1092 (1956); **32** 296 (1957); **33** 387 (1957) [*Sov. Phys. JETP* **3** 835 (1956); **5** 208 (1957); **6** 299 (1958)]
79. Freedman R, Fredkin D R *Phys. Rev. B* **11** 4847 (1975)
80. Nedorezov S S, Author's Thesis for Doctorate of Physicomathematical Sciences (Kharkov: Physicotechnical Institute of Low Temperatures, 1985)
81. Beuneu F *J. Phys. F* **10** 2875 (1980)
82. Silsbee R H, Beuneu F *Phys. Rev. B* **27** 2682 (1983)
83. Roth L M *Phys. Rev.* **145** 434 (1966)
84. Landau L D, Lifshitz E M *Quantum Mechanics: Non-Relativistic Theory* 3rd edition (Oxford: Pergamon Press, 1977)
85. Harrison W A *Phys. Rev.* **126** 497 (1962)
86. Reitz J R *J. Phys. Chem. Solids* **25** 53 (1964)
87. Kaganov M I, Slutskin A A *Magnitnyi Proboi* (Magnetic Breakdown) (Moscow: Znanie, 1985)
88. Gantmakher V F, Levinson Y B *Carrier Scattering in Metals and Semiconductors* (Amsterdam: North-Holland, 1987)
89. de Graaf A M, Overhauser A W *Phys. Rev.* **180** 701 (1969)
90. Cracknell A P, Wong K C *Fermi Surface: Its Concept, Determination and Use in Physics of Metals* (Oxford: Clarendon Press, 1973)
91. Van Dyke J P, McClure J W, Doar J F *Phys. Rev. B* **1** 2511 (1970)
92. Harrison W A *Solid State Theory* (New York: McGraw-Hill, 1970); Heine V *Solid State Phys.* **24** 1 (1970); Cohen M L, Heine V *ibid.* **24** 37 (1970); Heine V, Weaire D *ibid.* **24** 249 (1970)
93. Slutskin A A, Kadigrobov A M *Fiz. Tverd. Tela (Leningrad)* **9** 184 (1967) [*Sov. Phys. Solid State* **9** 138 (1967)]
94. Belokolos E D *Fiz. Tverd. Tela (Leningrad)* **19** 767 (1977) [*Sov. Phys. Solid State* **19** 444 (1977)]
95. Slutskin A A *Pis'ma Zh. Eksp. Teor. Fiz.* **4** 96 (1966) [*JETP Lett.* **4** 65 (1966)]
96. Abramowitz M, Stegun I A (Eds) *Handbook of Mathematical Functions with Formulas, Graphs, and Mathematical Tables* (New York: Wiley, 1972)
97. Gurzhi R N, Kopeliovich A I, in *Elektrony Provodimosti* (Conduction Electrons) (Moscow: Nauka, 1985) p. 7
98. Dyson F J *Phys. Rev.* **98** 349 (1955)
99. Azbel' M Ya, Gerasimenko V I, Lifshitz I M *Zh. Eksp. Teor. Fiz.* **31** 357 (1956) [*Sov. Phys. JETP* **4** 276 (1957)]
100. Cohen M H, Blount E I *Philos. Mag.* **5** 115 (1960)
101. Stark R W *Phys. Rev.* **135** A1698 (1964)
102. Useinov N Kh, Author's Abstract of Thesis for Candidate of Physicomathematical Sciences (Kazan: Kazan State University, 1992)
103. Lonzarich G G, Holtham P M *Proc. R. Soc. London Ser. A* **400** 145 (1984)
104. Pippard A B *Proc. R. Soc. London Ser. A* **287** 165 (1965)
105. O'Sullivan W J, Schirber J E *Phys. Rev.* **162** 519 (1967)
106. Buot F A, Li P L, Strom-Olsen J O *J. Low. Temp. Phys.* **22** 535 (1976)
107. Lifshitz I M, Kosevich A M *Zh. Eksp. Teor. Fiz.* **29** 730 (1955) [*Sov. Phys. JETP* **2** 636 (1956)]
108. Kochkin A P *Zh. Eksp. Teor. Fiz.* **54** 603 (1968) [*Sov. Phys. JETP* **27** 324 (1968)]
109. Joseph A S, Gordon W L *Phys. Rev.* **126** 489 (1962)
110. Thorsen A C, Joseph A S, Valby L E, in *Proceedings of Ninth International Conference on Low Temperature Physics, Columbus, OH, 1964* (New York: Plenum Press, 1965) p. 867
111. Winter J *Magnetic Resonance in Metals* (Oxford: Clarendon Press, 1971)
112. Platzman P M, Wolff P A *Waves and Interactions in Solid State Plasma* (Suppl. 13 to *Solid State Phys.*) (New York: Academic Press, 1973)
113. Azbel' M Ya, Gerasimenko V I, Lifshitz I M *Zh. Eksp. Teor. Fiz.* **32** 1212 (1957) [*Sov. Phys. JETP* **5** 986 (1957)]
114. Azbel' M Ya, Gerasimenko V I, Lifshitz I M *Zh. Eksp. Teor. Fiz.* **35** 691 (1958) [*Sov. Phys. JETP* **8** (1959)]
115. Lifshitz I M, Azbel M Ya, Gerasimenko V I *J. Phys. Chem. Solids* **1** 164 (1956)
116. Kaplan J I, Glasser M L *Phys. Rev.* **183** 408 (1969)
117. Czerwonko J *Phys. Status Solidi B* **67** K15 (1975)
118. Montgomery D S *J. Phys. F* **11** 711 (1981)
119. Bloembergen N, Purcell E M, Pound R V *Phys. Rev.* **73** 679 (1948)
120. Dupree R, Holland B W *Phys. Status Solidi* **24** 275 (1967)
121. Moore R A *J. Phys. F* **5** 2300 (1975)
122. Silsbee R H, Beuneu F *Phys. Rev. B* **27** 2682 (1983)
123. Lubzens D, Shanabarger M R, Schultz S *Phys. Rev. Lett.* **29** 1387 (1972)
124. Notley R P, Sambles J R, Cousins J E *Solid State Commun.* **25** 1125 (1978)
125. Stanley D J, Walker M B *Solid State Commun.* **21** 449 (1977)
126. Rahman T S, Parlebas J C, Mills D L *J. Phys. F* **8** 2511 (1978)
127. Couch N R, Sambles J R, Stesmans A, Cousins J E *J. Phys. F* **12** 2439 (1982)
128. Zubarev D N *Nonequilibrium Statistical Thermodynamics* (New York: Consultants Bureau, 1974)
129. Oseroff S, Gehman B L, Schultz S *Phys. Rev. B* **15** 1291 (1977)